Developing methods to prioritize *in vitro* drug combinations against *Mycobacterium tuberculosis*: fusidic acid as potential combination partner with known antitubercular agents.

Charles Omollo

Thesis presented for the degree of Doctor of Philosophy in the Department of Chemistry, University of Cape Town

12 March, 2017

DECLARATION

I declare that this thesis is my own unaided work. It is being submitted for the degree of Doctor of Philosophy at the University of Cape Town. It has not been submitted for any degree or examination at any other university.

Charles Omollo

Signed by candidate

Signature: Signature removed

Date: 12 March, 2017.

ACKNOWLEDGEMENTS

I would like to thank all the people who contributed one way or the other towards this PhD thesis.

Special thanks to Prof. Kelly Chibale my supervisor: You accepted me into your academic group, supported both my research activities as well as my attendance to various conferences. I have benefited greatly from your exceptional scientific guidance, mentorship and friendship throughout my PhD journey. *Ahsante!*

A/Prof. Digby F. Warner my co-supervisor: Thank you so much for walking me through every single step since I began to explore drug's synergistic interactions. You gave me the intellectual freedom and tools for my work, challenged me with new ideas and literally demanded high quality out-put of this effort. Indeed, you have taught me how to become a scientist.

I also thank Prof. Valerie Mizrahi for her insightful comments, constructive criticism and the hard questions during numerous group sessions at MMRU. All these contributed in shaping up this work. Your passion and dedication for science has inspired us to grow up as scientists.

I am very grateful to Drs. Elizabeth Kigondu and Krupa Naran for being my first teachers at UCT. You initiated me into the laboratory and impeccably guided me through the techniques involved with matrix screening assays which has been an integral part of this work. Additionally, thanks to Drs. Kawaljit Singh and Gurminder Kaur whose knowledge in organic synthesis and relentless work ethic successfully yielded the analogues of FSA, upon

which I relied on for most of the experimental work. Dr. Pooja Argawal and my colleague, Antonina Wasuna, your contributions with the macrophage work are highly appreciated. I benefited a lot from the support and immense knowledge of Drs. Vinayak Singh, Atica Moosa and Anastasia Koch. All members, both at the MMRU and KC groups: thank you for your support and friendship.

Elaine-Rutherford Jones and Gadija Hull-Conrad both deserve special mention for facilitating the logistics and keeping our work running smoothly both in and outside of the laboratories. Additionally, Lameeza seamlessly fitted into providing logistical support when Gadija retired.

I am grateful for the various sources and collaborators who availed funds for my graduate school studies: The Novatis Pharma Fellowship, IDM-Carnegie Corporation Fellowship and the Department of Science and Technology, through the South Africa Research Chairs Initiative administered through the National Research Foundation, the Department of Chemistry and the MMRU, University of Cape Town.

And most of all for my loving, supportive, and patient wife Rose, sons; Wayne and Curtis. Your undivided support throughout this PhD is so appreciated. To God Almighty be the glory.

ABSTRACT

The tuberculosis (TB) epidemic remains a major threat to public health globally, and is exacerbated by the escalating number of multi-drug resistant cases. These factors have highlighted the urgent need for new effective therapies or different approaches to augment the efficacy of current anti-TB drugs. Synergistic drug combinations present a feasible strategy towards expanding TB treatment options. Despite reported successes with combination screening, as well as the current reliance on combination therapy for TB, this approach remains largely underexplored. Evidence suggests that utilizing synergistic combinations might enable existing clinically-approved drugs to be readily re-purposed for TB treatment, including against multi-(MDR) and extensively- (XDR) drug resistant strains for current therapies are often ineffective.

This thesis focused on the development and application of improved methods to identify and advance novel drug combinations for TB therapy. There were two key aspects to this work: firstly, exploring mechanisms of synergy between fusidic acid (FSA), a natural product antibiotic, and current anti-TB agents and, secondly, characterizing antibiotic action by delineating bacteriostatic and bactericidal compounds.

In the search for synergy, a drug repurposing/repositioning approach was adopted, chapters 2 and 3, in which FSA and its semi-synthetic derivatives were selected for combination studies with a drug panel consisting of known anti-TB drugs as well as translational inhibitors. Checkerboard assays and subsequent analyses of time-kill kinetics revealed seven drugs that synergized with FSA in inhibiting the growth of *Mycobacterium tuberculosis*. These included the rifamycin, rifampicin (RIF), and the macrolides, erythromycin (ERY), clarithromycin (CLR), and roxythromycin (ROX). Other agents which

synergized with FSA included the oxazolidinone, linezolid (LZD), the aminoglycoside, streptomycin (STR), and spectinomycin (SPC), an aminocyclitol. Among these, FSA exhibited strongest synergies with SPC and ERY, both returning a fractional inhibitory concentration index (FICI) value of 0.25. Notably, synergy with FSA was achieved *in vitro* at concentrations lower than the reported peak plasma concentrations achievable for all the drugs, with the exception of ERY. Moreover, those compounds synergizing with FSA also exhibited less lipophilicity, i.e low clogP values, suggesting the potential to penetrate the caseum, a characteristic currently prioritized in many TB drug discovery programmes.

In order to inform judicious selection of FSA synergizing partners for further advancement, the activity of these compounds against drug-resistant mutants was also examined. No cross resistance was observed against a defined FSA-resistant (FSA-R) mutant and, furthermore, FSA-R mutant displayed increased susceptibility to STR and SPC compared to the WT strain. In chapter 3, combinations that exhibited varied degrees of potency against the WT strain were also tested against the resistant mutants. These studies revealed the potential for synergistic combinations to restore activity against strains resistant to either one of the two partner drugs. For example, combining FSA (or its analogues) with SPC against wild-type *M. tuberculosis* H37Rv and a derivative FSA-resistant (FSA-R) or SPC resistant (SPC-R) mutant showed that potent interactions such as FSA plus SPC (FICI ~ 0.15) retained synergistic inhibition against either resistant mutant. To leverage this finding, SPC was utilized in a three-drug interaction study that also included rifampicin (RIF) and isoniazid (INH). The combination of RIF-INH plus SPC used at sub-MIC's exhibited synergy against the wild-type and RIF-resistant, *rpoB* mutant. This inhibitory effect supported the potential for SPC to overcome a pre-existing genetic resistance against one of the drugs in a combination therapy.

Assigning bactericidal or bacteriostatic modes of action to experimental compounds has become an important consideration in early drug discovery programmes. The second major component of this thesis aimed to develop a rapid and robust method for assessment of bactericidal/bacteriostatic compounds by integrating different strategies, including flow cytometry (FCM), fluorescent microscopy, and the spot assay technique. The results established that assigning mode of antibiotic action could be rapidly accomplished. Using FCM analyses of *M. smegmatis*, chapter 4, results were available within 1 h of exposure to the applied drug. Moreover, the use of FCM enabled a tentative inference of the drug's target: cell wall synthesis inhibition *versus* the inhibition of other metabolic processes within the cell. Both FSA and SPC exhibited a late inhibition, 72 h post-exposure, suggesting an intracellular metabolic impairment. Morphological phenotyping by optical microscopy revealed heterogeneous mycobacterial populations composed of aggregated cells, triplets, doublets and singlets that differentially distributed across the two sub-populations of the exponential culture. The transition of *M. smegmatis* cell population from log phase to stationary phase was also accompanied with a cell size reduction. This may possibly be explained by the rearrangement in peptidoglycan in cell wall of the stationary phase bacteria leading to size reduction.

In conclusion, this thesis describes experimental and analytical approaches designed to enable the evaluation of synergistic drug interactions as a key component to the discovery and development of novel combination therapies and, moreover, suggests that application of high-throughput population biology techniques such as FCM enable rapid early triage of priority experimental compounds and combination therapies.

PRESENTATIONS

Omollo C, Chibale K, Warner DF. Developing synergistic combinations to restore sensitivity in drug-resistant *Mycobacterium tuberculosis*. Poster presentation at a *H3D Drug Discovery Symposium on Tuberculosis and Neglected Diseases* held on 15-18 November, 2016, Goudini Spa Resort, Cape Town, South Africa.

Omollo C, Chibale K, Warner D. 2D and 3D interactions of fusidic acid with front-line anti-tubercular drugs and selected translational inhibitors against *Mycobacterium tuberculosis* in vitro. Poster presentation at the Gordon Research Conference in Tuberculosis Drug Development held on 12-17 July, 2015, Melia Golf Catalan Business and Convention Center, Girona, Spain.

Omollo C, Kigondu E, Warner DF, Chibale K. *In vitro* synergistic interactions of fusidic acid with known antituberculosis drugs. Poster presentation at *H3D Drug Discovery Symposium*, 27-29 August, 2014, Victoria Falls, Livingstone, Zambia.

TABLE OF CONTENTS

LIST OF FIGURES

List of Tables

LIST OF ABBREVIATIONS

AMK	-	Amikacin
ATP	-	Adenosine Triphosphate
BDQ	-	Bedaquiline
CA-AM	-	Calcein AM
CFU	-	Colony Forming Unit
CLSI	-	Clinical and Laboratory Standards Institute
CLR	-	Clarithromycin
CIP	-	Ciprofloxacin
CPZ	-	Chlorpromazine
DCS	-	D-Cycloserine
DMSO	-	Dimethylsulphoxide
DNA	-	Deoxyribonucleic Acid
EMB	-	Ethambutol
ERY	-	Erythromycin
FACS	-	Fluorescence Activated Cell Sorting
FBS	-	Fetal bovine serum
FCM	-	Flow cytometry
FIC	-	Fractional Inhibitory Concentration
FICI	-	Fractional Inhibitory Concentration Index
FSA	-	Fusidic acid
FSC-H	-	Forward Scatter Height
GAT	-	Gatifloxacin

GEN - Gentamycin

HIV - Human Immunodeficiency Virus

HYG - Hygromycin

INH - Isoniazid

KAN - Kanamycin

LEV - Levofloxacin

MDR - Multidrug Resistant

MDRTB- Multidrug Resistant Tuberculosis

MIC - Minimum Inhibitory Concentration

MMRU- Molecular Mycobacteriology Research Unit

MXF - Moxifloxacin

NADH- Nicotinamide Adenine Dinucleotide Hydrate

OADC- Oleic Acid/Albumin/Dextrose/Catalase

OD - Optical Density

OFX - Ofloxacin

PAS - ρ-Aminosalicyclic acid

PBS - Phosphate Buffered Solution

PI - Propidium iodide

POA - Pyrazinoic Acid

PZA - Pyrazinamide

RIF - Rifampicin

RNA - Ribonucleic Acid

rRNA - ribosomal Ribonucleic Acid

ROS - Reactive Oxygen Species

SPC	-	Spectinomycin
SSC-H	-	Side Scatter Height
STR	-	Streptomycin
TB	-	Tuberculosis
TET	-	Tetracycline
VAN	-	Vancomycin
Wt	-	Wild-type
WHO	-	World Health Organization
XDRTB	-	Extensively Drug Resistant Tuberculosis

Chapter 1

Introduction

1.1. Background

Mycobacterium tuberculosis is responsible for significant morbidity and mortality as well as imposing a massive public health and economic burden (Zumla et al., 2014). In 2015, there were an estimated 1.4 million deaths from tuberculosis (TB) and a further 0.4 million deaths arising from TB disease among people infected with HIV (WHO,). Moreover, it is estimated that there are approximately two billion latent *M. tuberculosis* infections worldwide, which represents a massive reservoir of potential future disease (Zumla et al., 2015). Incident cases of TB were estimated at 10.4 million in 2015, equivalent to 142 cases per 100,000 population, with 61% in Asia, and 26% in the African region (World Health Organization, 2015). The Mediterranean accounted for 7% of the world's cases, while Europe and the America's each had 3% new cases (WHO, 2016). In addition, India, Indonesia, China, Nigeria, Pakistan and South Africa contributed to an estimated 60% of the global TB incidence in 2015 (WHO, 2016). **Figure 1-1**, shows the geographic distribution of TB incidence globally.

The existing TB prevalence can be ascribed to various features, notably, cases of increased drug resistance, co-infection with HIV, resettlement and migration of people, and active transmission in crowded environments such as prisons, refugee camps and hospitals (Ducati et al., 2006). The absence of a completely effective TB vaccine as well as the slow development of new antimycobacterial drugs have also exacerbated the re-emerging TB crisis (WHO, 2012).

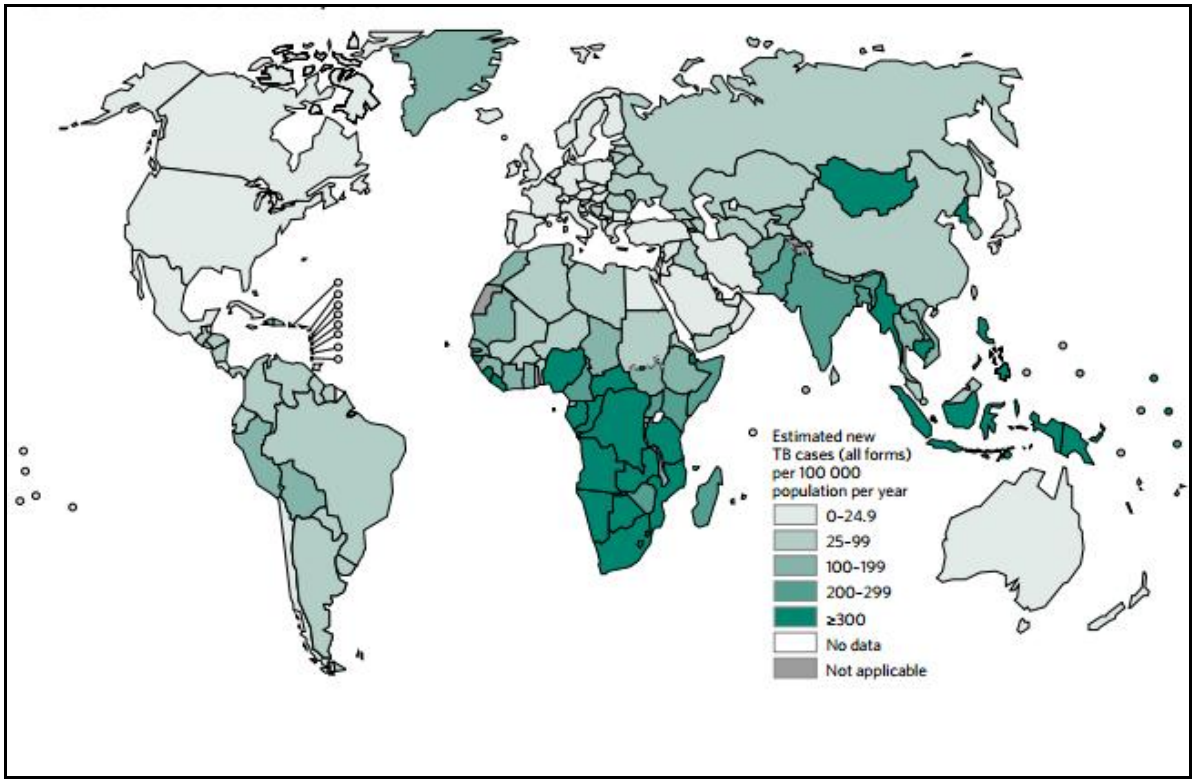

Figure 1-1 Estimated new TB cases, 2015 (WHO, 2016).

Worse still, an estimated 1.1 million (13%) of TB cases in 2013 were HIV-positive individuals. Among these, the African region bore the greatest burden with four out of every five HIV-positive TB cases and TB deaths reported (World Health Organization, 2014).

1.2. Mycobacteria

The genus *Mycobacterium* consists of mostly non-motile, Gram-positive bacilli whose genomes are characterized by high G+C percentage (62 – 72 %). They are rod-shaped, aerobic bacteria whose cell walls uniquely contain mycolic acids as a major component. The wax-like cell wall for this genus is associated with unique characteristics of acid-fastness and intense hydrophobicity. In addition, they are less prone to desiccation, changes in acidity/alkalinity and are generally tolerant of antibiotics (Barry et al., 1998; Daffe & Draper, 1998).

1.2.1. *M. tuberculosis* pathogenesis

In 1882, Robert Koch identified *M. tuberculosis*, a member of the Mycobacteriaceae family, as the causative agent of TB (Kaufmann & Schaible, 2005). *M. tuberculosis* is a clinically important bacilli that belong to the *M. tuberculosis* complex (or MTBC), a group comprised of closely related mycobacterial pathogens which includes *M. africanum*, *M. bovis*, *M. canettii* and *M. microti* (Russell, 2001). *M. tuberculosis* is a slow grower with a generation time of approximately 20 h under standard aerobic conditions *in vitro* (Dartois, 2014). It requires two to three weeks of incubation for any visible growth to be detected on solid media at 37°C (Murray et al., 2007). Moreover, it is known to replicate and survive within the host macrophage cells, which distinguishes *M. tuberculosis* from many other pathogens. *M. tuberculosis* is transmitted by aerosol into the lungs. It largely inhabits the professional phagocytic cells; macrophages, neutrophils, monocytes and dendritic cells (Kang et al., 2011; Wallgen, 1948). After phagocytosis, neutrophils, lymphocytes and macrophages move towards the lesion, leading to formation of a granuloma, a wall of macrophages and immune cells intended to contain the infection. In other infectious diseases, the recruitment of phagocytic cells restricts and even eliminates invading pathogens, whereas in *M. tuberculosis*, the granuloma structure allows it to continue growing and overcome the immune response during the early stages of infection (Davis & Ramakrishnan, 2009). Inside the granuloma, the bacilli can be metabolically quiescent leading to latent TB infection. In less than 10% of latent TB infections, there is reactivation of infection, exacerbated by many factors which result in an immunocompromised state. Such factors include HIV infection, immunosuppression, or treatment with anti-TNF-α (Kumar et al., 2011).

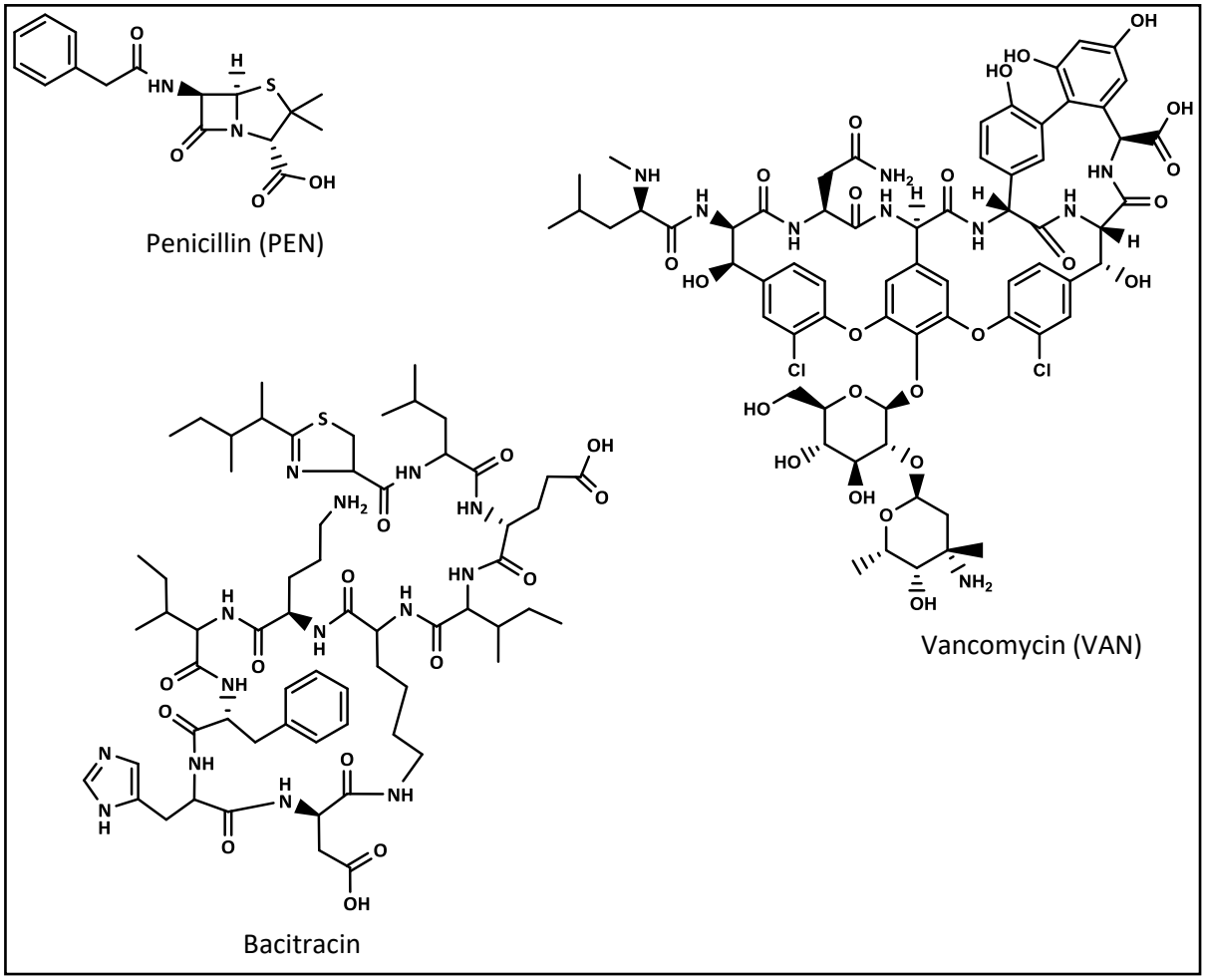

Figure 1-2 Examples of cell wall biosynthesis inhibitors

1.3. Antibacterial agents

Infectious diseases, for example TB, which are caused by bacteria can be treated or managed by using antibiotics. These agents are natural, semi-synthetic or synthetic compounds that kill, or inhibit the growth of, bacteria. The bacteria can be susceptible to antibiotics resulting in growth inhibition or death. Yet, in some cases, the bacteria may remain unaffected, or may even acquire resistance (Stefanovic-Racic et al., 2012).

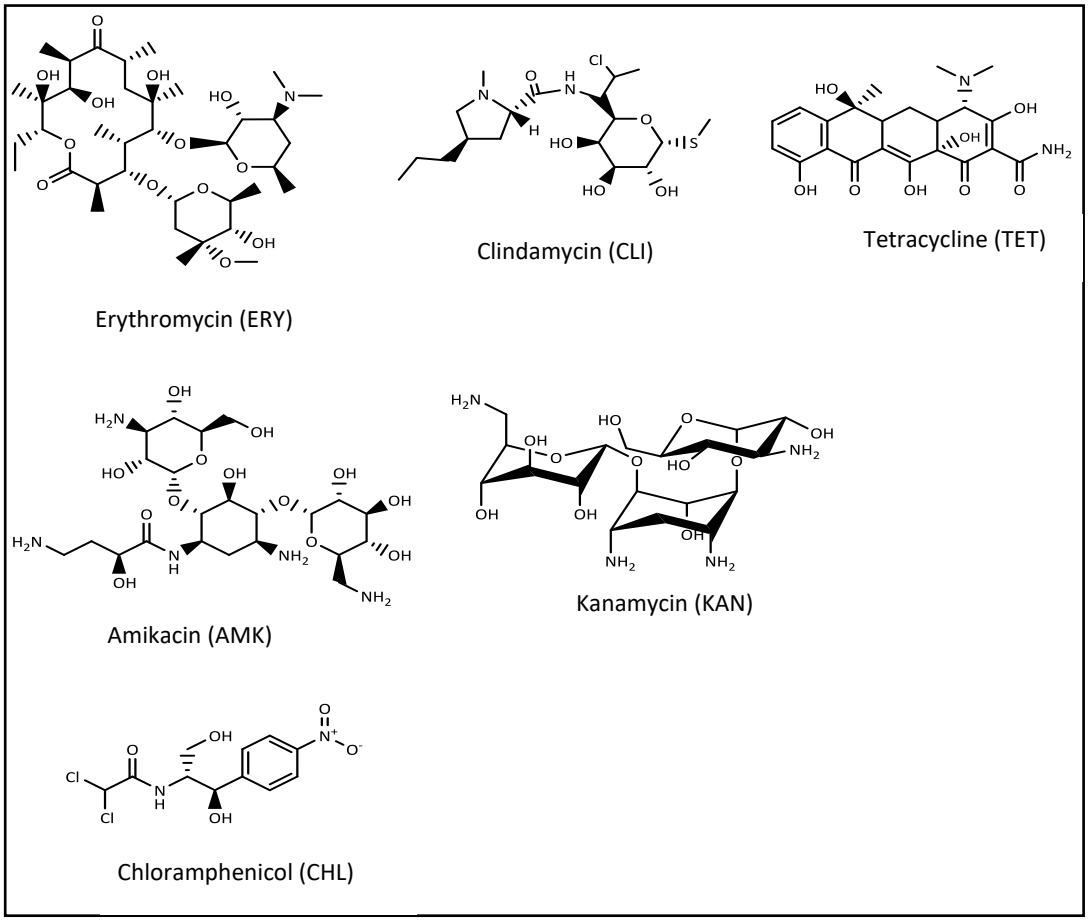

Figure 1-3 Examples of protein biosynthesis inhibitors

Antibiotics can be classified primarily into five groups based on the metabolic pathway or macromolecular structure they affect. These include: (i) cell wall biosynthesis inhibitors, for example penicillin (PEN), vancomycin (VAN), bacitracin (BAC), **(Figure 1-2)**. PEN, a beta lactam antibiotic, blocks the final step of peptidoglycan synthesis by inhibiting the action of transpeptidation enzymes. BAC and VAN, on the other hand, target the early stages of peptidoglycan synthesis (Baggot, 1998); (ii) protein biosynthesis inhibitors, which target certain subunits of microbial ribosomes, for example macrolides such as erythromycin (ERY) and clindamycin (CLI), the aminoglycosides, amikacin (AMK) and kanamycin (KAN), as well as tetracycline (TET) and chloramphenicol (CHL), **(Figure 1-3)**;

(iii) DNA replication/ repair inhibitors, including the fluoroquinolones ciprofloxacin (CIP), moxifloxacin (MXF) and ofloxacin (OFX) **(Figure 1-4)**; (iv) RNA synthesis inhibitors, for example rifampicin (RIF), a rifamycin (Ali et al., 1993) **(Figure 1-5)**, and (v) inhibitors of folic acid synthesis, for example pyrimethamine (PMT), trimethoprim (TMP) and the sulfonamide, sulfamethoxazole (SMX) (Baggot, 1998) **(Figure 1-6)**.

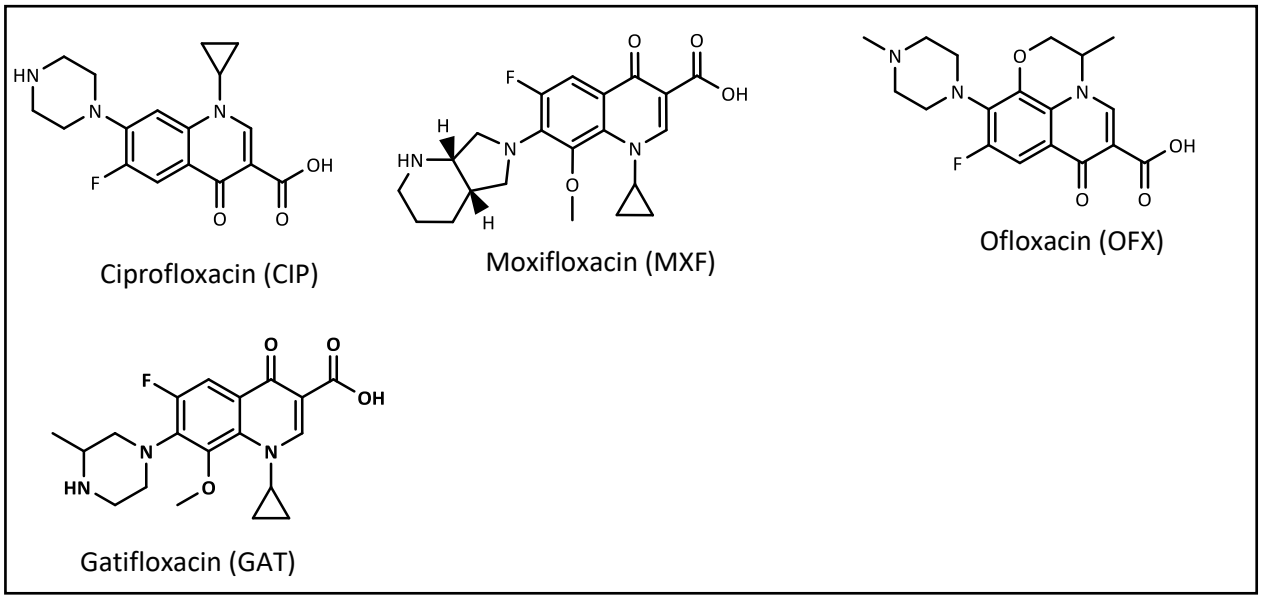

Figure 1-4 Examples of DNA replication/repair inhibitors

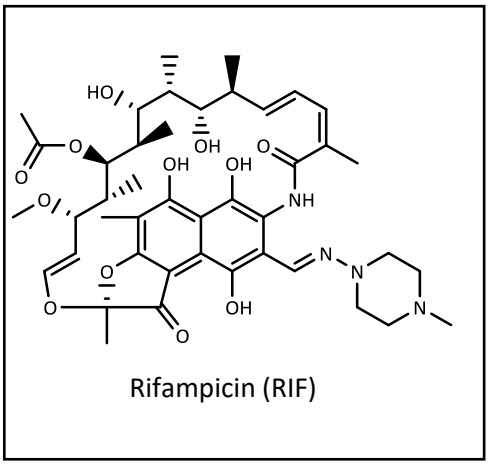

Figure 1-5 Example of RNA synthesis inhibitor

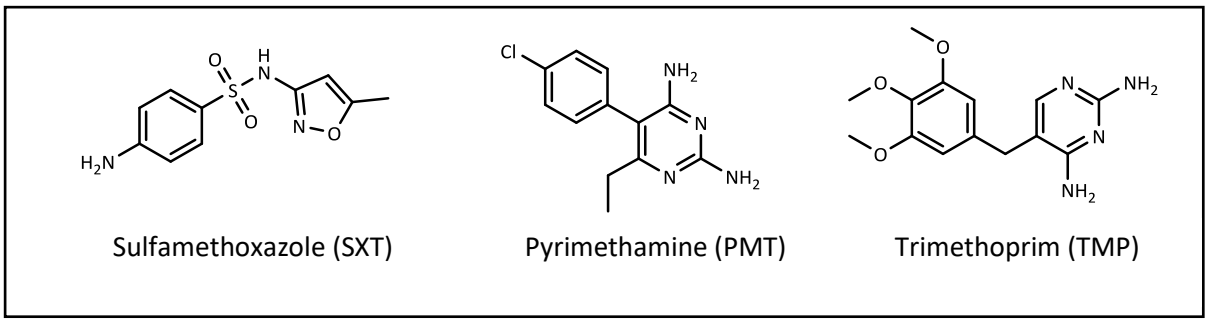

Figure 1-6 Examples of folic acid biosynthesis inhibitors

1.3.1. Translational inhibitors

The translational apparatus of bacteria has been shown to be a major target of antibiotics. In this case, the antibiotics act predominantly on the three functional centres of the ribosome: the messenger RNA (mRNA)-transfer RNA (tRNA) decoding region on the 30S subunit, the peptidyl transferase centre of the 50S subunit and, lastly, the ribosomal exit tunnel, which allows the passage of the nascent polypeptide chain. Protein translation can be categorized as: the initiation, elongation and termination or recycling **(Figure 1-7)**. With the exception of aminoglycosides, most antibiotics that act on the ribosome are bacteriostatic (Kohanski et al., 2007).

1.3.1.1. Antimicrobials acting on the 30S part of the ribosome

Aminoglycosides such as streptomycin (STR) and gentamicin (GEN) **(Figure 1-8)** trap the 30S initiation complex (30S-mRNA-tRNA) by binding at the 16S ribosomal RNA, thereby preventing any further initiation. They also induce misreading of mRNA, which results in slowing down of protein synthesis. Binding of aminoglycosides to the 16S rRNA enhances the binding of tRNA to the A site irrespective of the anticodon specificity.

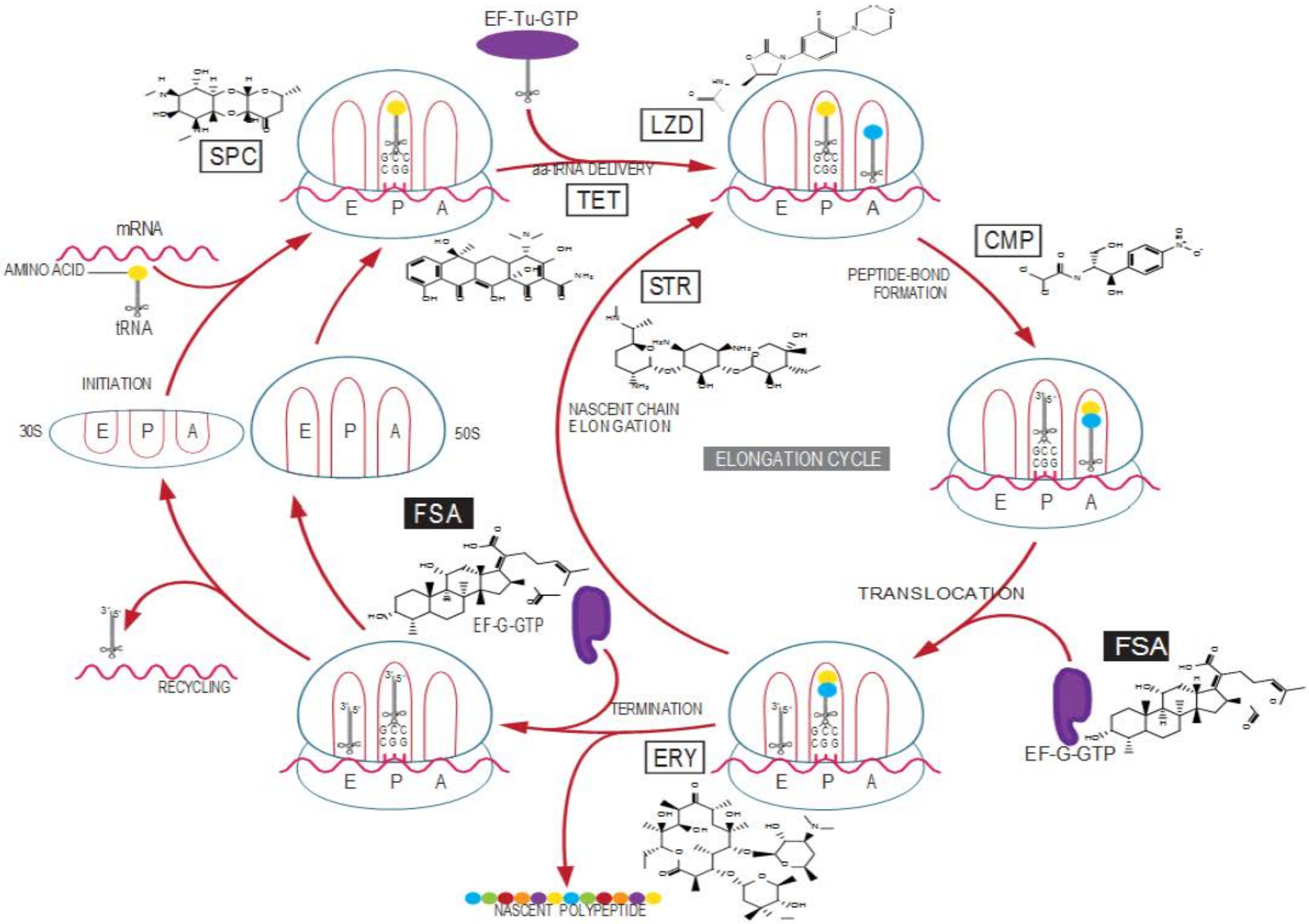
EF-Tu-GTP
SPC
LZD
aa-tRNA DELIVERY
TET
mRNA
AMINO ACID
tRNA
INITIATION
30S
50S
E P A
STR
CMP
PEPTIDE-BOND FORMATION
NASCENT CHAIN ELONGATION
ELONGATION CYCLE
FSA
EF-G-GTP
TRANSLOCATION
RECYCLING
TERMINATION
ERY
NASCENT POLYPEPTIDE

Figure 1-7 Antibiotic targets during protein synthesis. Schematic representation of antibiotics acting at different stages in the translation process. The three main tRNA binding sites on the ribosome; A-, P-, and E-sites. (Adopted and modified from Wilson, 2009)

Tetracyclines are bacteriostatic agents that include TET, minocycline (MIN) and doxycycline (DOX) **(Figure 1-9)**. They bind reversibly to the 30S subunit, and thereby prevent the accommodation of aminoacyl-tRNA to the acceptor site of the 70S ribosome (Wilson, 2009).

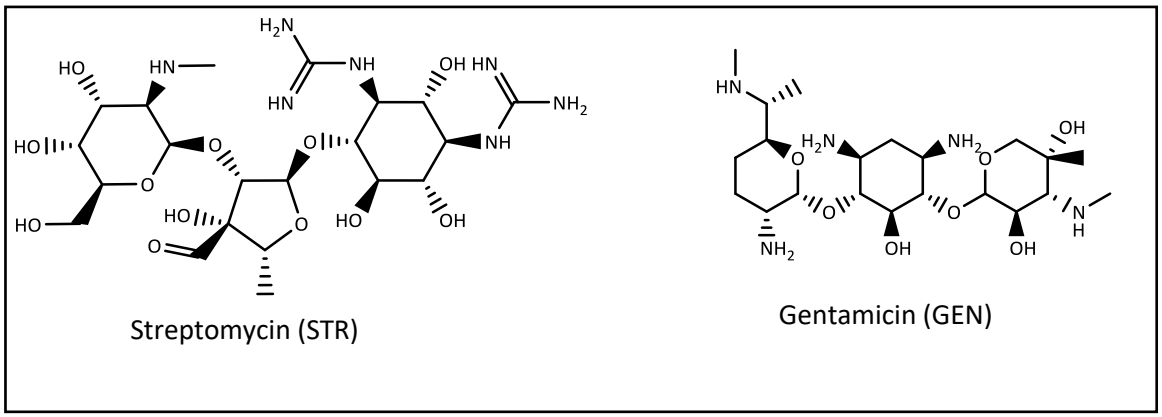

Figure 1-8 Examples of aminoglycosides

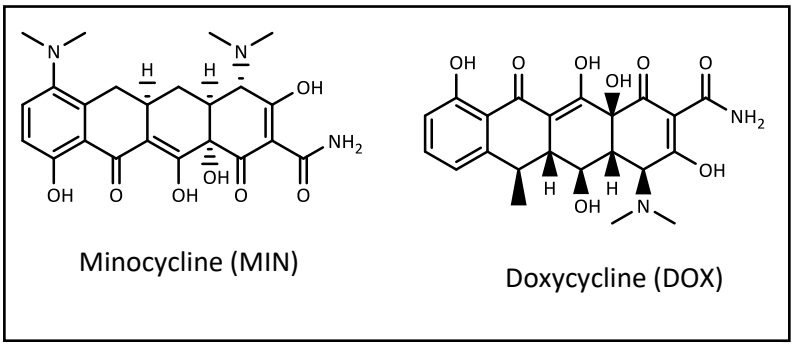

Figure 1-9 Examples of tetracyclines

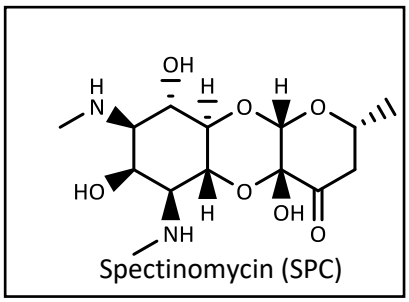

Figure 1-10 Example of an aminocyclitol

The *aminocyclitol* class is exemplified by SPC **(Figure 1-10)**, and is structurally similar to aminoglycosides; these antibiotics interfere with mRNA interactions with the 30S ribosome (Hoeksema & Knight, 1975; Lyutzkanova, Distler & Altenbuchner, 1997).

1.3.1.2. Antimicrobials that target elongation factors in protein synthesis

Fusidic acid (FSA) **(Figure 1-11)** is a focus of this study. This drug acts on elongation factor G (EF-G). FSA interferes with the release of EF-G from the EF-G/GDP complex (Turnidge & Collignon, 1999).

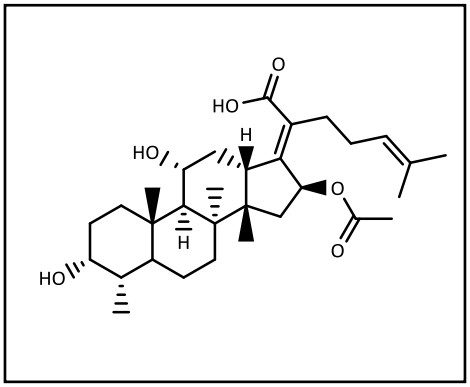

Figure 1-11 Fusidic acid (FSA)

1.4. TB treatment regimens

The difficulty encountered in eradicating *M. tuberculosis* with the currently available drugs, as well as the long treatment duration, are factors contributing to the increasing occurrence of MDR strains (Reddy et al., 2010). Moreover, about 11-13% of TB patients worldwide are co-infected with HIV, which complicates the treatment owing to drug-drug interactions or related toxic side-effects (Koul et al., 2011). Furthermore, TB-HIV co-infected patients are at risk of developing immune reconstitution inflammatory syndrome (Gengiah et al., 2011). The current first–line anti-TB chemotherapy consists of a four-drug combination: RIF, isoniazid

(INH), pyrazinamide (PZA) and ethambutol (EMB) **(Figure 1-12)** (Kaneko, Cooper & Mdluli, 2011)

RIF has been the backbone of TB chemotherapy since its discovery in the 1960s. It targets the *rpoB*-encoded β subunit of RNA polymerase, an enzyme that catalyses transcription (Zumla, Nahid & Cole, 2013; Cohen, 2013) INH, introduced in 1953, has been very effective since its development (Miesel et al., 1998; Almeida et al., 2007). It inhibits the synthesis of mycolic acids that form long chain fatty acids, which contribute to the structural composition of the cell wall (Miesel et al., 1998; Winder & Collins, 1970). PZA, which was developed in the mid-1980s, has structural similarities to INH (Shi et al., 2011; Scorpio & Zhang, 1996). Until recently, it was believed that PZA - through its bioactive derivative, pyrazinoic acid (POA) - exerted its action on *M. tuberculos*is by disrupting membrane energetics resulting in inhibition of membrane transport function (Zhang et al., 2003).

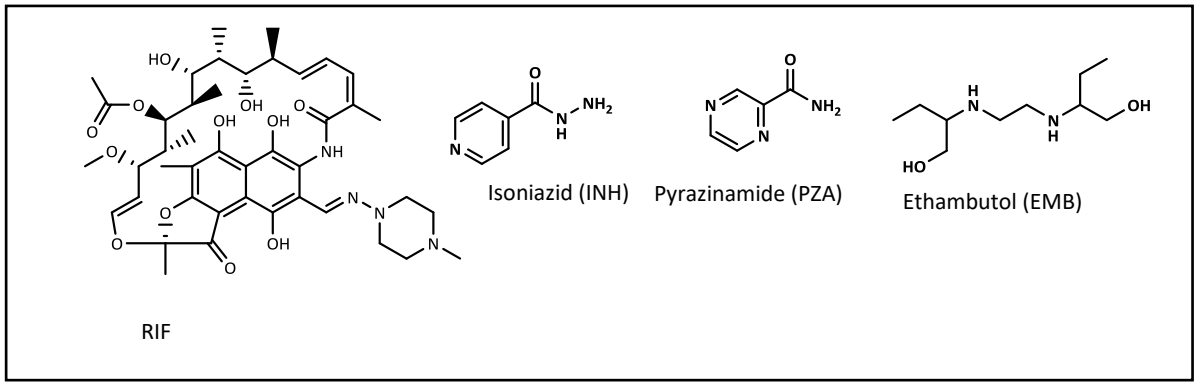

Figure 1-12 Current anti-TB first-line drugs.

However, recent findings suggest a different mode of action involving PZA/POA. Gopal *et al.* demonstrated that POA depletes coenzyme A (CoA), an essential acyl carrier, in wild type bacteria. In addition, they found resistance conferring mutations in two pathways: missense mutations in aspartate decarboxylase, *panD*, involved in synthesis of CoA and

frameshift mutations in the *in vitro* non-essential polyketide synthase genes, *mas* and *ppsA-E*, involved in the synthesis of the virulence factor phthiocerol dimycocerosate (PDIM) (Gopal et al., 2016). In another study, Shi *et al.* identified the ribosomal protein S1 (RpsA), encoded by the *rpsA* gene as the possible target of POA. RpsA is associated with protein translation process and maintenance of fidelity in protein synthesis; or trans-translation (Shi et al., 2011). Evidence by Yang *et al.* also suggested that the binding of POA to RpsA led to the inhibition of trans-translation. In this study, crystal structures of the C-terminal domain of RpsA in *M. tuberculosis* were reported in complex with POA, as well as the corresponding domains of two RpsA variants associated with PZA resistance (Yang et al., 2015). Lastly, EMB, discovered in 1961 kills actively multiplying bacilli by inhibiting arabinosyl transferases involved in cell-wall biosynthesis (Takayama & Kilburn, 1989; Shi et al., 2011).

Subsequent to the discovery and FDA approval of RIF, no new TB drug was developed for almost 50 years. Recently, however, bedaquiline (BDQ), also known as TMC 207 **(Figure 1-13)**, received FDA approval for the treatment of MDR-TB cases (Cohen, 2013). It is highly effective on non-replicating bacilli of drug-susceptible, MDR, and XDR *M. tuberculosis* strains and acts by inhibiting ATP synthase, blocking mycobacterial ATP generation (Andries et al., 2005; Rivers & Mancera, 2008). However, it has been shown to cause serious side effects such as irregular heart rhythms that can result in cardiac arrest. Results of clinical trials have revealed a 4.5-fold higher mortality of groups treated with BDQ compared to the control (Cohen, 2013). Moreover, it is not yet clear whether this drug can be safely combined with the current HIV medications (Giffin & Robinson, 2009). These shortcomings, and the fact that fewer than 10% of drug candidates pass clinical trials successfully, reinforce the pressing need for new anti-TB drugs (Giffin & Robinson, 2009).

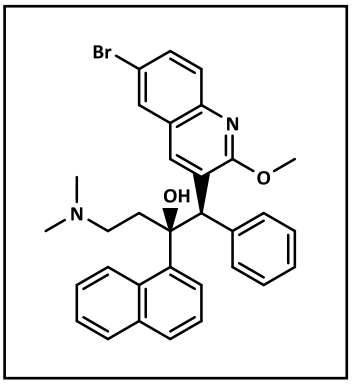

Figure 1-13 Bedaquiline, BDQ

1.4.1. Resistance of *M. tuberculosis* to current anti-TB treatment

The renewed search for new anti-TB drugs has been further necessitated by the emergence of MDR strains, which are defined as resistant to the frontline agents, INH and RIF. Extensively drug-resistant (XDR) TB strains are defined as MDR strains that have gained resistance to any fluoroquinolone and at least one of the three injectable second-line drugs **(Figure 1-14)** (Zignol et al., 2006; Basu & Galvani, 2008).

By the end of 2015, representative data from continuous surveillance in 88 WHO member countries within the five territories indicated an average of 9.5% of MDR-TB cases as XDR-TB.(WHO,) However, this representation could be an underestimation owing to the difficulty in the diagnosis of tuberculosis. As noted in a study by Dheda *et al*, the challenges include patients

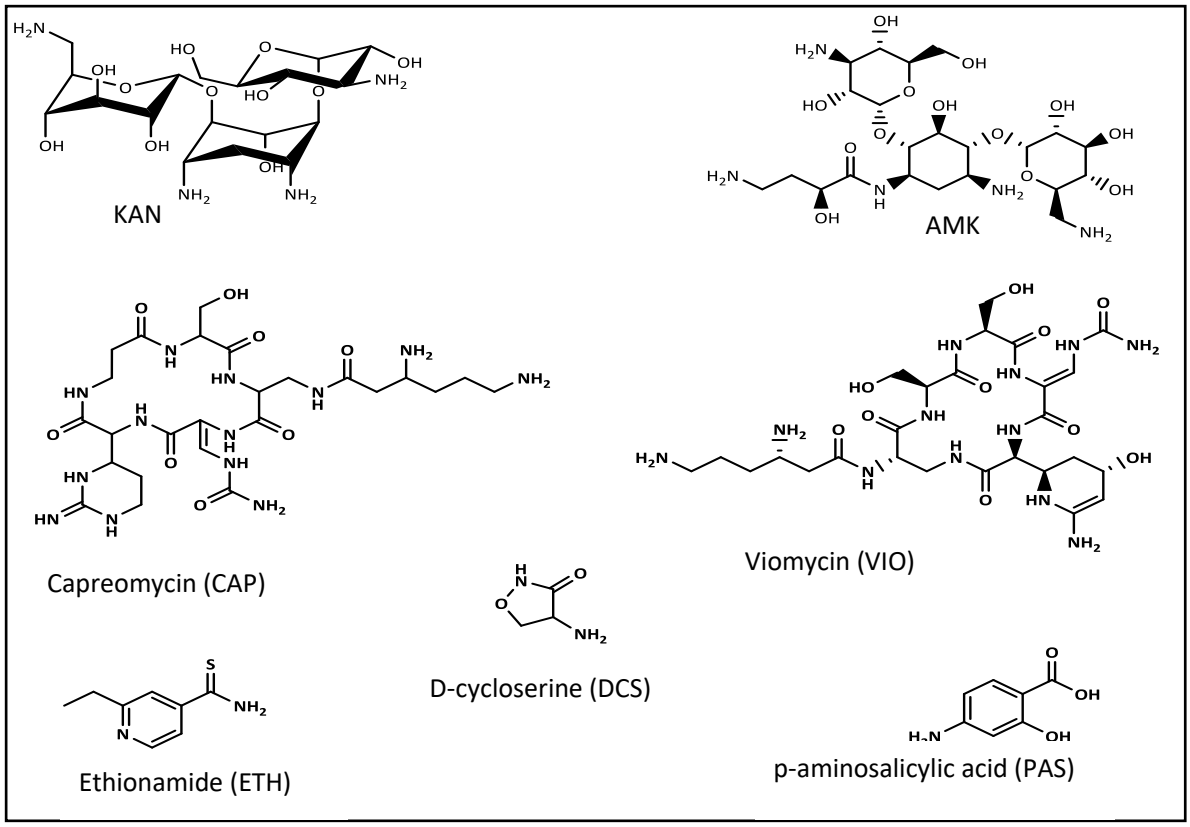

Figure 1-14 Examples of second-line anti-TB drugs.

with scant or no sputum, an extrapulmonary presentation or low sputum mycobacterial burden - same day sputum test negative. In some cases, sputum induction and organ or tissue biopsy might be needed, but are not always available in the resource poor settings. Accordingly, these challenges in diagnosis as well as other health-system associated factors add to the diagnostic gap of an estimated 3 million undiagnosed tuberculosis cases globally (Dheda, Barry 3rd & Maartens, 2015).

Chromosomal mutations are primarily responsible for the drug resistance in TB. These mutations affect either the drug target itself, or bacterial enzymes that activate prodrugs, or efflux pumps (Sandgren et al., 2009). The emergence of clinical drug resistance in TB **(Figure 1-15)** is categorized as *acquired resistance* when drug resistant mutants are selected as a result of ineffective treatment or as *primary resistance* when a patient is infected with a resistant strain (Johnson et al., 2007). A number of mutations in isolates resistant to

specific drugs have been elucidated in *M. tuberculosis* (Ramaswamy & Musser, 1998). In the case of drugs like INH and RIF, considerable mutations have been established that confer resistance (estimated spontaneous mutation frequency of 3.5×10^{-6} for INH and 3.1×10^{-8} for RIF), and these mutations account for most resistance observed with the clinical isolates (Dooley & Simone, 1994). Due to the fact that the respective gene locations associated with resistance to different drugs are not joined together, the probability of a simultaneous spontaneous mutation is extremely low: 9×10^{-14} for both INH and RIF (Sandgren et al., 2009). Mutations that occur throughout the *pncA* gene have also been shown to correlate closely with phenotypic PZA resistance (Barco et al., 2006). Besides, drugs such as STR and other second-line agents have far less resistant mutations within the drug-resistant population (Ramaswamy & Musser, 1998).

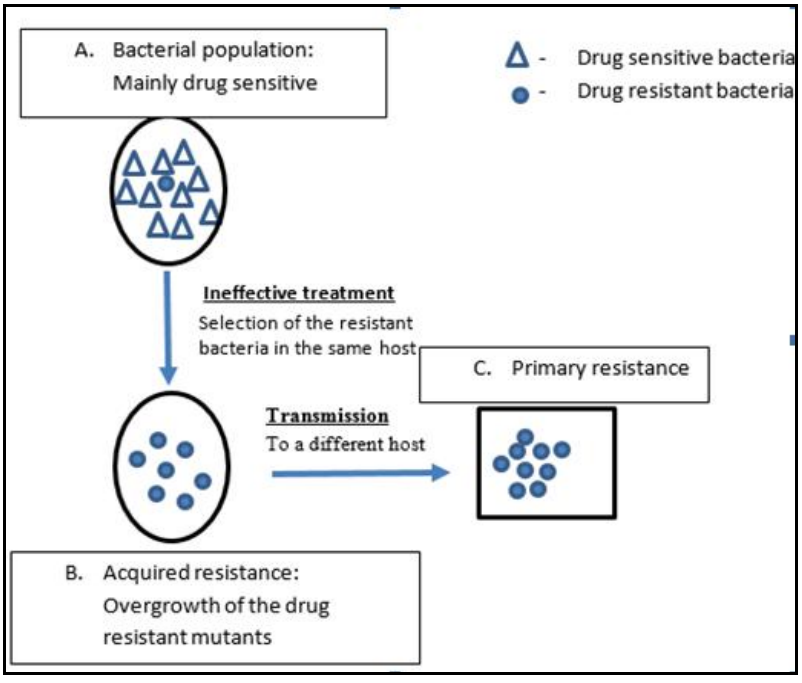

Figure 1-15 Acquired resistance versus Primary resistance in TB. (Adopted and modified from Zhang et al., 2007).

1.4.2. New anti-TB drug development

A number of clearly defined criteria are considered in developing new drug candidates for TB, of which a validated safety profile forms a critical aspect. Besides, the new drug should exhibit a superior potency in comparison with the existing drugs in order to shorten the duration of treatment; should potentially inhibit novel targets to successfully overcome MDR and XDR-TB; should allow for the concomitant administration with ART as many TB patients are co-infected with HIV; and should not have antagonistic effects with existing anti-TB drugs or those under development so that a regimen of three drugs or more can be administered (Global Alliance for TB Drug Development, 2001; Cole & Riccardi, 2011; Koul et al., 2011).

After about five decades of very limited activity in the field of anti-TB drug development, much more progress has been made in the very recent past. This has resulted in the emergence of a TB drug pipeline with promising drug candidates **(Figure 1-16)**. However, due to the high attrition rate of drug candidates during clinical development and new cases of drug resistance, the discovery of new lead molecules is without a doubt needed (Pethe et al., 2013). In this drug pipeline, it can be seen that many drug candidates are in lead optimization, preclinical development, as well as phase 2 and phase 3 clinical studies. However, phase 1 needs urgent attention in order to ensure a constant delivery of molecules in case of failure of advanced drug candidates. **Figure 1-17** shows the chemical structures of some of the current anti-TB drug candidates.

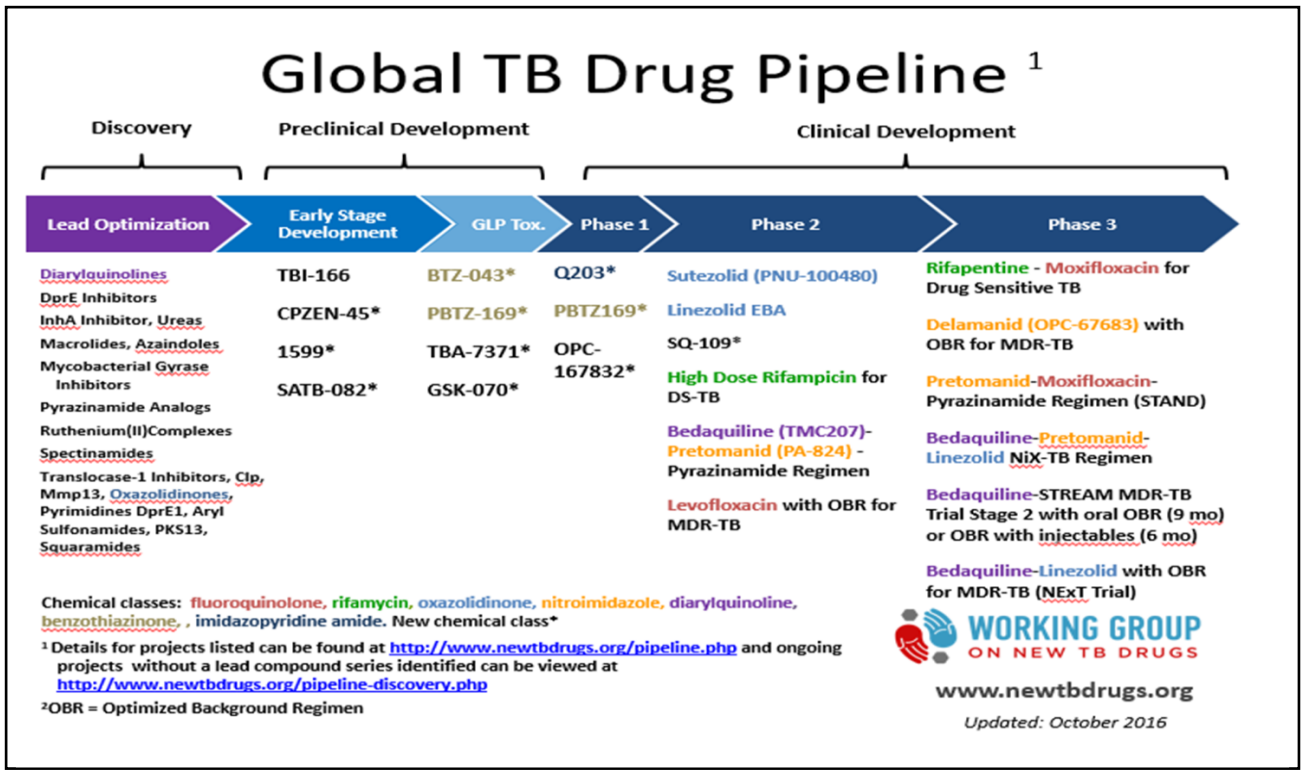

Figure 1-16 Current global drug pipeline (modified by www.newtbdrugs.org) updated October, 2016.

BDQ (Andries et al., 2005). PBTZ-169 (Makarov et al., 2009), and imidazopyridine amide Q-203 (Pethe et al., 2013), were identified through phenotypic screening of compounds against *M. tuberculosis.* SQ109, a 1, 2-ethylenediamine {N0-(2-adamantyl)-N-[(2E)-3, 7-dimethylocta-2, 6-dienyl] ethane-1, 2-diamine} was designed around the active 1, 2-ethylenediamine pharmacophore of EMB. It targets MmpL3, a member of the MmpL (*M*ycobacterial *m*embrane *p*rotein, *L*arge) family, in *M. tuberculosis* (Tahlan et al., 2012). MmpL3 is required for the transportation of mycolic acids, in the form of trehalose monomycolates (TMM), into the *M. tuberculosis* cell wall (Tahlan et al., 2012). It also plays an important role in haem uptake by helping in the acquisition of iron for mycobacterial survival. Therefore, MmpL3 is considered an attractive target for anti-TB drug discovery since it is the

only protein in this family, essential for the survival of *M. tuberculosis* (Nguta et al., 2015). In addition, recent results by Li *et al* showed the synergy potential of MmpL3 inhibitors with two different chemotypes, indolcarboxamides and adamantyl ureas. These inhibitors demonstrated synergistic interactions with RIF, BDQ, clofazimine and ß-lactams (Li et al., 2017). SQ109 possesses polypharmacological properties; exhibiting activity in bacteria and fungi that do not have mycolic acids (Biava et al., 2007). Delamanid (OPC-67683) and pretomanid (PA-824) are two new imidazooxazole-based prodrugs. They are activated intracellularly by Rv3547, a deazaflavin-dependent nitroreductase (Ddn) present in *M. tuberculosis*. The des-nitroimidazole metabolite was identified as the active form of PA-824. This molecule releases reactive nitrogen species, such as nitric oxide, leading to respiratory poisoning (Singh et al., 2008). Delamanid, on the other hand, inhibits mycolic acid biosynthesis and has shown potent *in vitro* and *in vivo* activity against MDR strains (Gler et al., 2012). Rifapentine (RFP), a semi-synthetic cyclopentyl rifamycin derivative, acts by binding the ß subunit of the RNA polymerase in *M. tuberculosis*, a similar mechanism utilized by RIF (Munsiff, Kambili & Ahuja,

2006)

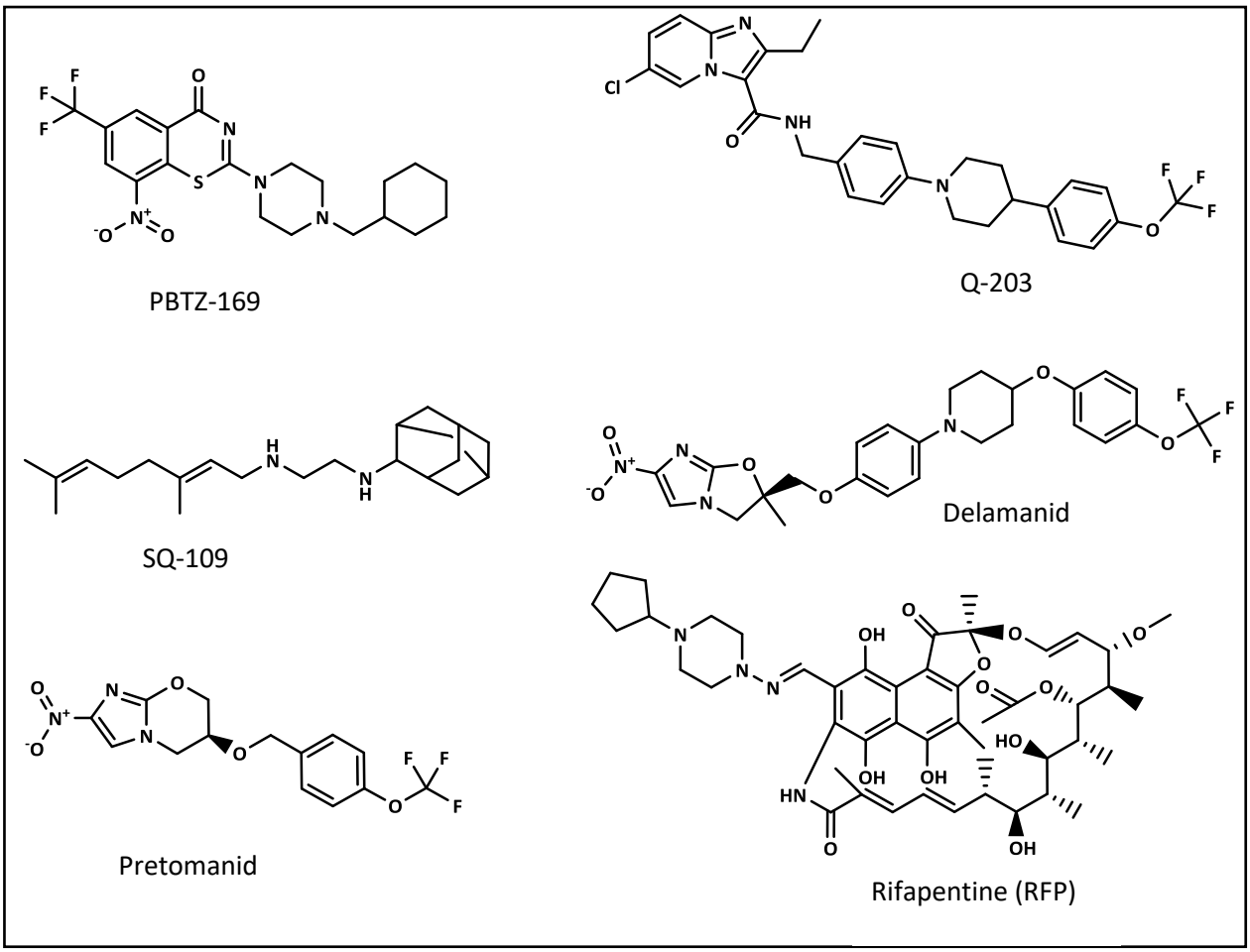

Figure 1-17 Anti-TB drug candidates

RFP is effective against both active and latent TB but shows cross-resistance with RIF (Pethe et al., 2013). Moreover, RFP is not recommended for use in patients infected with HIV owing to the high risk of developing RIF resistance. Q-203, an optimized imidazopyridine amide (IPA), blocks *M. tuberculosis* growth by interfering with cytochrome oxidase bc_1 complex, a component of respiratory electron chain, required for maintaining a proton gradient and ATP synthesis (Zumla, Nahid & Cole, 2013; Pethe et al., 2013). Despite the fact that both BDQ and Q-203 act on the respiratory chain of *M. tuberculosis,* the latter is more potent in ATP synthesis inhibition (Pethe et al., 2013) PBTZ-169, which is at the pre-clinical development stage of the drug pipeline, inhibits the enzyme decaprenylphosphoryl-β-

D-ribose 2´ epimerase (DprE1) (Merle et al., 2014), an oxidase involved in the biosynthesis of decaprenylphosphoryl-D-arabinose (DPA), which is a key precursor in the biosynthesis of the cell wall arabinans (Merle et al., 2014; Ribeiro et al., 2011). The mechanism of action of PBTZ-169 is similar to other benzothiazones, as it involves activation of an aromatic nitro group. The nitro group is required for activity conjointly with a *meta* electron-withdrawing group such as a trifluoromethyl or another nitro dinitrobenzenes **(Figure 1-18)** (Hoagland, Zhao & E Lee, 2016). The nitroaromatic group is selectively reduced to a corresponding reactive nitrosoarene. The nitroso group further reacts with the cysteine residue in the DprE1 enzyme to form a covalent bond between the two species and consequently inactivating the enzyme (Trefzer et al., 2010). Inhibition of this enzyme leads to cell lysis and bacterial death (Merle et al., 2014). Notably, the reductive metabolism in humans is not capable of activating PBTZ-169 or its related chemical series, thus providing an appropriate safety margin as confirmed by a negative Ames test for DNA mutagenesis (Hoagland, Zhao & E Lee, 2016).

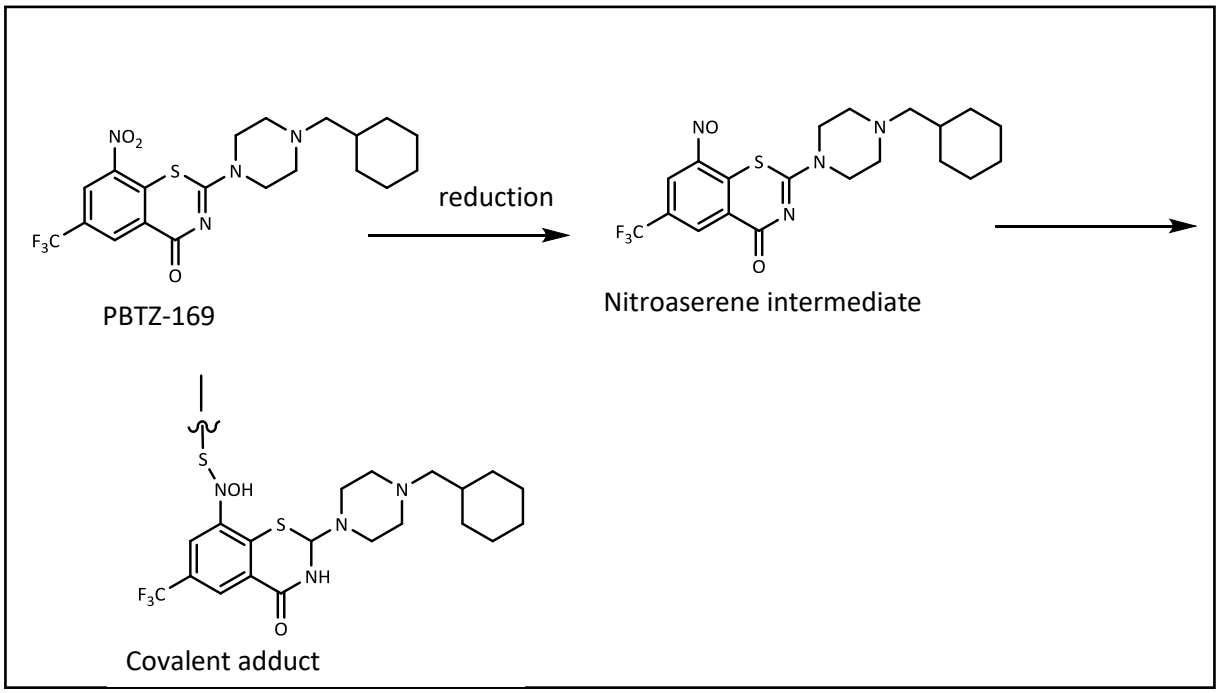

Figure 1-18 PBTZ -169 with the covalent inhibition mechanism of DprE1 (Hoagland, Zhao & Lee, 2016).

1.4.3. Repurposed drugs for TB treatment

The development of new drugs is onerous, costly and often time-consuming (Scannell et al., 2012). Moreover, besides efficacy, most of the compounds fail to progress to approval due to toxicity-related concerns (DiMasi et al., 2010). In order to overcome these bottlenecks, drug repurposing and/or repositioning have become attractive strategies (Strittmatter, 2014). *Drug repurposing* refers to the process of finding new use for existing, approved drugs (Strittmatter, 2014). On the other hand, *drug repositioning* involves carrying out structure modifications of an existing drug, abandoned or shelved compounds and candidates under development, for a new indication (Nzila, Ma & Chibale, 2011; Naylor, 2015).

There are several strategies that have been employed to identify drugs with the potential for new uses. The unintended second benefit may manifest as a result of clinical observation in one group, as observed with the treatment using clofazimine (CFZ; **Figure 1-20**) (O'Donnell, Padayatchi & Metcalfe, 2016). CFZ, is a highly lipophilic drug that readily gets into the fatty tissues with and is taken up by human mononuclear phagocytes, the cells affected with *M. tuberculosis*. In addition, a compound may target a condition, different from the one originally intended. For example, the compound AZD0530 targets tyrosine-protein kinase Fyn, encoded by the *fyn* gene in humans. AZD05030 may therefore be broadly utilized to target tyrosine-protein kinase Fyn, an enzyme that is key to the mechanism of Alzheimer's disease and in the proliferation of tumour cells (Nygaard, van Dyck & Strittmatter, 2014). A compound may also act on a novel target associated with various disease states (Strittmatter, 2014). The following drugs have been repurposed:

Fluoroquinolones: These drugs have been used widely since they possess a broad-spectrum antibiotic action and are quite potent (Zumla, Nahid & Cole, 2013). They act by inhibiting the

enzymes topoisomerase II and IV, thereby interfering with DNA replication (Drlica & Zhao, 1997). Examples include MXF and GAT **(Figure 1-4)**, which exhibit bactericidal properties against *M. tuberculosis* both *in vitro* and *in vivo* (Gillespie & Billington, 1999; Miyazaki et al., 1999). They are already used as second-line treatment for TB (Moadebi et al., 2007).

Oxazolidinones: These are exemplified by linezolid (LZD), sutezolid and AZD5847, **(Figure 1-19)**. LZD has originally been used for indications caused by Gram-positive bacteria such as skin infections and the hospital-acquired pneumonia (HAP) (Leach et al., 2011). In addition, LZD was reported to exhibit anti-TB properties and favourable clinical efficacy (Fortun et al., 2005; Yang et al., 2012). It inhibits protein synthesis by binding to the P site of the 50S ribosomal subunit **(Figure 1-7)**. Mutations at the 23S rRNA made possible the identification of a peptidyl transfer centre as the exact site of action (Kloss et al., 1999). Besides the *in vitro* and *in vivo* activity of LZD against *M. tuberculosis* (Ashtekar et al., 1991), other studies have shown that it exhibits a synergistic interaction with RIF in drug-susceptible *M. tuberculosis* strains, suggesting the potential to control selection of resistant mutants (Zurenko et al., 1996; Cynamon et al., 1999). Supported by these studies, LZD was used on a controlled number of TB patients to evaluate its efficacy and tolerability after long-term use. Results showed that, while LZD was effective in treating MDR-TB patients, its prolonged use was associated with toxicity causing anaemia and peripheral neuropathy (Ntziora & Falagas, 2007). However, the proven efficacy of LZD in treating MDR-TB cases has occasioned other investigations with sutezolid and AZD5847, belonging to a class of second-generation oxazolidinones with greater selectivity on *M. tuberculosis* and fewer side effects (Hoagland, Zhao & E Lee, 2016).

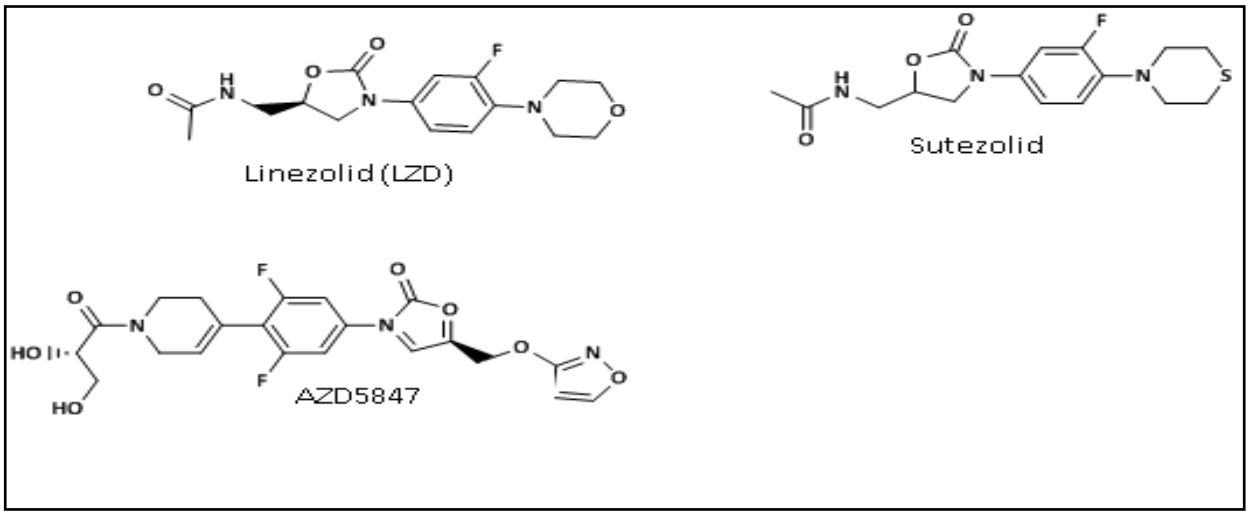

Figure 1-19 Oxazolidinone class of compounds

Riminophenazines: These are exemplified by **CFZ. (Figure 1-20)**, a lipophilic drug used for the treatment of leprosy. This drug may play a major role in the treatment of MDR-TB (Barry et al., 1957; Dey et al., 2013). Based on limited studies, and due to a shortage of therapeutic alternatives when dealing with more severe cases of drug resistant TB, CFZ is now included in group 5 of WHO's third-line drugs for MDR-TB (Cholo et al., 2012). The exact mode of action of CFZ is not completely known but recent studies have suggested the outer membrane as a possible target (Cholo et al., 2012).

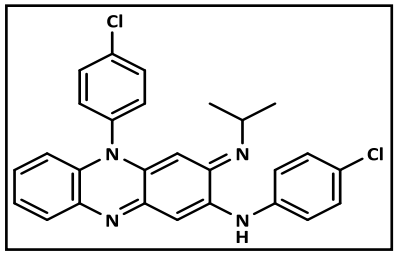

Figure 1-20 Clofazimine (CFZ)

In a different study, it was shown that NADH dehydrogenase in *M. tuberculosis* reduces CFZ and, after spontaneous reoxidation, subsequently releases levels of reactive oxygen species

(ROS) that are bactericidal (Yano et al., 2011). Hartkoon *et al.* reported that gene mutations in Rv0678, a transcriptional regulator, was associated with the up regulation of the multisubstrate efflux pump; MmpL5. These not only caused resistance to CFZ but also BDQ (Hartkoorn, Uplekar & Cole, 2014).

β lactams: Are a populous class of antibiotics **(Figure 1-21)**. Besides, they also form the mainstay of most of the antibacterial drug treatment regimens. Yet, the efficacy of β-lactams against *M. tuberculosis* has traditionally been considered very limited (Hoagland, Zhao & E Lee, 2016). Members of this class of antibiotics act by inhibiting membrane-bound transpeptidases, which play an important role in crosslinking the peptidoglycan layer of the cell wall (Hugonnet & Blanchard, 2007). Apart from its thick impermeable cell wall, *M. tuberculosis* has a highly active ß-lactamase enzyme, BlaC, which makes it inherently resistant to ß-lactam antibiotics (Hugonnet & Blanchard, 2007). Carbapenems, however, have so far been successful against *M. tuberculosis* since they interact with the penicilin binding proteins that have a high-molecular-weight. In addition, they inactivate the

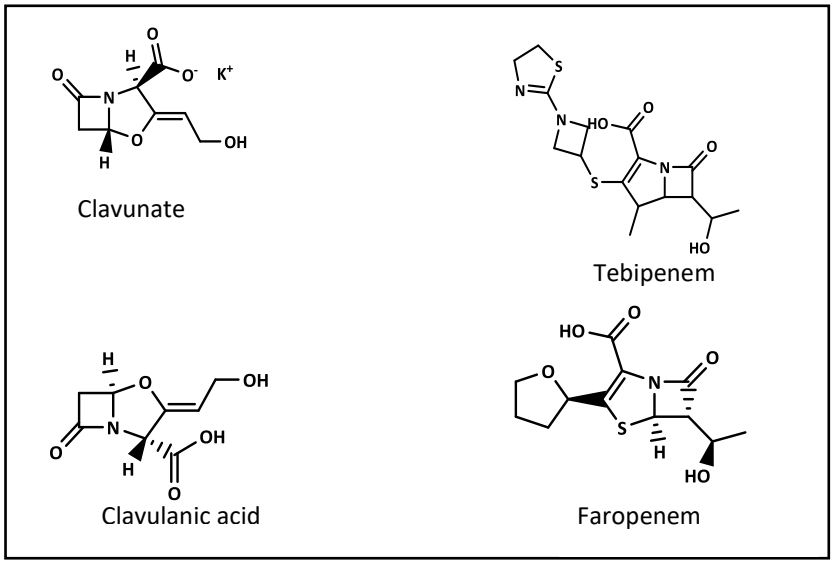

Figure 1-21 ß-lactams

L,D-transpeptidases that form the 3→3 crosslinks existing in the unique *M. tuberculosis* cell wall (Dubee et al., 2012). Carbapenems are also less favourable substrates for BlaC, which is expressed at high levels thereby inactivating most other ß-lactams. The combination of ß-lactamase inhibitor,clavulanate, with carbapenems displayed activity against *M. tuberculosis* i*n vitro* and in a murine model (England et al., 2012). Moreover, a case study showed that this drug combination was effective in treating six immunocompromised patients with XDR-TB infection (Payen et al., 2012). The ß-lactam tebipenem, originally developed to treat otolaryngoligical and respiratory infections in pediatrics, has been identified to be the most potent anti-TB oral carbapenem when combined with clavulanic acid (Horita et al., 2014). Structural modification of the carbapenem resulted in faropenem, a penem with a slightly less strained ring system and, consequently, improved chemical stability (Milazzo et al., 2003). Its prodrug ester, faropenem medoxomil, allows for oral administration, a desirable property in MDR-TB treatment (Milazzo et al., 2003; Schurek et al., 2007).

1.4.4. Fusidic acid/and or its derivatives as potential anti-TB agent(s).

FSA, a hydrophobic, narrow spectrum antibiotic was first isolated from the fungus *Fusidium coccineum* by Godtfredsen *et al.* in 1962 and developed for clinical use by Leo laboratories in Ballerup, Denmark (Godtfredsen & Vangedal, 1962). This drug, possess antibacterial activity against Gram-positive bacteria (Collignon & Turnidge, 1999; Hoffner et al., 1990), and is licensed for use as its sodium salt *sodium fusidate*. It is approved for use under prescription in South Korea, Japan, UK, Canada, Europe, Australia, New Zealand, Thailand, India and Taiwan. FSA inhibits bacterial replication and does not kill the bacteria, and is therefore termed *bacteriostatic*. However, at high concentrations between 2 to 32-fold higher than the MIC, it shows bactericidal tendency (Verbist, 1990).

It has a steroidal-like structure − bearing a well defined tetracycline ring, even though they differ from each other in the sterical conformation around the hexamer ring – 6

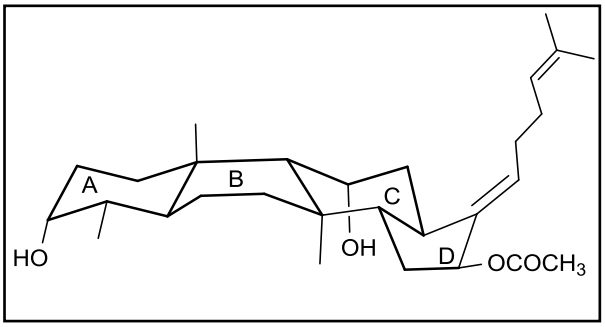

Figure 1-22 Trans-syn-trans arrangement of cyclopentanoperhydrophenanthrene ring system

membered carbon ring. Unlike tetracyclic triterpenes and sterols, fusidic acid has an unusual stereochemistry of the cyclopentanoperhydrophenanthrene ring system. Rings A, B and C are arranged in trans-syn-trans manner in contrast to usual trans-anti-trans arrangement in tetracyclic triterpenes and sterols. This unusual trans-syn-trans arrangement forces ring B to have a boat conformation (**Figure1-22**) (Godtfredsen et al., 1966). Thus, FSA and other fusidane antibiotics, assume a chair-boat-chair conformation which is essential for their function (Duvold et al., 2001). It is a weak acid (pKa of 5.7) and is mostly ionized in plasma and tissue at the physiological pH of 7.4

FSA is mainly used against staphylococci, including strains resistant to other antibiotics (Collignon & Turnidge, 1999). It is primarily used in the treatment of skin and eye infections. Occasionally, it is used systemically to treat bone and joint infections and septicaemia (Atkins & Gottlieb, 1999; Darley & MacGowan, 2004). Moreover, FSA has exhibited efficacy against other pathogens such as *Norcadia* sp. (Black & McNellis, 1970), *Actinomyces* and *Clostridia* spp. (Von Daehne, Godtfredsen & Rasmussen, 1979). The potential of FSA's therapeutic utility is demonstrated by its excellent tissue distribution, absence of known allergy, low toxicity as well as the nonexistence of clinically relevant cross

resistance with any of the commonly used antibiotics (Christiansen, 1999; Turnidge & Collignon, 1999). It distributes well into all human body compartments except the cerebrospinal fluid (Taburet et al., 1990), has a half-life of approximately 10 h, and exhibits minimal host toxicity (Reeves, 1987).

While FSA is the only fusidane antibiotic in clinical use, a number of steroid-like antibiotics from natural products have been identified (Chain et al., 1943). Ramycin, an antibiotic isolated from *Mucor ramannianus* (Vanderhaeghe, Van Dijck & De Somer, 1965), and helvolic acid, isolated from *Aspergillus fumigatus* and *Cephalosporium caerulens* (Okuda et al., 1964) (**Figure 1-24**) are examples of naturally occurring fusidanes with identical chemical structures to FSA. The other steroid-like related antibiotic is cephalosporin P1 produced by *Cephalosporium acremonium* (Von Daehne, Godtfredsen & Rasmussen, 1979)

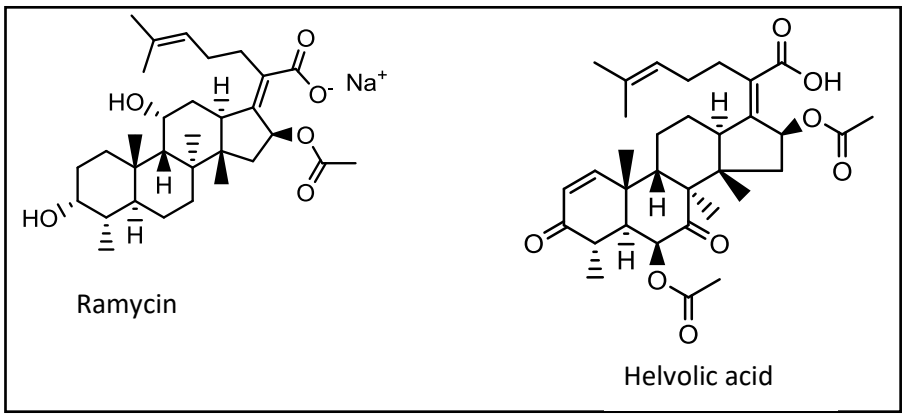

Figure 1-23 Examples of fusidanes

As already mentioned, FSA targets elongation factor G (EF-G) thereby inhibiting peptide elongation in the ribosome and the process of ribosome recycling (**Figure 1-7**). It stalls the ribosome in complex with EF-G and GDP (Turnidge & Collignon, 1999). Studies have shown that FSA has a low affinity for unbound EF-G but forms a strong complex when EF-G is bound to the ribosome (Okura, Kinoshita & Tanaka, 1971; Willie et al., 1975a). EF-

G has a dual role in bacterial protein synthesis in that it (1) catalyses mRNA translocation during the peptide elongation cycle, and (2) in conjunction with the ribosome recycling factor, speeds the dissociation of the ribosomal sub-units after a round of protein synthesis termination (Hirashima & Kaji, 1973) for the start of a new round of mRNA translation (Karimi et al., 1999). Thus, FSA inhibits both peptide elongation and ribosome recycling (Hoffner et al., 1996; Savelsbergh, Rodnina & Wintermeyer, 2009).

M. tuberculosis is susceptible to FSA. A previous study reported a MIC against *M. tuberculosis* of 16 to 64 µg/ml (Collignon & Turnidge, 1999). In another study that utilized the *in vitro* agar proportion method, 64 strains of *M. tuberculosis* were tested and the activity of FSA was reported at 16 µg/ml. Moreover, a study that investigated 30 *M. tuberculosis* strains (11 of them resistant to first-line drugs), the activity of FSA was below 32 µg/ml for all except three strains in which it was 64 µg/ml (Cicek-Saydam et al., 2001). Yet, another study involving FSA, was performed *in vitro* against 170 clinical isolates of *M. tuberculosis* using a proportion dilution method. This study revealed that nineteen isolates were resistant to at least one first-line anti-tuberculosis drug. A total of 1.8% of the isolates was resistant to FSA. In addition, no cross-resistance was found between first-line drugs and FSA (Cicek-Saydam et al., 2001)

When compared to other antibiotic classes, not much has been studied on the mechanisms and genetics of resistance to FSA (Turnidge & Collignon, 1999). Turnidge and Collignon (Turnidge & Collignon, 1999) have, however, shown that the FSA resistant mutants could readily be selected from an initial high inoculum. in *Staphylococcus aureus*. Furthermore, the entire bacterial populations revealed a spontaneous single-step chromosomal mutations were in *fusA*, the gene coding for EF-G, at a rate of 1 in 10^6 - 10^8

cell divisions. This occurs even for the isolates from individuals previously not exposed to FSA (Turnidge & Collignon, 1999). Chopra first showed that resistant mutants of *Staphylococcus aureus* selected on FSA-containing media had altered EF-G (Chopra, 1976). Moreover, altered EF-G has been shown in Gram-negative bacteria, which give MICs much greater than the wild type strains (Dahlfors & Kurland, 1990). In *Salmonella typhimurium*, altered EF-G has been reported to be caused by mutations in three specific regions of *fusA*, which encodes EF-G (Johanson & Hughes, 1994). A single mutation, F88L, has been identified as responsible for strong FSA resistance in *S. aureus* clinical isolates (Nagaev et al., 2001). This F88L mutation matches with the F90L mutation in *Thermus thermophiles* which also confers FSA resistance (Martemyanov et al., 2001). Studies have shown that the loss in fitness associated with FSA resistance is compensated by secondary mutations (Koripella et al., 2012). By characterizing three *S. aureus* EF-G mutants, Koripella *et al* reported that fitness defects in FSA-resistant mutants led to a significantly slower tRNA translocation and ribosome recycling. There was also an increase in peptidyl-tRNA drop off. The F88L mutant protein exhibited this defective function, whereas M16I showed high activity and hypersensitivity to FSA. Therefore, a direct correlation between fitness, caused by EF-G translocation and recycling, and FSA sensitivity was demonstrated (Koripella et al., 2012). Resistance to FSA may also arise due to plasmid-mediated alterations in cell wall/membrane permeability. The type I chloramphenicol acetyltransferase (CAT-I), found in Enterobacteriaceae, can also inactivate FSA by competitively binding the drug and sequestering it (Marcoli, Iida & Bickle, 1980; Turnidge & Collignon, 1999).

Finally, although very limited data have been published on FSA combination studies, Phee, *et al.* reported robust synergy between FSA and colistin against a panel of multidrug-resistant *Acinetobacter baumannii* clinical strains including some colistin-resistant strains.

Here, synergy was evaluated *in vitro* against 11 multidrug-resistant *A. Baumannii* isolates. Synergy was demonstrated against all strains, with an average fractional inhibitory concentration index (FICI) of 0.064. Furthermore, time-kill assays showed that colistin-FSA was synergistic and rapidly bactericidal, including against colistin-resistant strains (Phee et al., 2015). Myint *et al*. also reported the synergistic interaction between FSA and the phytochemical tannic acid, against the three clinical strains of methicilin-resistant *S. aureus* Moreover, the possible mechanism could be as a result of the phytochemical tannic acid potentiating the effect of FSA and/ or acting as alternative target that results in the lysis of bacteria (Myint, Sing & Wei, 2013). In mycobacteria, Hoffner *et al* reported synergistic interactions with EMB. Out of the 17 *Mycobacterium avium* complex strains studied, a combination of FSA and EMB exhibited synergistic effects against 11 strains (Hoffner et al., 1990) In addition, Ramon-Garcia and co-workers reported the combination between FSA and SPC as synergistic, FICI value = 0.25, against *M. smegmatis* (Ramon-Garcia et al., 2011).

In summary, the *in vitro* effect exhibited by FSA against *M. tuberculosis*, its unique mechanism of action─ specifically, inhibition of bacterial protein synthesis by binding to EF-G, the antimicrobial-potentiating effect with other antibiotics including the anti-TB drug, EMB, as well as lack of cross-resistance to other antimicrobial classes inspired its choice as a classic repurposing agent for the synergistic drug interaction study against both wild-type and multidrug- resistant strains of *M. tuberculosis*. This work, therefore, fits as part of a larger project that explores the activity of FSA and/ or analogues in an effort to identify potential anti-tuberculosis drugs.

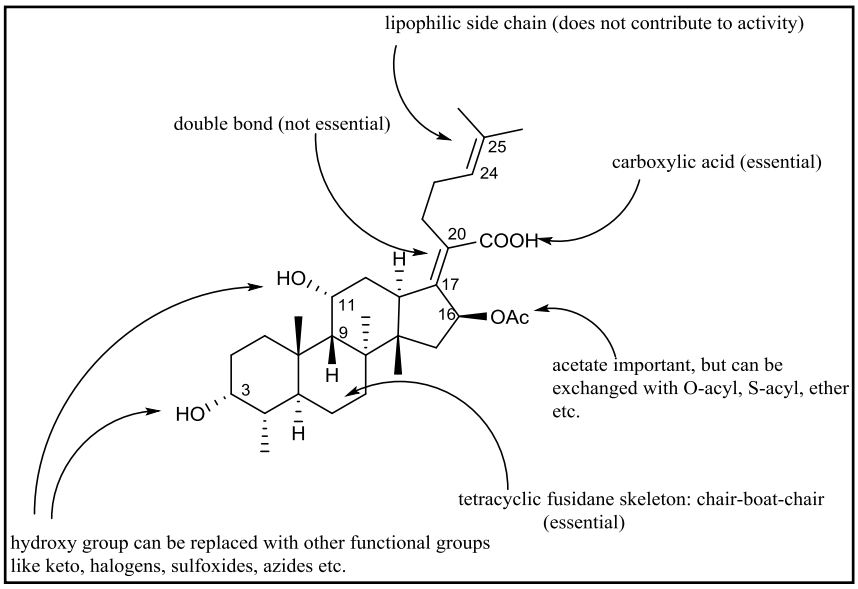

Figure 1-24 An overview of structure activity relationships of fusidic acids showing important and essential structural and functional features. (Adopted from Duvold, Tore 2001).

FSA analogues

Drug repositioning (**see section 1.4.3**) has continued to play a key role in drug discovery. This strategy has resulted in analogues with one or several characteristics separating them from their progenitors; improved *in vitro* or *in vivo* efficacies, no cross resistance with earlier antibiotics or a wide-spectrum of bacteria that are susceptible to the new molecule (Rolinson, 1998). The structure-activity relationships of FSA has extensively been studied and large number of FSA analogues synthesised (Von Daehne, Godtfredsen & Rasmussen, 1979; Duvold et al., 2001). However, only a few of these analogues have exhibited activities comparable with that of FSA . Most of these have similar antibacterial spectrum and are cross-resistant (Duvold et al., 2001). Four stereoisomers were prepared by reducing the double bond between C-17 and C-20 to explore the side chain which had not been previously explored. It was found that one stereoisomer (17*S*,20*S*), **Figure 1-25** was equipotent to FSA out of four

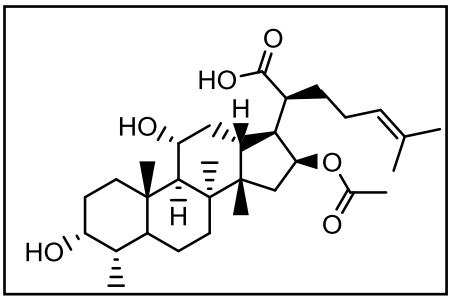

Figure 1-25 17*S,*20*S*-dihydrofusidic acid

stereoisomers (17*R*,20*S*), (17*R*,20*R*), (17*S*,20*S*), (17*S*,20*R*) while others had low or no antibacterial activity when compared to FSA. Yet, an interaction study of the antibiotic [^{3} H]-24,25-dihydrofusidic acid, an active analog of FSA , with the ribosome . EFG . GDP complex revealed the following (Willie et al., 1975b). (1) All components of the complex are essential for the [^{3} H]-24,25-dihydrofusidic acid binding, (2) the $C_{17\text{-}20}$ double bond of fusidic acid was critical for both binding and complex stabilization activitities. (3) Modifications of other functional groups in the molecule could result in a significant decreased stabilization of the ternary ribosome complex and /or ability to compete with the [^{3} H]-24,25-dihydrofusidic acid for binding to the complex, but do not demonstrate absolute structural requirements for either activity.

1.5. Antimicrobials and combination strategies

Increased knowledge of the biology of a disease as a perturbed system comprising a network of molecular pathways that are more susceptible to simultaneous action of several drugs provides scope for rational development of combination therapies (Smalley et al., 2006; Podolsky & Greene, 2011). Various factors can explain why a drug combination may have a particular effect. Key to this is the molecular interaction profiles of the constituent drugs, which describe their individual interactions with biomolecules, pathways or processes (Jia et

al., 2009). Other factors include genetic variations (Kim & Fay, 2007), environmental factors (Carvalho-Netto et al., 2006), host behaviour (Yang et al., 2012) and drug scheduling (Tabernero et al., 2008). Drug combinations are considered pharmacodynamically synergistic, additive or antagonistic if the elicited effect is greater than, equal to, or less than their summed effects (Chou, 2006). Coalistic combination occurs when all drugs involved are inactive individually but become active when combined (Greco, Bravo & Parsons, 1995). This kind of interaction may result, for example, when the expression of a target gene requires that two transcription factors each need to bind, with each constituent intervention activating one transcription factor only (Jia et al., 2009).

Synergistic drug combinations have been utilized to achieve one or more of the following desirable outcomes: shortened therapeutic duration, decreased dosage at equal or increased efficacy, reduced or delayed development of drug resistance, and simultaneous enhancement of therapeutic actions as well as reduction of unwanted action (Kitano, 2007; Zimmermann, Lehar & Keith, 2007). Bhusal *et al* reported the use of a three-dimensional checkerboard assay to quantitatively determine antimycobacterial synergy. In addition, using this assay, they showed that fluoroquinolones and antibacterial agents such as CLR are effective against multidrug-resistant isolates of *M. tuberculosis* when combined with RIF and INH (Bhusal, Shiohira & Yamane, 2005). In addition, Chen and co-workers employed an invitro BACTEC 460 system, that evaluated drug interactions based on the quotient values that were derived numerically from the growth indices of cultures treated with a single antibiotic or combination treatment with two antibiotics (Chen, 2006). These results suggested that SQ109 at 0.5 of its MIC demonstrated strong synergistic activity with 0.5 MIC INH and as low as 0.1 MIC RIF in inhibition of *M. tuberculosis* growth (Chen, 2006). Rodriguez *et al.*, also reported on the *in vitro* activity against *M. tuberculosis* of the

combination of fluoroquinolones and LZD with classical drugs. The combination of INH with fluoroquinolones had synergic activity in nine of the ten INH-susceptible strains. Furthermore, they reported synergism between RIF and LZD in five of the 15 strains susceptible to RIF (Díaz, Juan Carlos Rodriguez 2003)

1.5.1. *In vitro* combination testing techniques

There are different methods which have been developed to determine the *in vitro* activities of drug combinations against bacteria (Kurien & Lorian, 1980). These include the checkerboard technique, and serial broth dilutions of fixed proportions of the combined drugs (Garrod & Waterworth, 1962) Other methods include time-kill assays with the broth media, agar dilution method, paper-strip and double-disk agar diffusion with agar media (Hartkoorn et al., 2014; Willie et al., 1975). Checkerboard and time-kill assays have been reliably used in most antimicrobial experiments (Odds, 2003).

(i) Checkerboard assays

The checkerboard method is normally carried out in microtitre culture plates. In a standard two-drug combination, the first drug (drug A) is serially diluted along the ordinate and the second drug (drug B) along the abscissa. The result is that each well in the plate contains a unique combination of the two drugs being tested. The effect resulting from the combination of the two drugs is interpreted using the fractional inhibitory concentration index (FICI). This is defined as the sum of the fractional inhibitory concentration (FIC) of drug A (FIC_A) + FIC of drug B (FIC_B), where FIC_A is the minimum inhibitory concentration (MIC_{90}) of drug A in the combination ($MIC_{A(comb)}$) as a proportion of the MIC of drug A alone (MIC_A), and the FIC_B is $MIC_{B(comb)}$)/ (MIC_B). A FICI $\leq$ 0.5 is interpreted as synergistic, FICI > 0.5 but $\leq$ 4 is

considered as no interaction, and a FICI > 4 is designated as antagonistic (Odds, 2003; Johnson et al., 2004). In order to perform combinations of three antibiotics, a standard checkerboard titration of the two agents was adopted and modified (Bhusal, Shiohira & Yamane, 2005; Berenbaum, 1978). Herein, the third antibiotic was dispensed throughout the wells as an overlay at subinhibitory concentrations and synergistic interactions analyzed as already described with the two-drug combinations

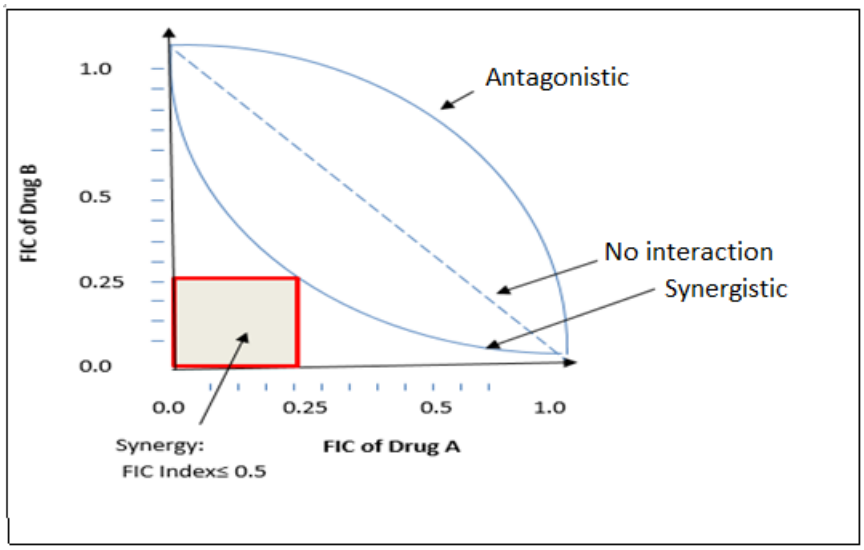

Figure 1-26 Isoboles for synergistic, antagonistic or no interaction. (Adopted and modified from Cuenca-Estrella, 2004).

Isobolograms have been used for the evaluation of drug interaction effects (Loewe, 1953). The calculated FICs, from the experimental data for agents used alone and in combination at equi-effective level, are plotted as shown in **Figure 1-26**. A combination is said to have no interaction if the data points are on the straight line connecting the FICs of drugs A and B at the X - and Y-axis intersections, respectively (Sühnel, 1990). Points below this line indicate synergy, while those above the line indicate an antagonistic interaction (Sühnel, 1990).

(ii)Time-kill curves

The checkerboard assay is relatively easy to perform but provides only the inhibition data. In contrast, time-kill curves are more dynamic and provide a measure of bactericidal activity (Mueller, de la Pena & Derendorf, 2004). However, limited concentrations can be tested at a given time owing to the number of tubes required. Therefore, a prior knowledge of test concentrations is necessary (Lorian, 2005). In time-kill assays, flasks containing broth media are inoculated with about 10^5 -10^6 colony-forming units (CFU/ml) of the test organism. Antibiotics are added to the flasks alone and in combination at relevant concentrations. The flasks are incubated and samples removed at set time intervals to determine the number of viable bacteria. Synergism is defined as $\geq 2\log_{10}$ decrease in colony count of the combination compared with that of the more active drug tested alone, and as $\geq 2\log_{10}$ decrease in colony count below the starting inoculum. A $< 2\log_{10}$ change (increase or decrease) in colony count compared to that of the most active drug tested alone is interpreted as no change or indifference, whereas $\geq 2\log_{10}$ increase in colony count compared with that of the most active drug tested alone shows antagonism (Entenza & Moreillon, 2009).

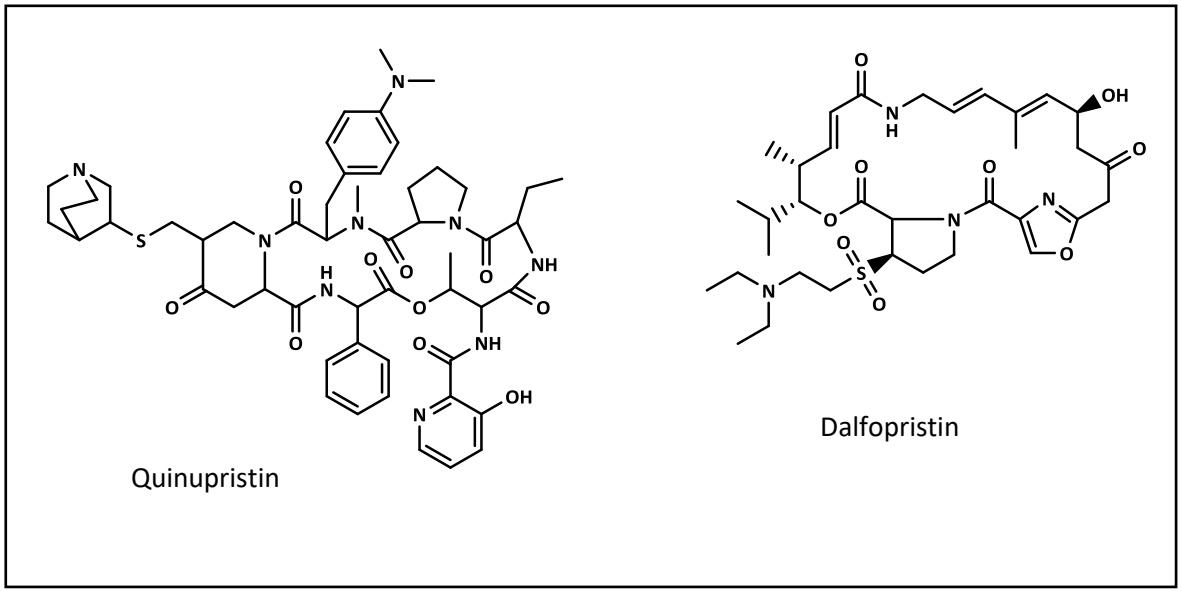

Figure 1-27 Quinupristin and Dalfopristin

1.5.2. Drug combinations: interaction mechanisms and selection against resistance

Drug combination studies may reveal different mechanisms that result in synergism against bacteria. It is therefore important to characterize the underlying mechanisms of drug interactions, which are still largely unknown. In many cases, the individual modes of action (MOAs) of each drug cannot explain observed drug interactions in an obvious way (Ankomah, Johnson & Levin, 2013). Drug interactions leading to synergy can be as a result of a simple uptake effect, in the sense that an increase in permeability by one drug may cause accumulation of the other, hence synergy. Such an uptake effect has been shown with interactions between aminoglycosides and ß-lactam antibiotics (Plotz & Davis, 1962). In their study, Plotz and Davis showed that synergism of PEN with STR ensue from cell membrane damage by PEN resulting in further destruction by STR. This effect promotes subsequent access of PEN to intracellular sites (Plotz & Davis, 1962). Drug interactions can also result from direct physical interactions between the drugs at their target— a mechanism that has been observed for the antibiotics quinupristin and dalfopristin, **(Figure 1-27)** which bind to

the ribosome at different sites and jointly stabilize their binding (Yonath, 2005). The interaction between these two drugs reveals a unique bactericidal mechanism of action (Vannuffel & Cocito, 1996). Dalfopristin, an olefinic macrolactone, binds to the 50S subunit of the prokaryotic ribosome. This results into (i) inactivation of the donor and acceptor sites due to interference with the peptidyl tranferase enzyme, and (ii) change in ribosome conformation, leading to an increase in the affinity of quinipristin, a peptidic macrolactone, which also binds to the 50S subunit. Quinipristin binding halts peptide chain elongation. The action of both of these drugs together permanently halts protein synthesis, leading to a synergistic and bactericidal activity, which is concentration-independent. In contrast, their action individually only causes a transient halt in protein synthesis, consequently resulting in a bacteriostatic effect (Cocito et al., 1997; Porse & Garrett, 1999).

Interactions between bactericidal and bacteriostatic antibiotics have long been theorized to be generally antagonistic since killing by bactericidal antibiotics often requires cell growth, which is prevented by bacteriostatic drugs (Jewetz et al., 1952). There are other drug interactions that have more complex causes when the drugs perturb cell physiology and cause cellular responses subsequently affecting the activity of other drugs. (Bollenbach, 2015). Nichols *et al*, have shown that the synergistic interaction between SMX and TMP is as a result of the two drugs targeting the tetrahydrofolate (THF) biosynthesis pathway (Nichols et al., 2011). In that study, the authors compared the growth of a library of *E. coli* deletion mutants in the presence of the two drugs, which target sequential steps in folic acid biosynthesis, namely dihydrofolate reductase and dihydropteroate synthetase, respectively. Based on their findings, they provided evidence that the synergism between these two drugs was partially caused by secondary effects on parallel branches of this pathway, downstream

from the main targets (Nichols et al., 2011). Consequently, these effects augment synergism that is expected from inhibiting the drug's primary target (Harvey, 1978).

The impact of drug combinations on the differential selection between sensitive and resistant bacterial populations has been evaluated. Exposure of a bacterial population to a drug usually confers an advantage any resistant mutants in competition with the wild-type population (Levy & Marshall, 2004). By applying a direct competition assay between doxycycline (DOX)-resistant and DOX-sensitive *Escherichia coli*, Chait *et al.* showed that this differential selection can be upended with the hyper-antagonistic class of drug combinations (Chait, Craney & Kishony, 2007). In this kind of combination, and at sub-lethal concentrations, a drug can render the combined treatment to be selective against it its own resistant mutants while maintaining inhibition of the wild-type (Chait, Craney & Kishony, 2007).

1.6. Antimycobacterial potency of compounds: cidal *versus* static drugs.

Antibacterial agents are often tested *in vitro* not only for their ability to inhibit bacterial growth but also to ascertain if the agents actually kill the bacteria (Pankey & Sabath, 2004). Although it would be preferable to kill pathogenic bacteria as opposed to inhibiting their growth, clinical outcomes provide the ultimate guide to the treatment of the infection (Pankey & Sabath, 2004). The target, therefore, should be achievement of good clinical outcomes, with clinical/bacteriological cure and no relapse and minimal toxicity (Pankey & Sabath, 2004). In terms of the definitions, "bacteriostatic" refers to those agents which prevent the growth of the bacteria - that is, those that prevent an increase in biomass through cell division - while the term "bactericidal" refers to agents that actually result in bacterial death, which is complete loss of function without capacity for regeneration. In reality, however, this

classification of bactericidal *versus* bacteriostatic drugs is problematic. Agents classified as "bactericidal" normally fall short of killing every organism, for instance due to the inoculum effect, or as a consequence of persister cells. On the other hand, "bacteriostatic" agents may often kill a certain proportion of the population, but not large enough to be called "bactericidal" (Pankey & Sabath, 2004).

Many factors influence the *in vitro* determination of bactericidal or bacteriostatic drug effects including growth conditions, bacterial density, test duration, and extent of reduction in bacterial numbers (Peterson & Shanholtzer, 1992). In bactericidal test determination, antibiotic tolerance presents a particularly difficult form of resistance to detect from the perspective of the clinical laboratory (Tuomanen, Durack & Tomasz, 1986). While 'resistance' is used to describe the inherited ability of microorganisms to grow at high antibiotic concentrations, irrespective of the duration of treatment, 'tolerance' describes the ability, whether inherited or not, of microorganisms to survive transient exposure to high concentrations of an antibiotic without a change in the MIC (Brauner et al., 2016). In antibiotic tolerance, bacteria evade only the killing action of an antibiotic (Tuomanen, Durack & Tomasz, 1986; Brauner et al., 2016). Phenotypic tolerance may arise in cells without sufficient nutrients, which characteristically multiply slowly or do not grow, such as evident with the β-lactams (Peterson & Shanholtzer, 1992). As β-lactams require active cell wall assembly to kill bacteria, slower growth will result in a longer minimum treatment duration to achieve the same level of killing regardless of the concentration of the antibiotic (Brauner et al., 2016).

1.6.1. In vitro evaluation methods for bactericidal versus bacteriostatic drugs for *M. tuberculosis*

A number of available screening systems such as BACTEC-TB 460 and MGIT-TB 960 are used for quantitative analysis of antibacterial susceptibility in *M. tuberculosis*. However, these methods are not high-throughput and require specialized instruments and media. High-throughput assays such as Microplate Alamar Blue Assay (MABA) and the Resazurin-based Microplate Assay (REMA) are routinely applied to provide MIC information, but these do not provide a measure of the cidality of test compounds. In addition, reporter-based assays, such as luciferase *(lux)*, or green-fluorescent protein (GFP) require modifications for each strain. None of these strategies has been shown to select bactericidal compounds (Franzblau et al., 2012). Instead, the gold standard test of "true" cidality remains the cumbersome, agar-based colony forming unit (CFU) enumeration screens (Gilchrist et al., 1973). The following two methods have been reported for rapid evaluation in cidal *versus* stasis experiments (Zhang et al., 2007; Ramon-Garcia et al., 2011; Hendon-Dunn et al., 2016).

***(i) Cell regrowth assay (MBC/MIC) analysis*:** Zhang *et al*. investigated the fungicidal *versus* fungistatic activity of small molecule combinations using a cell regrowth assay (Zhang et al., 2007). This technique was adopted to differentiate bactericidal or bacteriostatic effects of a single drug or drug combination against *M. tuberculosis* (Ramon-Garcia et al., 2011; Ramon-Garcia et al., 2012). In that study, a drug panel consisting of CLR, ketoconazole, bromperidol, RIF, and INH (a positive control), individually and as a combination with SPC, were tested *in vitro* to determine whether they were bacteriostatic or bactericidal. A compound or drug combination was considered bactericidal if the ratio between the minimal bactericidal concentration (MBC) and the MIC was equal to or smaller than 2 (MBC/MIC ≤

2). The reported results for the individual drugs indicated bactericidal activity with INH and bromperidol. Furthermore, an assay of SPC, a bacteriostatic drug, in combination with the sub-MIC concentration of bromperidol revealed a bactericidal activity, suggesting that the bactericidal character of bromperidol was dominant in the combination. The same effect was not observed when SPC was combined with ketoconazole, CLR, or RIF (Ramon-Garcia et al., 2011).

(ii) Flow cytofluorometric method: The usefulness of this technique has been investigated by many authors for antibacterial and antifungal analysis (Green et al., 1999; Ramani & Chaturvedi, 2000; Paparella et al., 2008). Using a rapid dual-fluorescence flow cytometry method, Hendon-Dunn *et al.* recently demonstrated that the fluorescent marker, Calcein Violet-AM (CV-AM), could differentiate between populations of *M. tuberculosis* bacilli growing at different rates, while SYTOX-green (SG) could differentiate between live and dead mycobacteria (Hendon-Dunn et al., 2016). Paparella *et al.* earlier reported the usefulness of this technique to discriminate clearly between three different subpopulations of *Listeria monocytogenes*: viable, dead and injured cells following treatment with different types of essential oils (Paparella et al., 2008).

1.7. Research Objectives

The main objective of this research was to explore the potential of synergistic drug combinations, focusing on drug repurposing, as a strategy for the identification of potential TB drug combination partners. The concept behind this work stems from previous studies which have shown that antibiotics that are currently in clinical use, but have limited efficacy against *M. tuberculosis*, could be used in TB treatment when administered in combination

with standard anti-TB drugs. To test the potential of combination screening approaches to drug repurposing for TB drug discovery and development, this research focused on the clinically used natural product antibiotic FSA and its selected analogues.

1.7.1. Specific objectives

1) Develop screening assays for the identification of synergistic drug interactions between FSA in combination with standard anti-TB drugs and selected translational inhibitors.

2) Determine the extent to which synergistic drug combinations can overcome pre-existing drug resistance.

3) Perform a novel 3-drug combination assay to determine the potential of including a third drug into RIF-INH; two main-stay TB treatment regimens.

4) Develop methods to delineate the bactericidal/bacteriostatic effect of antibiotics against mycobacteria.

Chapter 2

The search for synergy: Interaction of FSA in combination with anti-TB agents and selected translational inhibitors.

2.1 Background

Drug combinations have been widely envisaged as a promising strategy in the treatment of various diseases including cancer, malaria and tuberculosis (TB) (Caminero, 2010). Within this context, synergistic drug combinations have resulted in more efficacious and specific therapies (Lehár et al., 2009). In addition, cases of drug resistance emerging during therapy have been greatly reduced (Owens et al., 2013). For example, it has been shown that synergy results in rapid clearance of the infection thereby decreasing the time in which resistant mutants can occur (Torella, Chait & Kishony, 2010). A study by Lehar *et al.* further underpinned the use of drug combinations as a promising strategy to overcome the make-up mechanisms and unwanted off-target effects that limit the utility of many potential drugs. Results from large-scale simulations of bacterial metabolism and several multi-dose experiments suggested that synergistic drug combinations were generally more specific to particular cellular contexts than are single agent activities. Besides, selectivity with these combinations was achieved as a result of the differential expression of the drug's target in the cell types associated with therapeutic, but not toxic, effects (Lehár et al., 2009). This finding tempers the concern that the therapeutic synergy of a combination will be accompanied by synergistic side effects (Lehár et al., 2009). Despite reported success with combination screening, including the current TB drug regimen, very few systematic studies have been undertaken to show how these drugs interact with each other. Furthermore, very

little attention has been paid to exploring synergistic interactions involving drugs which are not clinically effective against TB (Ramon-Garcia et al., 2011).

As a drug repurposing strategy, we focused on FSA to develop matrix screening assays aimed at identifying optimal drug combination(s) that might be considered within the existing TB drug pipeline for potential clinical efficacy evaluation. More than that, the essence of this work was to explore the potential of synergistic drug interactions and demonstrate the integral role played by synergy towards realizing successful therapeutic outcomes. This chapter presents the analysis of *in vitro* interactions between FSA and a panel of drugs consisting of agents currently used in TB treatment as well as selected translational inhibitors. The latter were prioritized in this study in order to evaluate the outcome of their combination with FSA since they act on the same pathway **(Figure 1-7).**

2.2 Results

2.2.1 Identification of synergistic drug combination partners for FSA

A presumptive study was performed using *M. smegmatis* mc^2155, a non-pathogenic mycobacterium whose genetic relatedness to *M. tuberculosis* and faster growth has identified this bacillus as a useful surrogate in drug efficacy studies *in vitro*, allowing assays to be completed within a shorter duration (Cordone et al., 2011).

Checkerboard experiments using the selected panel of drugs exhibited either synergistic or no interaction combination profiles with FSA **(Table 2.1)**. More specifically, SPC, ERY, CLR and TET exhibited synergy with FSA. Synergy was defined as FICI ≤ 0.5. No antagonistic effects were observed in any of the combinations tested. Those combinations which elicited synergistic interactions against *M. smegmatis* displayed a 4–16 fold reduction in the MIC for each of the individual drugs **(Figure 2-1)**.

Table 2-1 *In vitro* synergistic interactions between fusidic acid (FSA) and anti-TB agents or selected translational inhibitors in *M. smegmatis.*

Compound[a]	**MIC**[b] **(µM)$_{individual}$**	**MIC**[b] **(µM)$_{combined}$**	**FIC**	**FICI**[c]
FSA RIF	81-162 10	20 5	0.12-0.25 0.5	0.62-0.75
FSA INH	162 13	81 13	0.5 1	1.5
FSA EMB	162 1.6-0.8	81 0.4	0.5 0.5-0.25	0.75-1.0
FSA STR	81 0.5	41 0.1	0.51 0.2	0.71
FSA KAN	81 4	81 2-4	0.51 0.5-1	1.01-1.51
FSA OFX	41 0.5	41 0.5	1 1	2
FSA SPC	81 50	5 13	0.06 0.26	**0.32**
FSA ERY	41 8	10 2	0.24 0.25	**0.49**
FSA CLR	81-162 5	20 1	0.12-0.25 0.2	**0.32-0.45**
FSA TET	81 0.7	10 0.2	0.12 0.29	**0.41**

[a]Compounds selected for this *in vitro* interaction assay included RIF, INH, EMB, STR, KAN, OFX, SPC, ERY, CLR and TET.

[b]MIC_{90} was determined using the resazurin assay. MIC values were determined as the lowest concentration of each drug(s) that prevented colour change.

[c]The FICI values represent the lowest values taken from two biological replicates. FICI ≤ 0.5 synergy; $0.5<FICI \leq 4$ no interaction; >4 antagonistic.

FICI values of drug combinations displaying synergy are shown in bold.

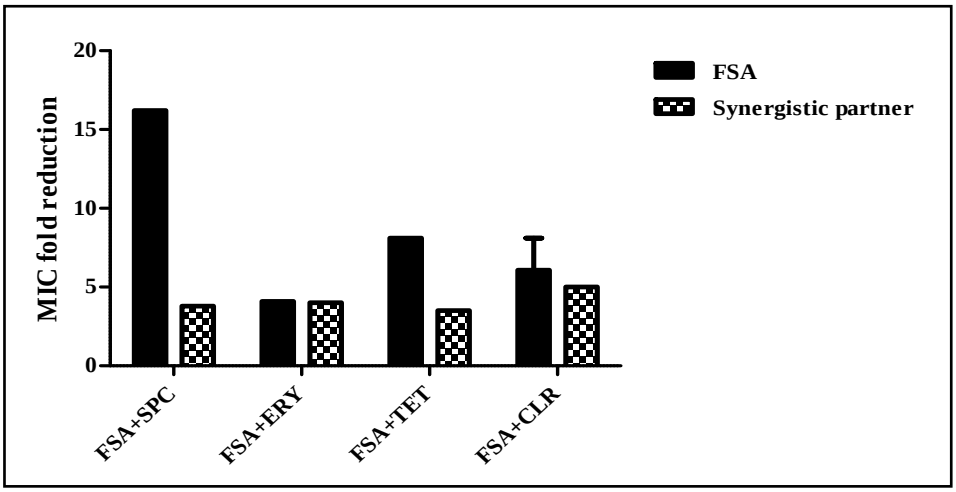

Figure 2-1 MIC fold-reduction of combinations exhibiting *in vitro* synergistic interactions when tested against *M. smegmatis* showing mean ± SD from duplicate samples.

On the basis of the synergies evident in *M. smegmatis*, further interaction studies were performed using the checkerboard method with an *M. tuberculosis* H37Rv reporter strain expressing green fluorescent protein (GFP); this strain has been used previously in high-throughput antimicrobial drug screening (Srivastava et al., 1998). **Figure 2-2** provides an example of an interaction study in which FSA and ERY were analysed in the checkerboard assay using *M. tuberculosis*::GFP. Representative drugs consisting of clinically used anti-TB agents (first- and second-line) and selected translational inhibitors were also tested in combination with FSA. Hits identified using *M. smegmatis*, except for TET owing to its unavailability at the time, were also included for comparative analysis.

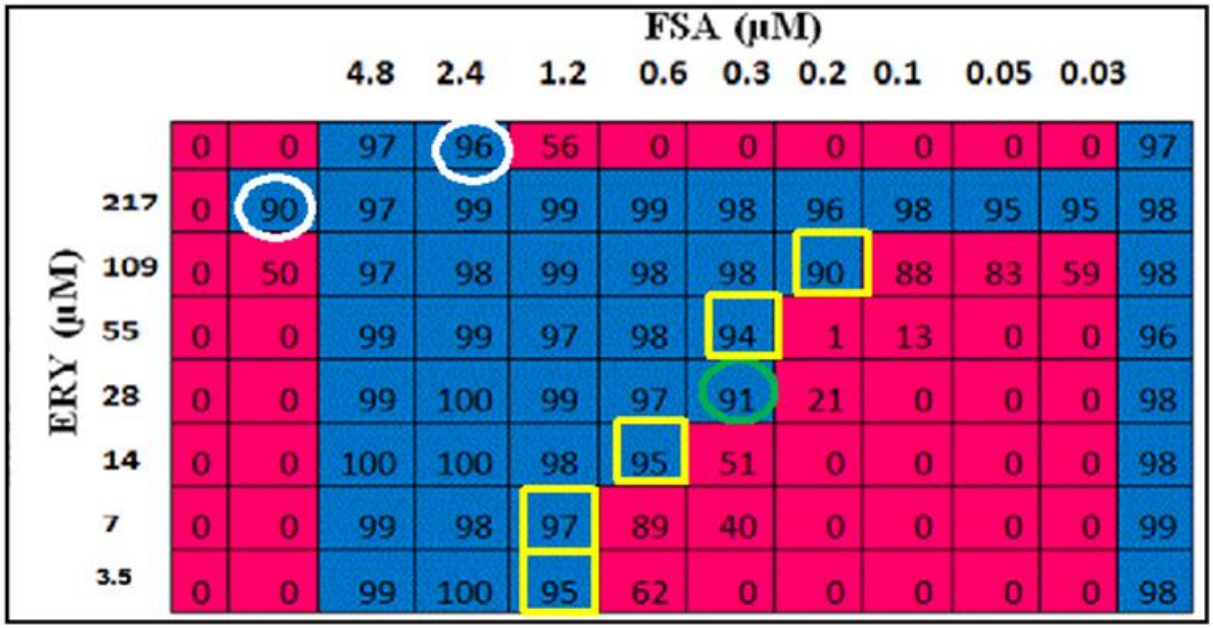

Figure 2-2 Checkerboard assay: Investigating the *in vitro* interaction between FSA and ERY against *M. tuberculosis*::gfp strain in a 96-well microtitre plate. Combinations with > 90% (blue) and < 90% inhibition (pink). MIC_{90} wells for both FSA and ERY are shown in white oval and the iso-effective concentrations from which FICs were calculated are indicated in yellow rectangles. The combination with the lowest FICI (*i.e* 0.25) is shown in green oval.

Results in **Table 2.2** show similarity to those obtained for *M. smegmatis*, such that SPC, ERY and CLR exhibited synergy with FSA in *M. tuberculosis.* As highlighted **(Figure 2-2)**, the combination between FSA and ERY showed a FICI value of 0.25, suggesting a synergistic interaction. Other drugs that synergized with FSA included RIF, STR, roxithromycin (ROX), and LZD. These synergistic interactions resulted mainly in a 4- to 8- fold reduction in the MICs of each drug within the combination. Even though the combination of FSA and BDQ did not result in a FICI value of ≤ 0.5, it is important to note that the two displayed approximately a 4-fold reduction in their respective MICs, and the observed FICI (0.55) is very close to that defined as "synergy". No antagonistic interaction was observed between FSA and any of the compounds tested.

Table 2-2 *In vitro* synergistic interaction between fusidic acid FSA and anti-TB agents or selected translational inhibitors against *M. tuberculosis*::gfp

Compound[a]	**MIC_{90}**[b] **$(\mu M)_{individual}$**	**MIC_{90}**[b] **$(\mu M)_{combined}$**	**MIC_{90}fold-reduction**	**FIC**	**FICI**[c]
FSA	2.5	0.61	4	0.24	**0.48**
RIF	0.003	0.0008	4	0.24	
FSA	2.4	1.2	2	0.50	1.00
INH	0.6	0.3	2	0.50	
FSA	2.4	1.2	2	0.50	1.00
EMB	2.5	1.25	2	0.50	
FSA	2.4	0.6	4	0.25	**0.50**
STR	0.4	0.1	4	0.25	
FSA	2.4	1.2	2	0.50	0.94
AMK	0.9	0.4	2	0.44	
FSA	2.4	2.4	1	1.00	1.30-1.50
OFX	1.4-2.8	0.7	2-4	0.25-0.5	
FSA	2.4	0.3	8	0.13	**0.26**
SPC	201	26	8	0.13	
FSA	2.4	0.3	8	0.13	**0.25**
ERY	217	27	8	0.12	
FSA	4.6	0.7	7	0.15	**0.30**
CLR	2.0	0.3	7	0.15	
FSA	2.4	0.6	4	0.25	0.73
GAT	2.1	1.0	2	0.48	
FSA	2.4	0.6	4	0.25	**0.50**
ROX	3.6	0.9	4	0.25	
FSA	5.0	1.3	4	0.26	0.55
BDQ	1.4	0.4	4	0.29	
FSA	4.8	1.2	4	0.25	**0.50**
LZD	1.4	0.4	4	0.25	
FSA	1.4	0.6	2	0.43	0.93
CYC	196	98	2	0.50	

[a]Compounds selected for this *in vitro* interaction assay included rifampicin (RIF), isoniazid (INH), ethambutol (EMB), streptomycin (STR), kanamycin (KAN), ofloxacin (OFX), spectinomycin (SPC), erythromycin (ERY), clarthromycin (CLR), gatifloxacin (GAT), roxithromycin (ROX), bedaquiline (BDQ), linezolid (LZD) and cycloserine (CYC). [b]The FICI values represents the lowest values taken from two biological replicates FICI $\leq$ 0.5 synergy; 0.5<FICI $\leq$4 no interaction; >4 antagonistic. *Values representing synergistic interactions are shown in bold.

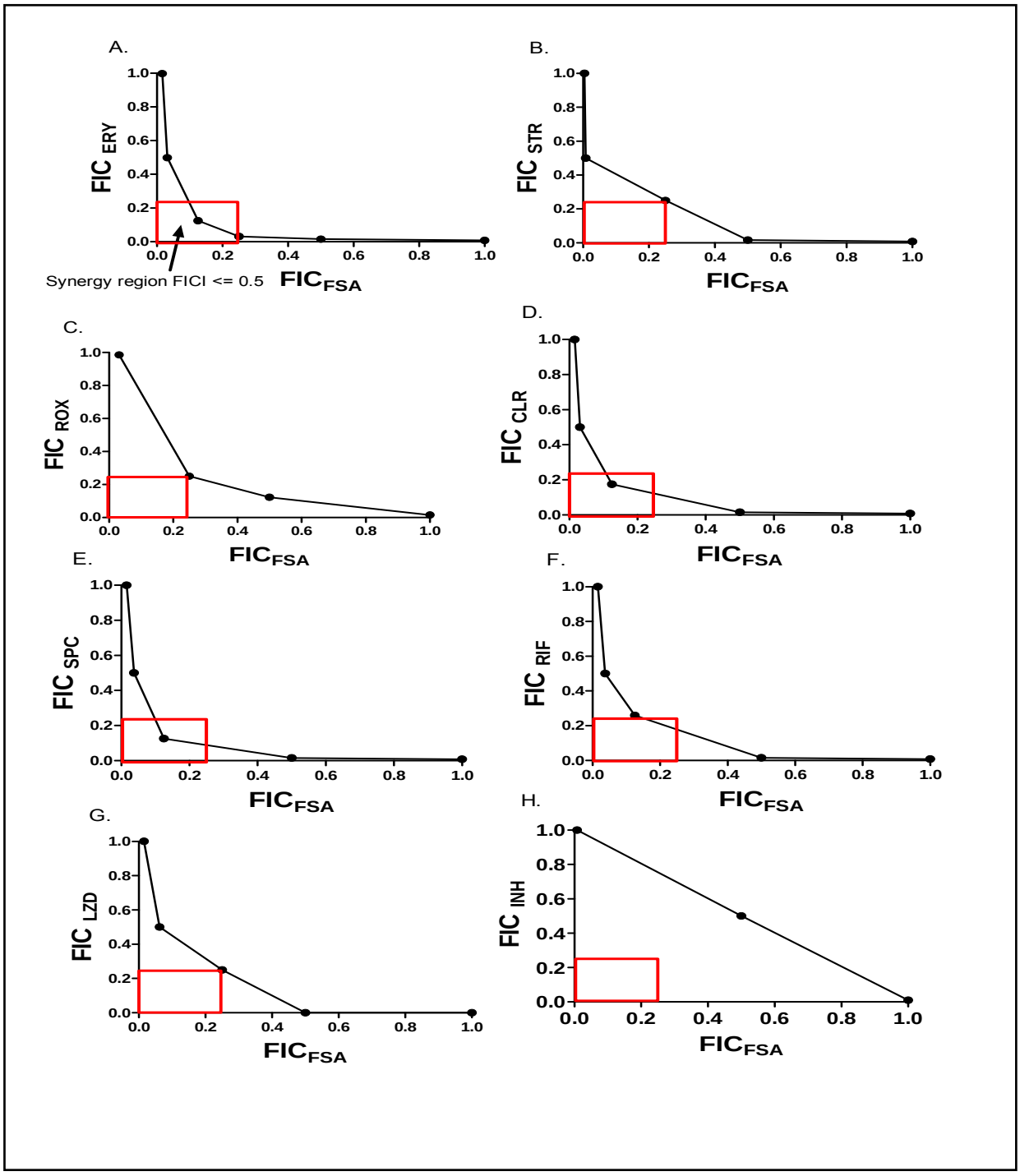

Figure 2-3 Isobolograms of FSA *versus* selected partner compounds. FIC curves of FSA versus (**A**) ERY (**B**) STR (**C**) ROX (**D**) CLR (**E**) SPC (**F**) RIF) (**G**) LZD (**H**) INH control drug. Synergy region (FICI ≤ 0.5) is defined by the red square. Data are representative of two biological replicates.

For the combinations exhibiting synergy with FSA, isobolograms were constructed by plotting the FIC curves of the FSA-drug combinations **(Figure 2-3)**. Interactions between FSA and SPC, CLR and RIF were well within the 'synergy region' (FICI < 0.5) whereas FSA with STR, LZD, and ROX indicated borderline synergy (FICI = 0.5). The FSA-INH interaction was included as a reference for a no interaction drug combination.

Time-curve Assay: The time-curve study was used to confirm results obtained using the checkerboard assay. In time-curve, FSA and ERY, a combination that exhibited potent interaction, was evaluated, **(Figure 2-4)**. FSA and ERY were used at 0.3 and 27 µM respectively, since these are the concentrations at which the lowest FICI value was displayed in the checkerboard assay **(Figure 2-2)**. RIF, at a concentration of 0.015 µM, was included as a control. In the absence of drug, the population of *M. tuberculosis* increased over 14 days post-inoculation. In contrast, the population of viable cells remained relatively constant over the same duration when the broth contained the FSA and ERY combination. Similarly, the test broth that contained FSA, ERY plus sub-MIC RIF did not display any increase in the number of viable bacterial population over a 14-day period. However, the broth containing individual antibiotics (FSA or ERY) showed equivalent growth to the untreated control.

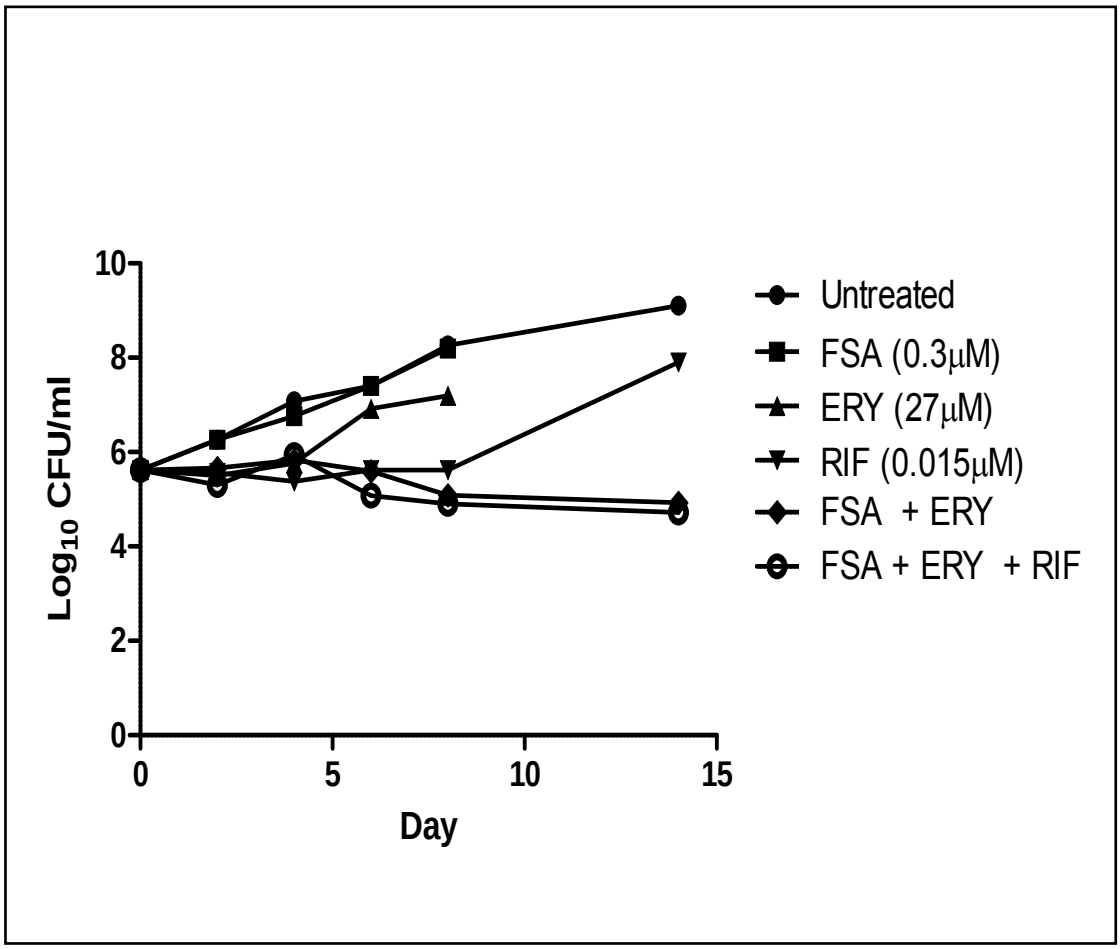

Figure 2-4 Kinetic Assay. Time-curve experiments for FSA, ERY and RIF alone and in combination. Viable cell concentrations in culture broth at the indicated time were determined on Middlebrook 7H10 agar. CFU, colony forming units. Data are from a single experiment only, owing to limited compound availability.

2.2.2 Assessing synergistic and peak plasma concentrations (C_{max}) as well as cLogP values of FSA synergizing drugs for optimal therapy.

As a key consideration for the clinical potential of FSA combinations, the respective concentrations at which synergy was observed were compared with the reported peak plasma concentrations (C_{max}) for each drug. This is important in understanding whether or not the concentrations required to achieve the desired response are therapeutically feasible – in the absence of such knowledge, investigating combinations might be criticized as representing an academic exercise.

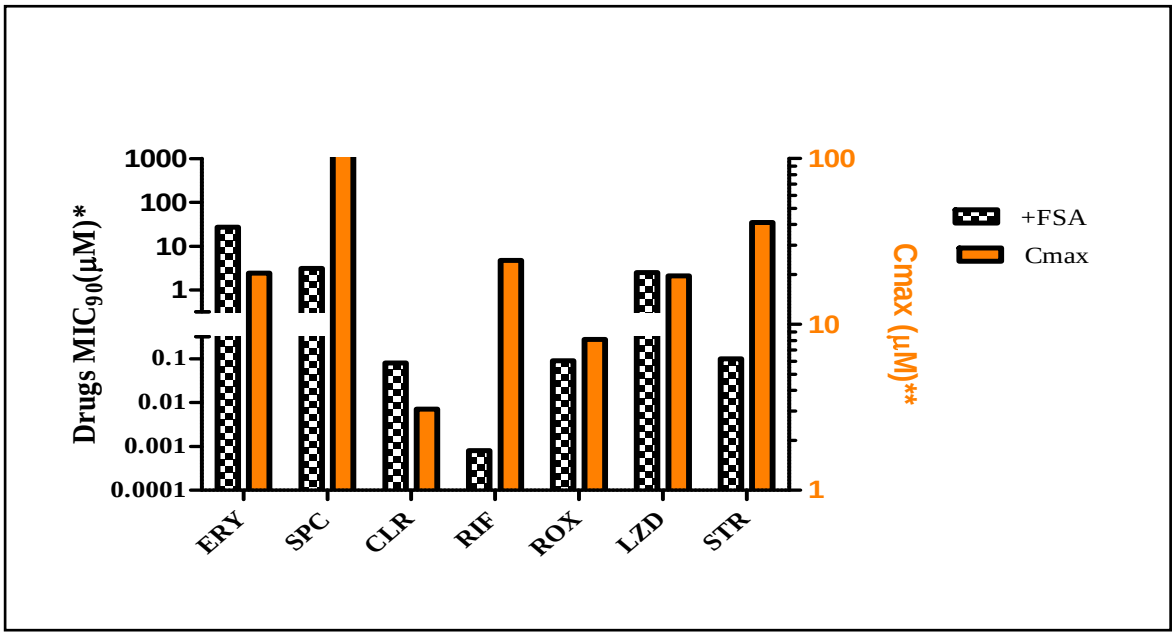

Figure 2-5 Synergy vs C_{max}. Comparison between synergistic concentrations of various drugs in the presence of FSA and their published Cmax values. With the exception of ERY, all drugs - SPC, CLR, RIF,ROX, LZD, and STR - exhibited synergistic concentrations lower than their known Cmax values**.** *Synergistic concentration values obtained from a representative experiment performed in triplicate. **C_{max} values from literature (Lee,R.E. 2014; Mensa,B. 2011).

Except for the FSA-ERY interaction, synergies between FSA and its partners were achieved at concentrations predicted to be below the maximum plasma concentrations, suggesting that these concentrations are therapeutically achievable, **(Figure 2-5)**. For example, the presence of FSA decreased the MIC of SPC from 201 µM to 3.14 µM, which represents a greater than 98% reduction in the MIC **(Table 2.3)**. This reduced concentration is far below the C_{max} value of SPC in humans (30.8 µM) after a 1000- mg intramuscular dose.

Apart from the peak plasma concentrations, it is noteworthy that the site of many infectious diseases is outside the blood or plasma compartment. In TB for example, the mycobacteria can reside in caseous lesions that are devoid of vascular supply, thus impacting any drug's ability to be effective against the pathogen at the site of infection.

Table 2-3 Reduction of MIC following addition of FSA at sub-inhibitory concentrations

Antibiotic	**[a] MIC_{90} (µM)**		**% MIC_{90} reduction**	**[b]Peak plasma concentration (µM)**
	-FSA	**[c]+FSA**		
ERY	217	27	87.6	20.4
CLR	1.3	0.08	93.8	323
SPC	201	3.14	98.4	30.8
RIF	0.003	0.0008	73.3	24.3
ROX	3.55	0.09	97.5	8.12
LZD	9.9	2.5	74.7	19.6
STR	0.4	0.1	75	41.2

[a]MICs of synergizing partner drugs in the absence (-) and presence (+) FSA. [b]Literature C_{max} values for the respective drugs (Lee et al., 1977; Mensa et al., 2011) [c]Sub-inhibitory concentrations of FSA that exhibited the respective synergies in these checkerboard experiments are between (0.3 – 1.2 µM)

Recent work has shown that the octanol-water partitioning coefficient, also referred to as lipophilicity (cLogP), is likely to play an important role in determining caseum penetration (Sarathy, Jansy P 2016). .As a drug's lipophilicity increases, non-specific protein binding also increases. This consequently results in a reduced free fraction to passively diffuse through the caseum, and an increase in intracellular macrophage permeation due to uptake of protein-drug complex through such means as endocytosis and lysosomal trapping (Prideaux et al., 2015). Therefore, the cLogP values of FSA synergizing drugs were examined in relation to other drugs including PZA, a drug that achieves excellent sterilizing activity of extracellular anaerobic bacteria (Prideaux et al., 2015); RIF, which has previously been shown to balance between relatively low uptake into macrophage and ideal caseum binding leading to continued build-up into the necrotic core; and clofazimine (CFZ), which does not diffuse into the necrotic core due to its high lipophilicity. A quadrant model **(Figure 2-6)** was generated that relates the potency of these synergizing drugs when combined with FSA to their respective cLogP values. This understanding enabled us to hypothesize the action of the drug

combinations at the two phases - the cellular macrophage and the avascular caseum - which are considered critical to determining sterilizing action.

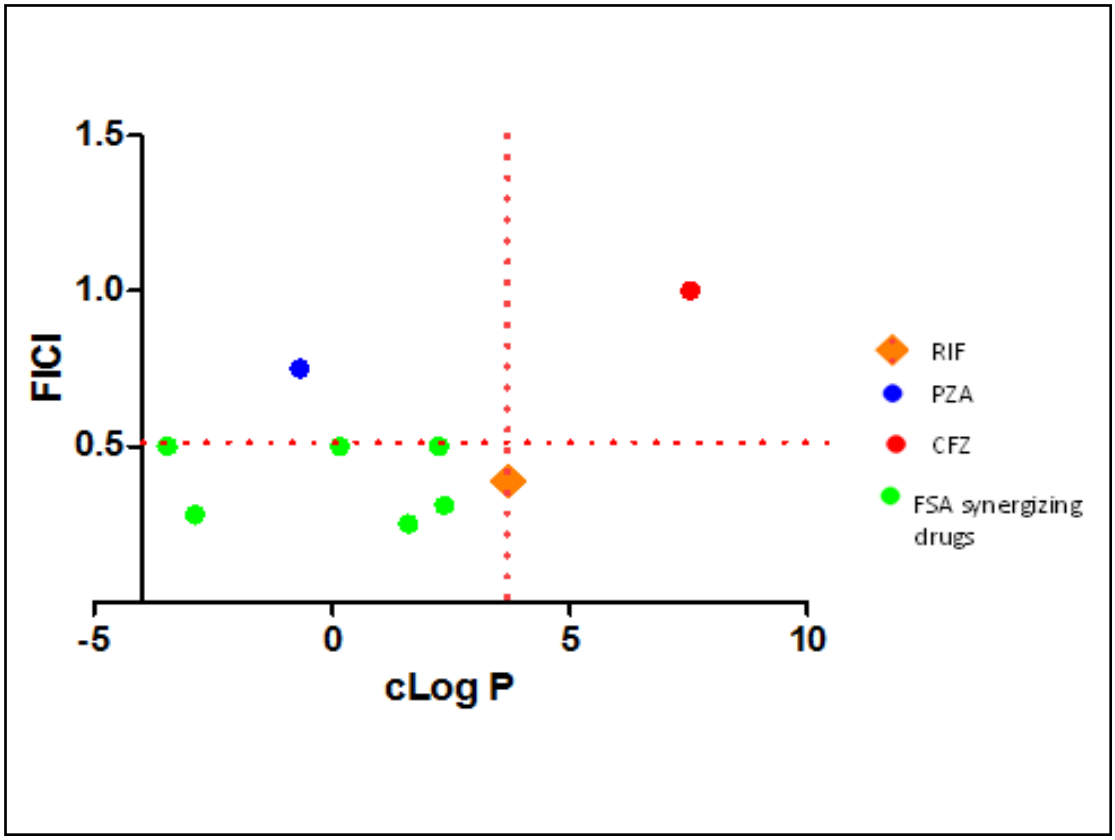

Figure 2-6 A comparison of cLogP value vs FICI for FSA synergizing drugs (in green), and selected reference drugs (RIF, CFZ and PZA).

Considering RIF as a reference for "desirable" cLogP values, drugs with low cLogP values would generally be expected to exhibit greater accumulation into the necrotic core whereas the more lipophilic compounds would spatially distribute within the cellular macrophages. Thus, a combination comprising high potency and low lipophilicity is preferred for targeting the extracellular (anaerobic) bacteria residing inside the caseum. From our plot, all the drugs, which synergized with FSA were spatially distributed within the 'desirable' quadrant. This suggests their potential as sterilizing agents for caseum bacilli.

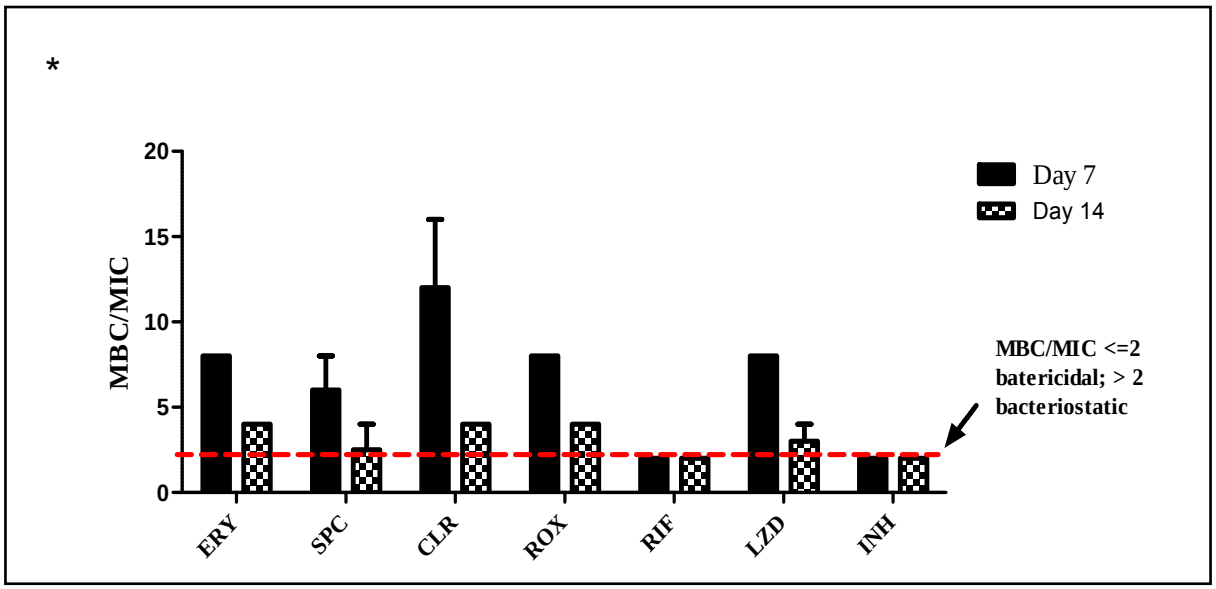

Figure 2-7 Bactericidal *versus* static effects of drug combinations against *M. tuberculosis*. Analysis of FSA in combination with synergizing drugs; ERY, SPC, CLR, ROX, RIF, and LZD. INH was used as reference drug. MBC/MIC ratio 1-2: cidal; MBC/MIC ratio > 2: static**.**
***Sub-inhibitory concentrations** of FSA that exhibited the respective synergies in these checkerboard experiments are between (0.3 – 1.2 µM) Data are from a representative experiment performed in triplicate. Error bars indicate standard deviations, calculated from the mean of triplicate samples.

2.2.3 A cidal *versus* static analysis of FSA interactions

To determine whether or not FSA interactions resulted in killing or merely inhibited the growth of *M. tuberculosis*, the method of Zhang *et al*. was utilized (Zhang et al., 2007). INH, a bactericidal agent, was used as a reference drug. The drugs were tested alone and in combination using the *M. tuberculosis* H37Rv::*gfp* strain. Results for the bacteriostatic or cidal effects of the drug combinations with FSA are illustrated, **(Figure 2-7)**. The FSA-RIF combination displayed a MBC/MIC ratio of 1-2 on day 14 of evaluation, suggesting cidality. The other FSA combinations tested – with SPC, ERY, CLR, ROX or LZD – all exhibited a MBC/MIC ratios >2, implying static effects. The bacteriostatic/cidal action of individual drugs is shown below **(Figure 2-8).**

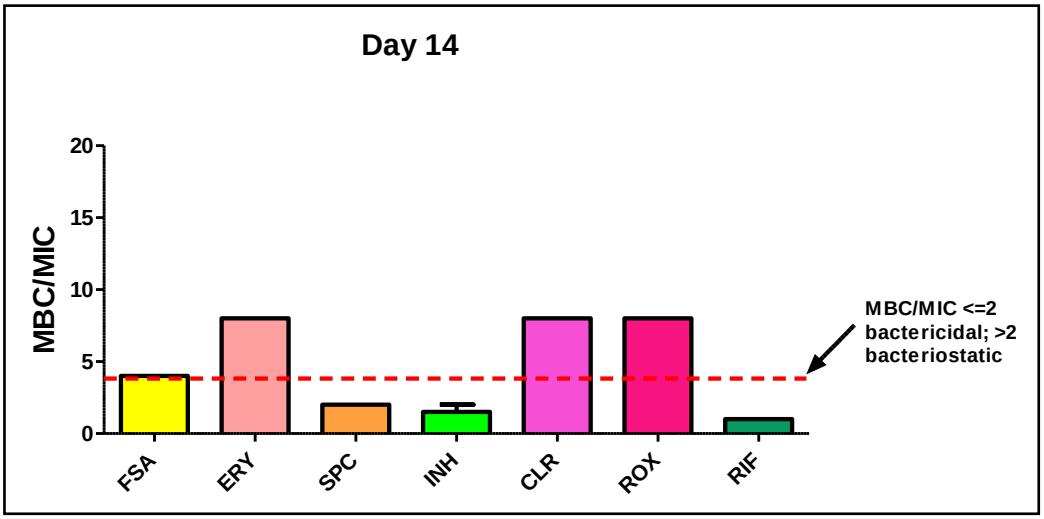

Figure 2-8 Bactericidal-static assay. Bactericidal versus static effects of individual drugs against H37Rv::gfp.FSA,ERY, SPC,CLR,ROX, and RIF. INH was used as reference drug. MBC/MIC ratio 1-2 cidal; > 2 static**.** Data are from a representative experiment performed in triplicate. Error bars indicate standard deviations, calculated from the mean of triplicate samples.

2.2.4 FSA synergizing partners are active against the FSA-resistant mutant.

A cross-resistance study was undertaken using a FSA-resistant *fusA1* mutant strain of *M. tuberculosis* H37Rv. The *fusA1* mutation was selected as a spontaneous FSA-resistance mutation in EF-G, H462Y. Briefly, this mutant was generated by plating 10^9 CFU per plate in 7H10/OADC. The colonies were isolated from 20X MIC plate. (Moosa, unpublished data). The FSA-resistant mutant exhibited a > 100-fold MIC compared to the FSA susceptible strain. Six FSA synergizing partners (RIF, SPC, CLR, ERY, STR and ROX) were evaluated using the resazurin reduction microplate assay (REMA). The results **(Figure 2-9)** indicated that the MIC_{90} values of these drugs remained the same against the FSA-resistant mutant relative to the wild-type strain, confirming that there was no cross-resistance to each of the tested compounds.

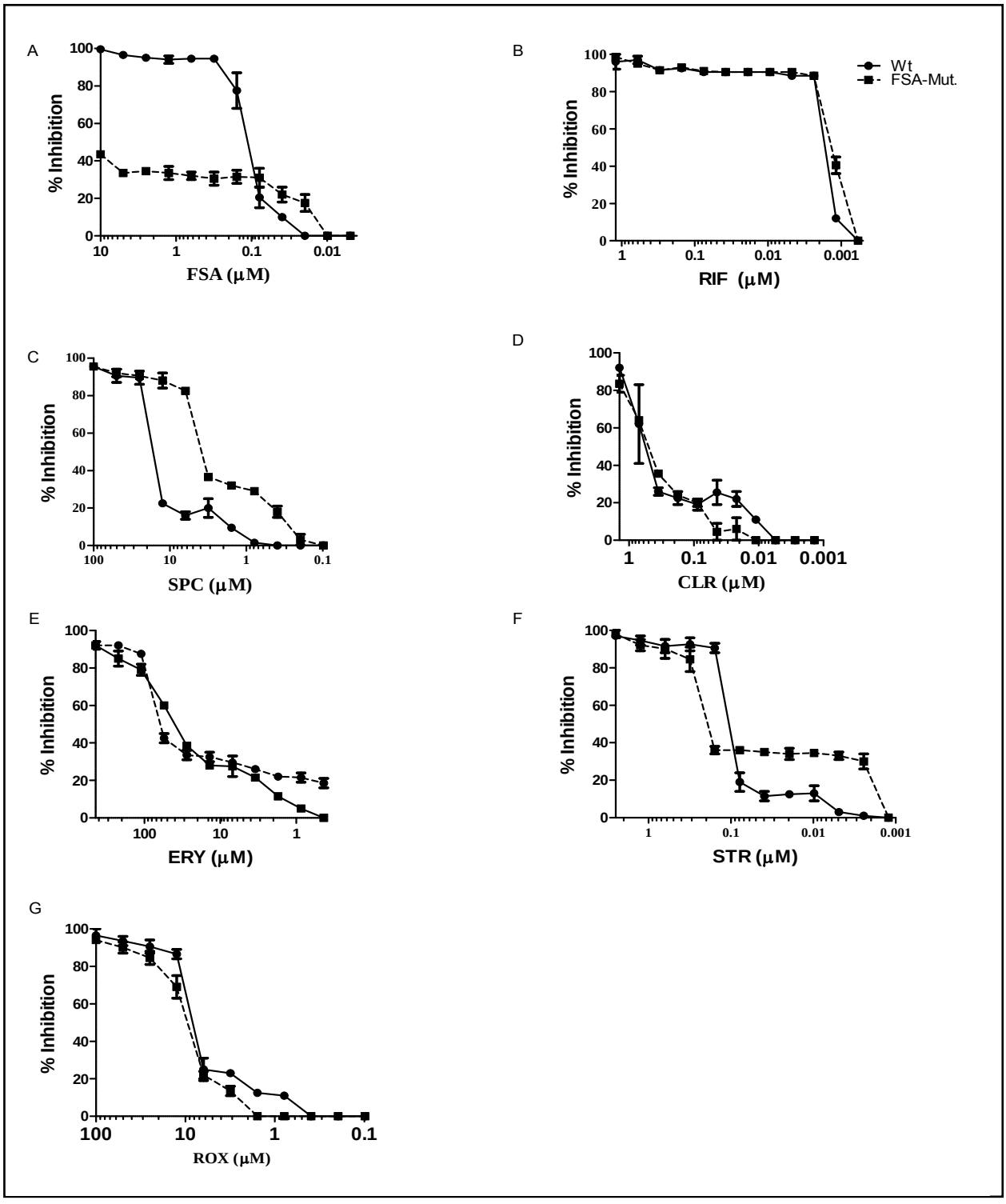

Figure 2-9 Cross-resistance study. Investigating cross-resistance of the FSA resistant mutant against FSA synergizing drugs. FSA synergizing partners are tested (**A**) FSA (control drug) (**B**) RIF (**C**) (CLR (**D**) (ERY) (**E)** STR (**F**) ROX (**G**) SPC. Data are from the representative experiment performed in triplicate. Error bars indicate standard deviations, calculated from the mean of triplicate samples.

Table 2-4 Selected chemically and structurally diverse drugs

Compound	Abbreviation	Chemical classification	Therapeutic use[a]
Isoniazid	INH	Isonicotinyl-hydrazide	Antituberculosis
Ethambutol	EMB	Ethylenediamine	Antituberculosis
Thiostrepton	THS	Cyclic oligopeptide	Antibacterial
Bedaquiline	BDQ	Diarylquinoline	Antituberculosis
Chlorpromazine	CPZ	Phenothiazine	Antipsychotic
Moxifloxacin	MOX	Fluoroquinolone	Antibacterial

[a]From PubChem(http://pubchem.ncbi.nlm.nih.gov/)

2.2.5 Interaction of FSA synergizing partners with selected chemically unrelated compounds

Using a set of six chemically and structurally diverse drug agents **(Table 2.4)**, a combinatorial assay was performed with four drugs that had displayed synergistic interaction with FSA, namely RIF, ERY, CLR and SPC. The aim was to determine whether these FSA synergizing partners displayed synergy only in combination with FSA, or were possibly associated with a wide spectrum of synergistic interactions. The results of these pairwise interactions **(Figure 2-10)** revealed synergy between all FSA synergizing partners (except RIF) with BDQ and CPZ. CLR, in particular, displayed strong synergies with BDQ and CPZ (FICI = 0.23 in both cases). The interaction between ERY and THS was also synergistic, while the remaining compounds (INH, EMB and MOX) exhibited no interactions in combination with RIF, ERY, CLR and SPC.

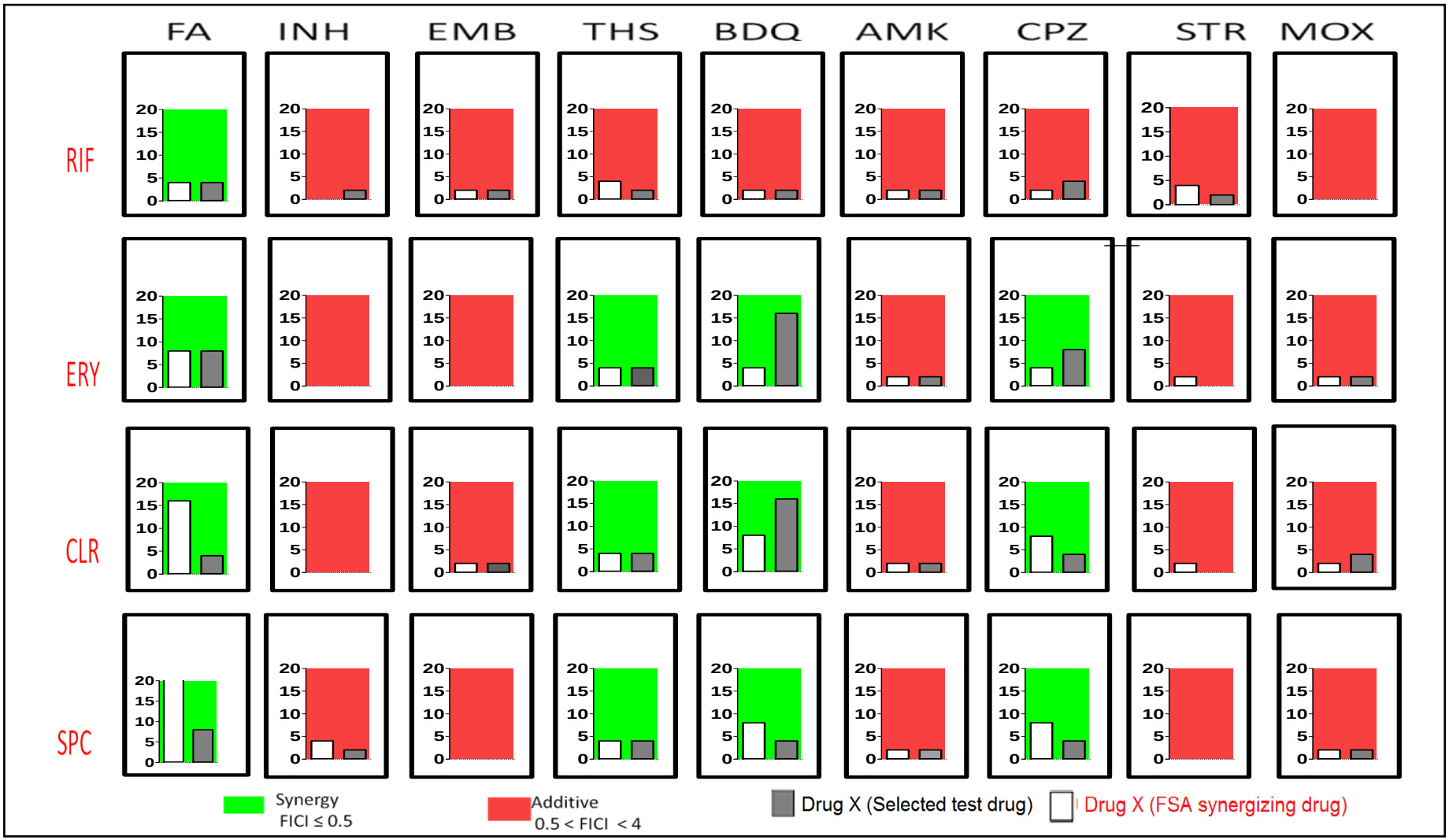

Figure 2-10 Drug interaction study. Pairwise interactions between selected drugs (Drug X) and synergizing agents of FSA (Drug Y) using *M. tuberculosis* H37Rv::*gfp*. Green panels indicate synergistic interactions (FICI ≤ 0.5), while red panels are no interaction (0.5 > FICI ≤ 4). The bars indicate the fold-reduction in MIC required to achieve the same effect in combination *versus* single-drug assays. Panels with no bars indicate no change in MIC_{90} for the drug combination compared to their respective MICs when used alone. Data are from the representative experiment performed in duplicate.

2.3 Discussion

Using a combination of checkerboard and time-kill kinetic assays, seven drugs were identified that synergized with FSA *in vitro*. These include the rifamycin, RIF, and the macrolides, ERY, CLR, and ROX. Others included the oxazolidinone, LZD, the aminoglycoside, STR, and an aminocyclitol class compound, SPC. Moreover, the fold-reduction in the MIC_{90} of the interacting drugs was demonstrated. As an example, ERY enhanced the potency of FSA to a much-reduced MIC of 0.3µM from 2.4 µM, representing an 8-fold reduction in the MIC_{90}. Apart from the synergy observed, other two-drug combination results showed that most of the interactions had FICI values between 0.5 and 4.0, indicating a no interaction effect. None of the combinations with FSA showed any antagonistic effects, FICI value ≥ 4.0. Validation of the synergy displayed between FSA and ERY using the checkerboard assay was achieved using the time-kill kinetics experiment. The reason for this FSA-ERY synergy remains unknown. However, a systematic study of drug interactions reveals that compounds inactivating the same cellular function act efficiently when combined (Yeh, Tschumi & Kishony, 2006). This might explain the observed synergy since ERY, and indeed other macrolides, targets the ribosome. ERY inhibits protein synthesis by binding to the 23S rRNA molecule, located in the 50S subunit of the bacterial ribosome, thereby blocking the exit of the nascent peptide chain (Gupta, Agarwal & Srivastava, 2014). On the other hand, FSA is presumed to target elongation factor G when in complex with the ribosome (Gao et al., 2009).This interaction might account for the synergy observed.

A vital aspect to consider for the clinical utilization of (synergistic) drug combinations is whether or not the synergistic concentrations required for realizing an effective response is therapeutically achievable (Bruhn et al., 2015). Sufficient concentrations of the drug combinations in the blood stream and affected tissues are needed to achieve the desired

therapeutic effect (Winglee et al., 2015). If both drugs are present with the concentration of one of the drugs being lower than the concentration for synergy, this can result in a mismatched exposure where the bacteria are exposed to long periods of monotherapy. Consequently, the induction of transient resistance mechanisms may ensue, hence selection of genetic mutants (Drusano et al., 2010). The results demonstrated that synergies with FSA were achieved at concentrations lower than the respective peak plasma concentrations for all the drugs except ERY. In addition, all of the FSA synergizing drugs fitted into the "desirable" quadrant, suggesting their potential to access the caseum, a critical site of mycobacterium residence. When FSA synergizing partners were tested in combination with other chemically diverse agents, BDQ and CPZ exhibited the most promising synergistic interactions. The synergy with CPZ may be attributed to its efflux pump inhibitory effect, resulting in the accumulation of the partner compound (Winglee et al., 2015). Work from Weinsten *et al* has previously described the biochemical characterization of the aerobic respiratory chains from *M. tuberculosis* and shown that phenothiazine analogs specifically inhibit NADH:menaquinone oxoreductase activity (Weinstein et al., 2005). Therefore, it is possible that CPZ-mediated inhibition of energy metabolism might impact activity of the efflux pumps such as Rv1258c thereby conferring sensitivity to FSA. However, the mechanism responsible for synergistic interactions between BDQ and FSA synergizing partners, requires further investigation. The possible hypothesis for this synergy may also be a result of deleterious effect caused by combining FSA with BDQ, the agent affecting energy metabolism.

The challenge of overcoming antibiotic resistance continues even with the use of drug combinations. The bacteria can evolve resistance to one drug thereby risking the possibility that the bacteria will also be able to resist the other drug(s) in the combination regimen. An understanding of cross-resistance between drugs is an important first-step in determining the

drug combinations that would provide effective therapy (Sanders et al., 2001). .Here, the cross-resistance studies showed a mechanism of resistance specific to FSA when compared to the tested drugs that synergized with it. Interestingly, FSA-resistant mutants exhibited increased susceptibility to the inhibitory action of SPC and STR at sub-MIC concentrations. The significance of this susceptibility and the related mechanism is yet to be established. However, hypersusceptibility to different classes of antibiotics against FSA-resistant mutant of *Salmonella typhimurium* has earlier been reported (Macvanin et al., 2000). Moreover, it has been shown that *fus* A1 mutations, associated with FSA-resistance, have pleiotropic phenotypes that affects the fitness of FSA-R mutants *in vitro* and *in vivo* (Macvanin et al., 2000). Some or all of these phenotypes may be related to the down-stream effects of altered transcriptional regulators ppGpp and RpoS in FSA-R mutants (Macvanin & Hughes, 2005). In the case of norfloxacin, for example, increased susceptibility parallels increased sensitivity to DNA damaging agents as seen with ultra-violet (UV) light. Thus one of the pathways of DNA repair may be under-expressed in the *fus A1* strain (Macvanin & Hughes, 2005). *fus A1* mutations associated with altered cell shapes might result to increased susceptibility to ß-lactam antibiotics (Macvanin et al., 2000; Macvanin & Hughes, 2005). Resistance to STR caused by mutations is very strongly associated with reduced affinity for its binding site on the ribosome (Bohman et al., 1984; Bilgin et al., 1992).. Therefore, it has (Bohman et al., 1984) been suggested that the hyper-susceptibility to STR associated with *fus A1* might be due to mutant EF-G influencing access of the antibiotic to its ribosomal binding site.

In view of these promising synergistic interactions, it would be important to carry out further larger scale *in vitro* combinations, *ex vivo* and follow-up *in vivo* experiments to evaluate the effect of these drug interactions against various clinical isolates as well as multi-

drug resistant *M . tuberculosis* strains. In large scale *in vitro* combinations, a syncretic cross-(or matrix) screening approach (Keith et al., 2005), has been utilized to uncover interactions involving off-patent ("re-purposed") drugs inhibiting sphingolipid biosynthesis or modulating membrane permeability potentiating fluconazole against *Candida* and *Cryptococcus* (Spitzer et al., 2011). In addition, Small *et al.*, applied a genetic algorithm (evolutionary computing) strategy to hone all possible combinations of probe drugs inhibiting the cellular release of cytokines down to the best combinations; this allowed for the simultaneous identification of the best targets as well as the best dose ratios to apply (Small et al., 2011).

Chapter 3

Developing synergistic combinations to restore drug sensitivity in drug-resistant *Mycobacterium tuberculosis*.

3.1. Background

In order to treat multi-drug resistant (MDR) tuberculosis effectively, drug regimens are required that not only affect essential cellular processes, but also act synergistically with each other. Therefore, it is important to prioritize combination therapies that extend beyond biologically active individual molecules. This chapter explores the potential use of more potent synergistic combinations to circumvent resistance emanating from individual drugs in combination therapies, even restoring susceptibility to compounds for which genetic resistance is present.

Herein, the checkerboard assay was used to investigate the relationship between the inferred potency of drug combinations against wild-type, drug-susceptible *M. tuberculosis* (as determined by FICI) and activity against cognate drug-resistant mutants. Specifically, interactions with FSA, its semi-synthesized structurally modified analogues GKFA17, GKFA 37, GKFA51 and GKFA61 **(Figure 3-1)** were investigated. Furthermore, the *in vitro* and *ex vivo* interactions between SPC, a drug that exhibited synergy with FSA and its analogues, and the standard frontline TB drugs, RIF and INH, were evaluated. This was carried out using a three-drug combination assay against both the susceptible and drug resistant *M. tuberculosis* strains.

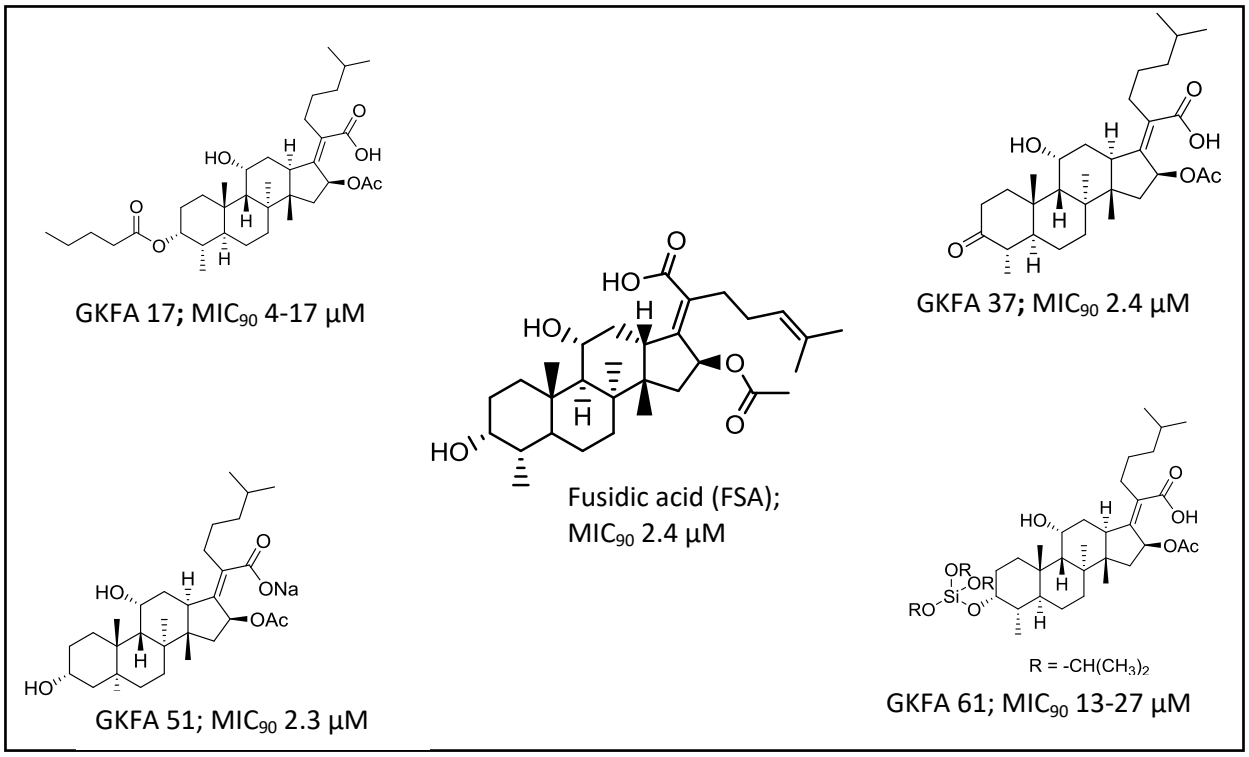

Figure 3-1 FSA and selected analogues

The specific objectives for this chapter were to:

1. Determine the potencies of FSA and selected analogues in combination identified FSA synergizing partner drugs.

2. Establish a correlation between the potency of a combination and its efficacy against cognate resistant mutants.

3. Investigate the potential of adding a third drug to the standard two–drug continuation regimen consisting of RIF and INH for treatment of susceptible and resistant *M. tuberculosis* strains.

3.2. Results

3.2.1. Synergistic interactions between analogues of FSA with selected partner compounds.

This experiment, undertaken using the drug susceptible *M. tuberculosis* H37Rv, was performed to allow for the prioritization of synergistic interactions that would subsequently be tested on the resistant mutants. As highlighted, the study hypothesized that strong synergies against the wild-type strain would equally elicit greater inhibitory activity against the resistant mutant, even to the extent of restoring drug susceptibility. Four drugs - SPC, ERY, CLR and RIF - were selected based on previous results which suggested their synergistic interaction with FSA **(Chapter 2 Table 2.2)**. The *in vitro* synergistic assay was performed using these drugs in combination with FSA, GKFA17, GKFA37, GKFA51 and GKFA61 in checkerboard assays, from which isobologram curves were derived **(Table 3.1, Figure 3-2)**. The combination of ERY or SPC with FSA yielded the lowest FICI values of 0.15 and 0.18 respectively, suggesting strong synergy. SPC generally displayed lower FICI values, implying better synergistic interactions with the FSA and its analogues. All interactions assessed resulted in either synergistic (FICI $\leq$ 0.5) or no interaction, > 0.5 FICI $\leq$ 4. No antagonistic interactions (FICI > 4) were observed with the compounds selected.

Table 3-1 Checkerboard assay. *In vitro* interaction of FSA, its analogues GKFA17, GKFA37, GKFA51, GKFA61 vs (**A**) ERY (**B**) SPC (**C**) CLR (**D**)RIF against *M. tuberculosis*, H37Rv strain. Interaction is interpreted as synergy FICI ≤ 0.5; no interaction 0.5<FICI ≤ 4; antagonistic > 4. **.** Data are representative of two biological replicates.

	Drug combination	**Compound**	**MIC_{90} $(\mu M)_{individual}$**	**MIC_{90} $(\mu M)_{combined}$**	**FIC**	**FICI**
A	FSA/ analogues and ERY	FSA ERY	2.42 109	0.30 3.41	0.12 0.03	0.15
		GKFA17 ERY	17 109	4.25 13.63	0.25 0.13	0.38
		GKFA37 ERY	2.42 109	0.61 27.25	0.25 0.25	0.50
		GKFA51 ERY	5.26 109	0.61 27.25	0.12 0.25	0.37
		GKFA61 ERY	13.87 218	3.47 54.5	0.25 0.25	0.50
B	FSA/ analogues and SPC	FSA SPC	2.42 201	0.3 12.5	0.12 0.06	0.18
		GKFA17 SPC	8.30 201	2.08 12.56	0.25 0.06	0.31
		GKFA37 SPC	2.43 101	0.30 25.25	0.12 0.25	0.37
		GKFA51 SPC	4.62 201	1.16 50.25	0.25 0.25	0.50
		GKFA61 SPC	27.73 201	6.93 50.25	0.25 0.25	0.50
C	FSA/ analogues and CLR	FSA CLR	1.21 0.3	0.31 0.08	0.26 0.26	0.52
		GKFA17 CLR	4.25 0.15	2.12 0.04	0.50 0.27	0.57
		GKFA37 CLR	2.50 0.30	1.25 0.04	0.50 0.13	0.63
		GKFA51 CLR	2.31 0.15	0.58 0.08	0.25 0.53	0.78
		GKFA61 CLR	13.87 0.15	3.47 0.04	0.25 0.27	0.52
D	FSA/analogues and RIF	FSA RIF	2.42 0.01	0.61 0.003	0.25 0.30	0.55
		GKFA17 RIF	4.16 0.005	2.08 0.0006	0.50 0.12	0.62
		GKFA37 RIF	1.21 0.005	0.61 0.001	0.50 0.20	0.70
		GKFA51 RIF	2.31 0.005	1.16 0.001	0.50 0.20	0.70
		GKFA61	13.87	1.73	0.13	0.63

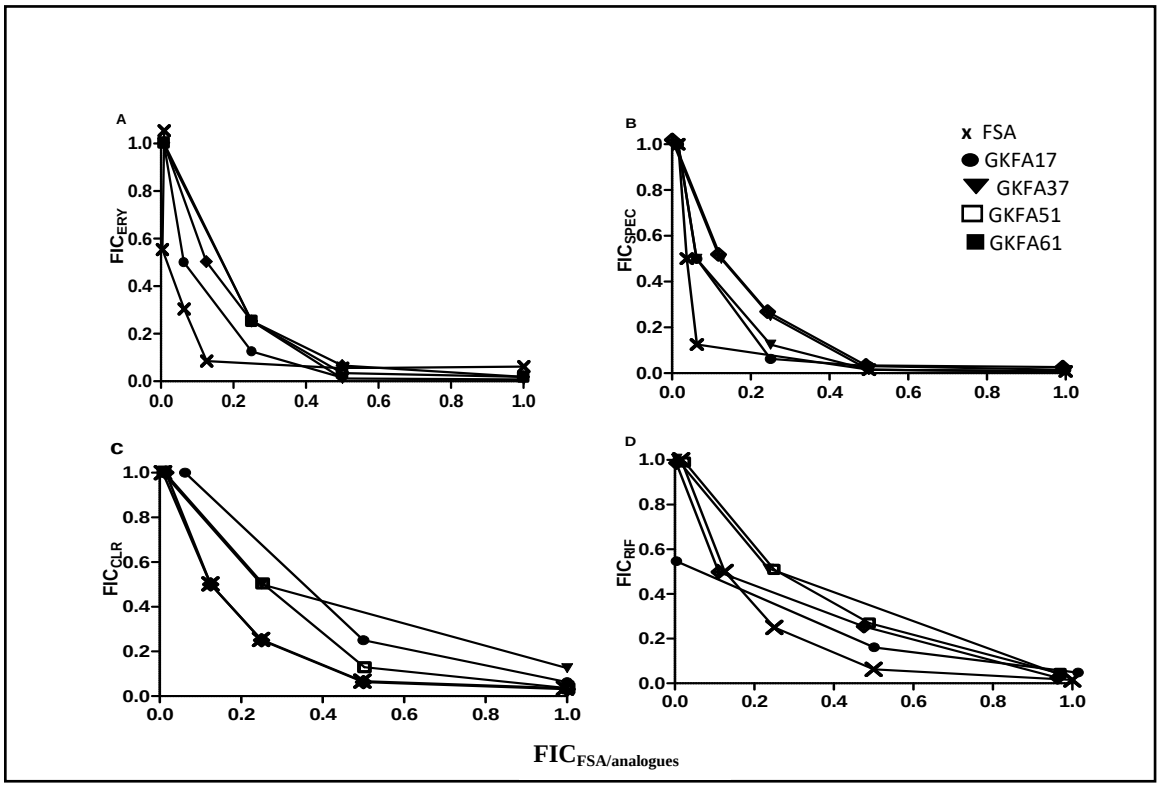

Figure 3-2 Interaction assay on 96-well plates. Interactions between FSA and its analogues when combined with (**A**) ERY, (**B**) SPC, (**C**) CLR, (**D**) RIF against wild–type *M. tuberculosis* H37Rv. Data are representative of two biological replicates.

3.2.2. Synergy and ability to restore susceptibility to drug-resistant isolates

On the basis of the synergy displayed by FSA and/or its analogues with SPC **(Table 3.1)**, a comparative evaluation was performed on wild-type *M. tuberculosis* and two resistant strains: FSA-R, which is resistant to FSA, and SPC-R, which is resistant to SPC. The SPC-R resistant mutants in *rrs* gene, G1379T, generated in the presence of 5X MIC_{99} SPC showed > 64 fold increase in MIC_{99} (Kigondu, 2015), whereas the FSA-R mutants were obtained as already mentioned **(Chapter 2 section 2.2.4).**

Here, the potential to counter pre-existing drug resistance using strongly synergistic combinations was examined. The interaction between SPC and FSA **(Figure 3-3A)**, with FICI value = 0.15, displayed a higher inhibitory activity against both the FSA-R and SPC-R

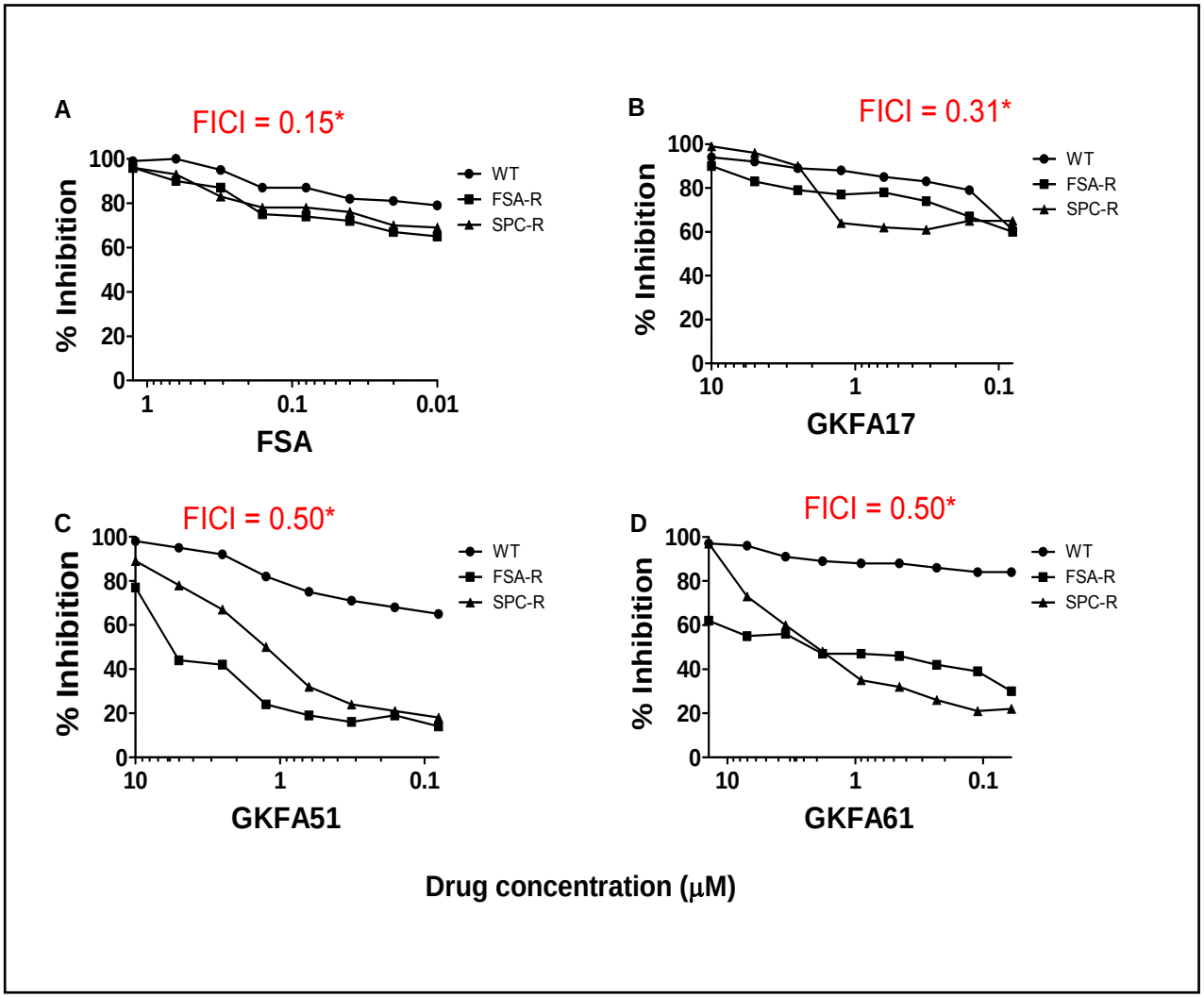

Figure 3-3 Compairing potency in WT strain vs inhibition in mutants. Two-drug interactions between FSA its analogues GKFA17, GKFA51, GKFA61 in combination with sub-inhibitory concentrations of SPC against wild–type, FSA-R and SPC-R mutants. *FICI values indicated are data obtained in experiment discussed (section 3.2.1, Table 3.1) Data are representative of two biological replicates.

strains. On the other hand, the interaction between SPC and GKFA51 **(**FICI value = 0.5), and SPC and GKFA61 **(**FICI = 0.5) **(Figure 3-2C & D)** was less inhibitory.

Figure 3-4 shows the correlation between the FICI values determined against wild-type *M. tuberculosis*, and the inhibitory effects of the respective combinations against the corresponding FSA-R and SPC-R mutants. A SPC derivative, 1599, which has been reported to overcome native drug efflux was also evaluated

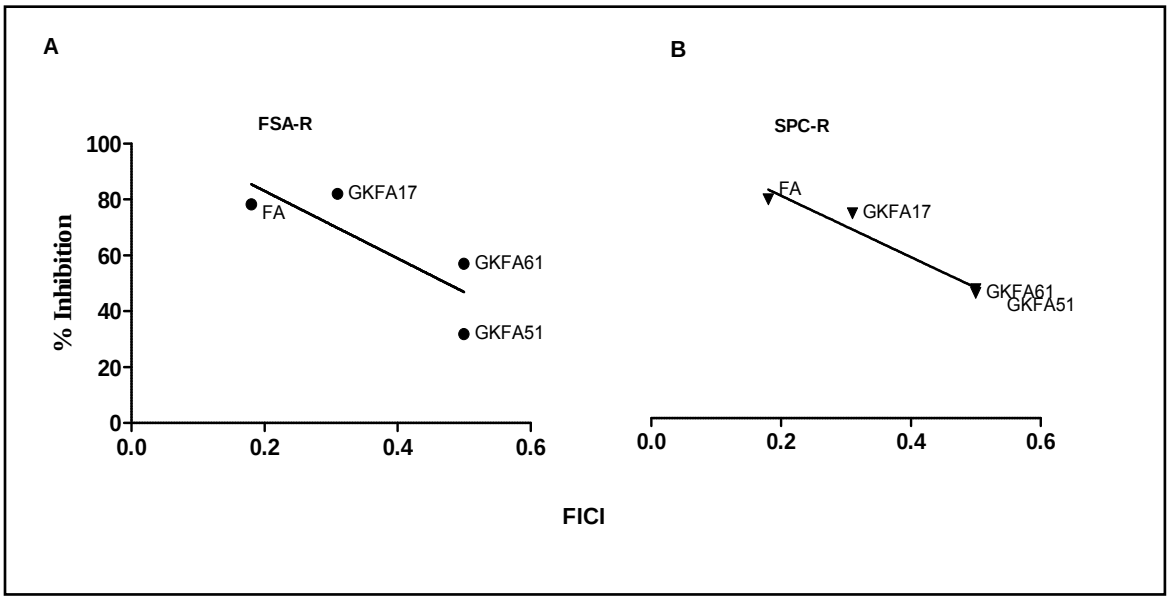

.

Figure 3-4 Compairing potency in WT strain vs inhibition in mutants. Correlation between potency (FICI values) versus activity (% Inhibition) of FSA and its analogues GKFA17, GKFA51, GKFA61 in combination with sub-inhibitory concentration of (SPC). Assay performed on checkerboard using H37Rv wild–type, and resistant mutants, FSA –R; r^2=0.679 and SPC-R ; r^2 = 0.947 respectively.

When the subinhibitory MIC_{90} of 1599 was combined with FSA and its analogues, the values

0.5 > FICI < 4 were obtained, which suggested no interactions (**Table 3.2).**

Table 3-2 *In vitro* interaction of fusidic acid (FSA), its analogues GKFA17, GKFA37, GKFA51, GKFA61 vs a spectinamide, 1599, against *M. tuberculosis*, H37Rv strain. Interaction is interpreted as synergy FICI ≤ 0.5; no interaction 0.5< FICI ≤ 4; antagonistic > 4 Data are representative of two biological replicates.

Drug combination	Compound	MIC_{90} $(\mu M)_{individual}$	MIC_{90} $(\mu M)_{combined}$	FIC	FICI
Fusidic acid/ analogues and 1599	FSA	2.40	0.61	0.25	0.75
	1599	1.04	0.52	0.50	
	GKFA17	33	8.30	0.25	0.75
	1599	1.04	0.52	0.50	
	GKFA37	0.52	0.07	0.13	0.63
	1599	1.04	0.52	0.50	
	GKFA51	5.26	2.63	0.50	1.00
	1599	1.04	0.52	0.50	
	GKFA61	14	7.0	0.50	1.00
	1599	1.04	0.52	0.50	

Furthermore, these combinations did not display any significant inhibitory effect against the FSA-R mutant, **(Figure 3-5)**. The apparent efficacy displayed by these FSA derivatives against the FSA-R mutant in the combination **(Figure 3-5)** was attributed to their disparate activities when tested individually **(Appendix 2).**

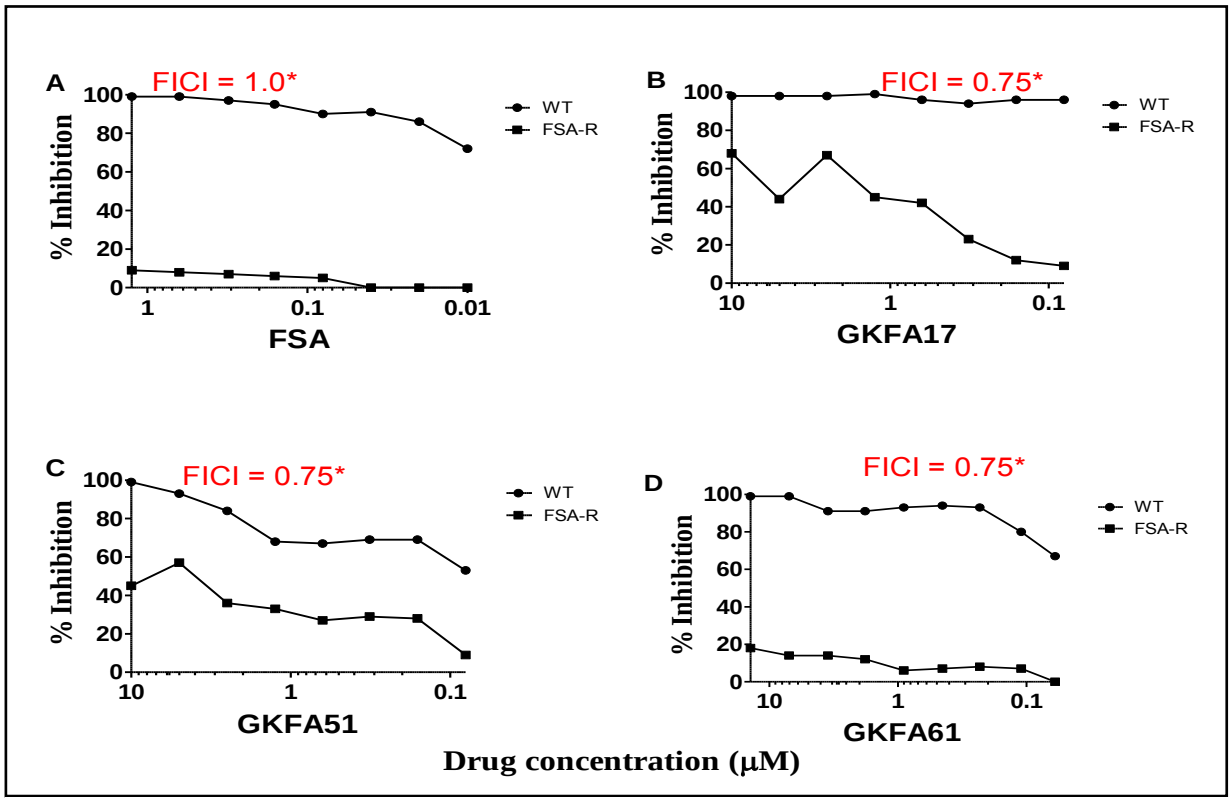

Figure 3-5 Compairing potency in WT strain vs inhibition in mutants. Two-drug interaction between FSA and its analogues GKFA17, GKFA51, GKFA61 in combination with the spectinamide, 1599 using wild–type H37Rv and the resistant strain, FSA-R .

*FICI values indicated are data obtained in experiment shown (Table 3.2) Data are representative of two biological replicates.

3.2.3. Potential use of synergistic combinations to overcome drug resistance in standard TB treatment regimens.

In order to investigate synergy as an approach to overcoming drug resistance, SPC was selected for use in this drug combination study because (i) it exhibited potent synergistic interactions with FSA and its selected analogues, and (ii) greater inhibitory effects were elicited by the potent interactions consisting of SPC against the drug resistant mutants, FSA-R and SPC-R, of *M. tuberculosis.* SPC was therefore included for a further combination study with RIF and INH, the two frontline drugs that form the backbone of TB treatment. RIF and INH were titrated using checkerboard titration in 96-well microtiter plates with decreasing sub-inhibitory concentrations of SPC added as an overlay into the individual plates (½X, ¼X,

1/8X. 1/16X MIC) as illustrated **(Figure 6-2)** experimental **chapter 6** . The result of the experiment performed against the susceptible *M. tuberculosis* **(Figure 3-6A)** suggests synergy with both ¼ X and ½ X MICs of SPC. This finding from the checkerboard assay was further confirmed with time-kill kinetics **(Figure 3-6B)**. The time-kill assay showed that the addition of SPC to the RIF-INH combination maintained a constant viable bacterial population over 14 days after inoculation.

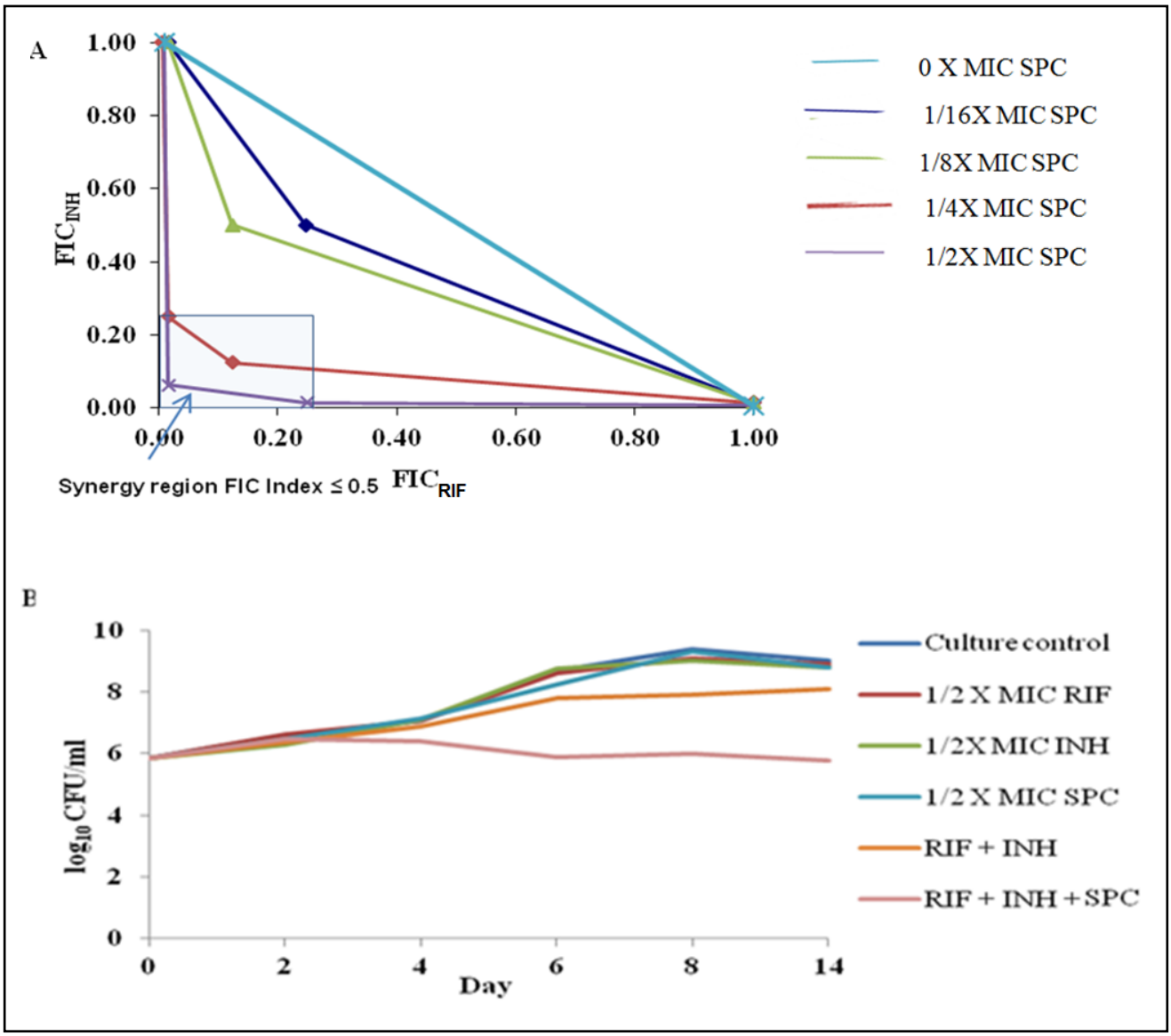

Figure 3-6 Three-drug *in vitro* assay Interaction between RIF, INH and SPC against *M. tuberculosis* (**A**) Checkerboard experiment on five 96-well microtitre plates at SPC concentrations of ½ , ¼ , 1/8, 1/16, and 0X MICs. (**B**) Time-kill assay of drug combination consisting of RIF, INH and SPC at ½ x MICs. Data are from the representative experiment performed in triplicate.

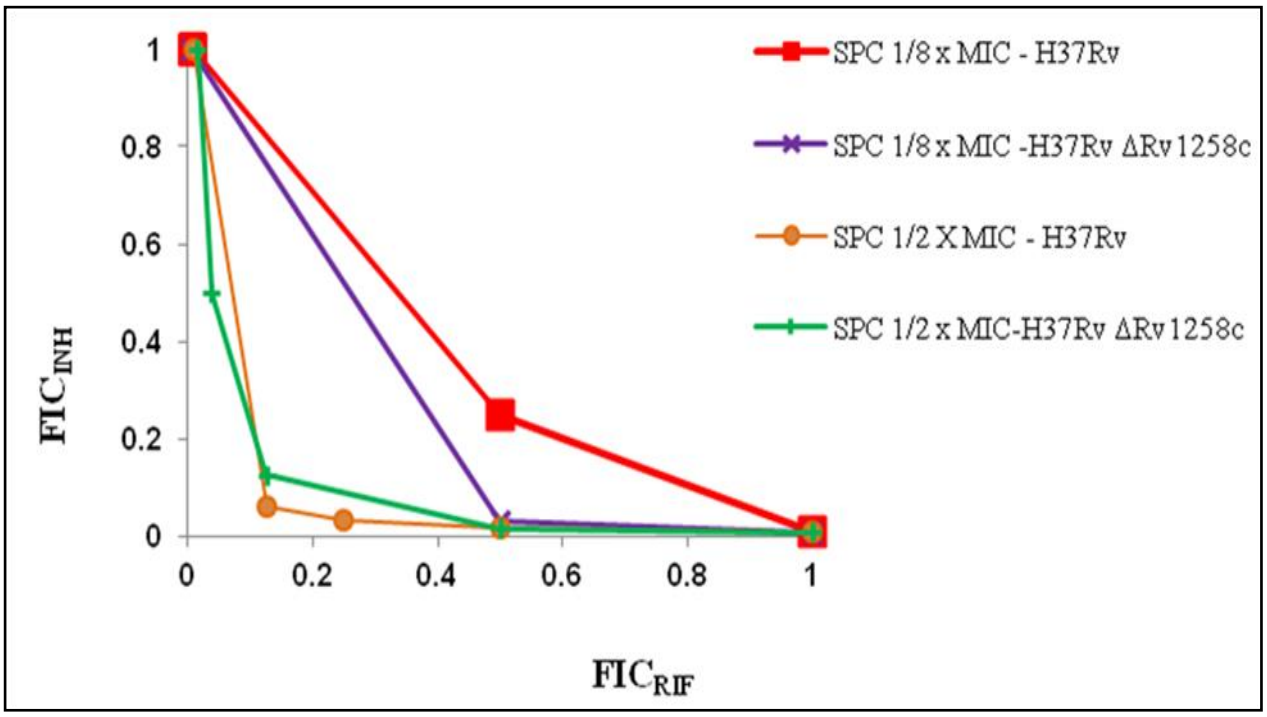

Figure 3-7 Interaction of RIF, INH and SPC against a knock-out H37Rv mutant. Checkerboard experiment at SPC concentrations of ½ X, and 1/8 X MIC against wild-type *M. tuberculosis* and Δ1258c deletion mutant. Data are from the representative experiment performed in biological duplicate.

The multidrug drug transporter Rv1258c has been associated with intrinsic resistance to SPC.[2] To explore the influence of Rv1258c in the RIF-INH plus SPC interaction, the three drugs were tested against a deletion mutant, Δ1258c **(Figure 3-7)**. No significant change in susceptibility was observed with this mutant compared to the wild-type strain. This suggests that a different mechanism may be responsible for the synergistic interaction displayed by the RIF-INH plus SPC combination. Since *M. tuberculosis* survives and replicates in macrophages using different mechanisms, the synergy of the RIF-INH plus SPC combination was evaluated against intracellular bacilli in *M. tuberculosis*-infected THP-1 cells. The three-drug combination, RIF-INH and SPC, showed inhibitory activity at 1X concentration **(Figure 3-8)**. No inhibition was observed when similar concentrations of each drug were applied individually. Likewise, no inhibition was exhibited with the RIF-INH combination. These key observations may require validation with other experiments such as CFU enumeration.

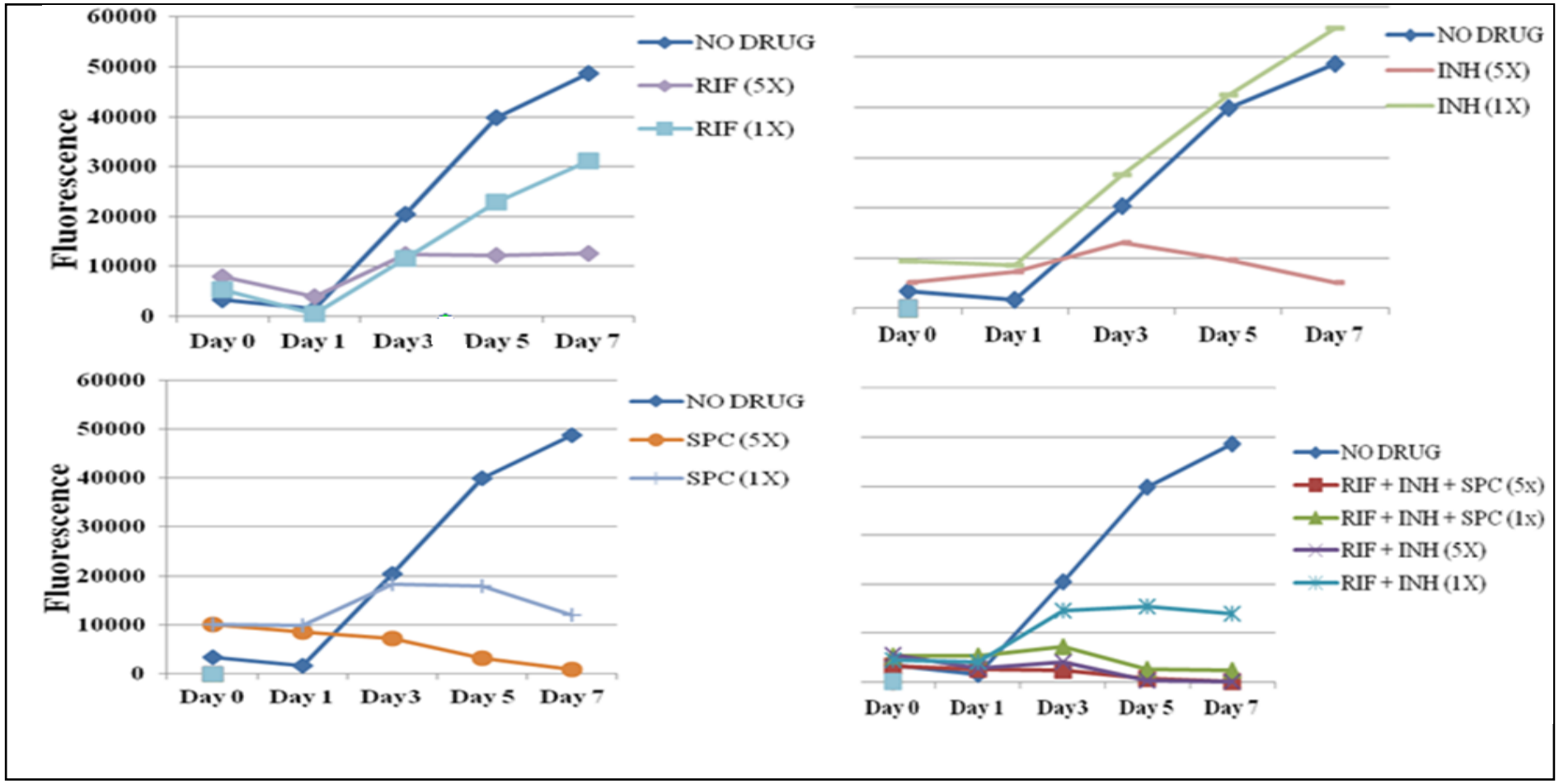

Figure 3-8 Intracellular activity of RIF, INH and SPC combination using THP-1 cells. *M. tuberculosis* H37Rv ::gfp at a multiplicity of infection (MOI), cells:bacilli 1:10 were subjected to several concentrations of test drugs (1X and 5X MICs) . Plots detail the inhibitory activity of the drugs as determined by fluorescence intensity. Data are from the representative experiment performed in technical duplicate.

On the basis of the potency observed with the three-drug combination in both *in vitro* and *ex vivo* experiments, the ability of this synergistic combination to overcome genetic resistance to one of the combination partner drugs was explored. A RIF-resistant mutant with the genetic mutation S531L encoded on the *rpoB* ß-clamp subunit was used for this investigation. Duplicate checkerboard experiments showed that, upon the addition of ½X MIC SPC to the RIF–INH plate, the drugs exhibited synergy against the *rpoB* mutant (FICI ≤ 0.5) **(Figure 3-9)**.

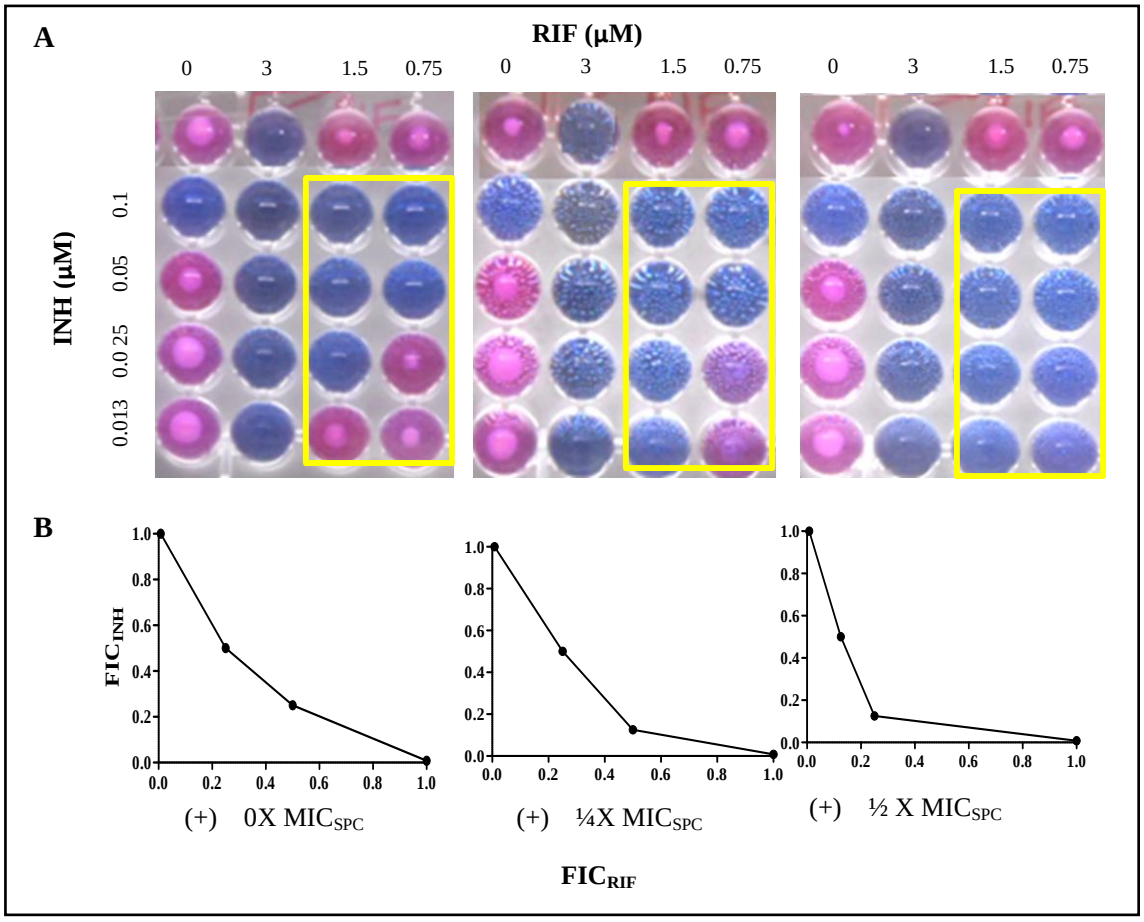

Figure 3-9 Activity against pre-MDR *M. tuberculosis* . (A) Resazurin assay against *M. tuberculosis rpoB* mutant with drug combination RIF-INH-(0X MIC)SPC ; RIF-INH-(1/4X MIC) SPC and RIF-INH-(1/2X MIC)SPC (B) Isobolograms showing RIF-INH-(0X MIC)SPC; RIF-INH-(1/4X MIC) SPC and RIF-INH-(1/2X MIC)SPC

3.3. Discussion

Bacterial evolution makes it difficult and conceivably impossible to overcome antibiotic resistance (Wright, 2016). However, different approaches can be used to circumvent and achieve efficacy in the presence of a resistant bacterium. Combination therapies offer one method. In a previous study, Chen *et al*. demonstrated a synergistic interaction between SQ109 and RIF when tested against RIF^R isolates: at 0.5X MIC, SQ109 was able to increase RIF's activity against *de facto* resistant organisms in a dose-dependent manner (Chen et al., 2006). Recently, Yang *et al* reported the enhanced efficacy of a imipenem-colistin combination against multiple drug-resistant *Enterobacter cloacae* using both *in vitro* activity and a *Galleria mellonela* model (Yang et al., 2016). Despite the above mentioned efforts, very few studies have been undertaken to illustrate the association between the degree of synergy and the ability of the particular drug combination to overcome pre-existing genetic resistance. In a clinical study, Ankomah *et al*. suggested that drugs acting synergistically can prevent treatment failure even when bacteria resistant to one of the drugs are present at the beginning of therapy (Ankomah, Johnson & Levin, 2013).

In the first part of this study, the checkerboard assay was used to investigate synergistic interactions between FSA and selected analogues in combination with ERY, SPC, CLR and RIF. The notable synergy displayed with ERY and not other macrolides such as CLR may suggest a specific ERY-FSA interaction which may not exist with other macrolides. Synergy was also evident between FSA/analogues and SPC. The conventional wisdom, "hitting it hard" for the best outcome, was used to demonstrate that the more potent acting synergistically antibiotics are effective at overcoming pre-existing drug resistance emanating from either of the combined partners. As shown in this study, the combination of FSA and SPC resulted in greater potency, that is, a low FICI value, against drug susceptible

bacteria compared to the interaction between its analogues and SPC. Notably, the same FSA-SPC combination exerted a greater inhibitory effect against the FSA-R and SPC-R mutants. There is no definitive explanation for this finding at the present moment. However, it is likely that the sustained drug pressure emanating from potent synergistic interactions results in an increased effective dose of the drug combination. In addition, some studies have suggested that the drug susceptibility of pathogens is significantly enhanced as a result of a reduced efflux pump efficiency either by genetic manipulation (Lomovskaya et al., 1999) or addition of efflux pump inhibitors (Markham & Neyfakh, 1996; Markham, 1999). The clinical relevance of this finding is that, despite the existence of bacterial resistance against a combination partner, it would still be possible to achieve optimal therapeutic outcomes with the use of appropriate potent drug combinations.

The second part of this study was aimed at developing a novel combination(s) in a three-drug assay. Previous studies have demonstrated the potential of having three-drug combinations when compared to individual or two-drug regimens. Recently, Tekin *et al.* reported that combinations of three different antibiotics can often overcome bacteria resistance to antibiotics, even when none of the three antibiotics on their own — or even two of the three together — is effective (Tekin et al., 2016). In addition, based on the drug interaction studies, Ramon-Garcia *et al.* hypothesized that the synergistic activity of the triplet combination might have multiplicative effects (Ramon-Garcia et al., 2011). SPC, a drug that exhibited potent interaction with FSA **(Table 2.1)**, was used in this study. Here, SPC was deployed as part of a three-drug regimen which also included RIF and INH;- the two drugs that form the cornerstone of TB treatment. Previous studies have shown the interaction between RIF and INH against *M. tuberculosis* to have a no interaction effect (Bhusal, Shiohira & Yamane, 2005). The inclusion of SPC in this drug regimen was

underpinned by studies elsewhere, which reported that 24 out of 70 random combinations tested were synergistically active in *M. smegmatis* (Ramon-Garcia et al., 2011). This suggests a large unexplored pool of synergistic combinations. Besides, SPC exhibited synergy with several compounds both *in vitro* and *ex vivo* (Ramon-Garcia et al., 2011). However, SPC is not active against *M. tuberculosis* when administered individually (Lee et al., 2014).

In the three-drug combination assay, synergy resulted when sub-inhibitory concentrations (½ and ¼X MICs) of SPC were titrated into media containing RIF and INH **(Figure 3-5A)**. This finding correlated well with the results of time-kill kinetics **(Figure 3-5B)**. The time-kill assay suggested, however, that the inhibitory effect of this three-drug interaction was bacteriostatic ($0 \geq \log_{10}$ CFU <3 reduction) and not bactericidal. This observation supports previous work which noted that, if bactericidal drugs are most potent with actively dividing cells, then the inhibition of growth induced by a bacteriostatic drug may result in an overall static effect when the drug is used in combination with a bactericidal drug (Ocampo et al., 2014). However, the resulting synergistic interaction achieves a more efficient clearance at lower concentrations.

Towards elucidating the mechanism of action for this synergistic interaction, a knockout mutant was used which was deficient in major superfamily multidrug exporter protein, Rv1258c. This protein has been shown to be responsible for intrinsic SPC resistance (Lehár et al., 2009). The interaction of RIF-INH plus SPC using the Rv1258c-deficient mutant did not reveal significant hyper susceptibility, implying that the evident synergy may be as a result of a different antibiotic target interaction.

In attempting to exploit synergy for potential optimal treatment outcomes, an investigation of the RIF-INH plus SPC interaction was performed in a RIF-resistant mutant. The *rpoB* resistant strain had an MIC value > 50 times the MIC for the drug susceptible *M.*

tuberculosis. **Figure 3-9** shows that the addition of ½ and ¼X MICs of SPC also facilitated inhibition of the drug resistant *M. tuberculosis* strain. As with the drug susceptible H37Rv strain, a clear explanation for the synergy between RIF-INH plus SPC combination against the *rpoB* mutant is presently lacking. INH targets mycobacterial cell wall synthesis, presumably allowing more SPC to get into the bacteria. However, access alone may not necessarily contribute to the synergistic interaction. Chen *et al.* reported synergy between SQ109, a presumed cell wall synthesis inhibitor, and RIF. On the other hand EMB, which also affects mycobacterial cell wall synthesis, did not exhibit synergy with RIF (Torella, Chait & Kishony, 2010).

Studies have shown RIF to be an efficient inducer of cytochrome P450 (CYP 450), a superfamily of haem-containing enzymes involved in the biosynthesis of compounds such as sterols, steroids, and fatty acids as well as detoxification of xenobiotics and chemicals (Sarathy et al., 2016). RIF has been linked with the induction of CYP both in humans and in *M. tuberculosis* (Zhang et al., 2007). The elevated levels of CYP has been associated with drug resistance due to the enhanced rate of elimination of the drugs by metabolism and detoxification pathways. INH, on the other hand inhibits CYP in *M. tuberculosis* (Zhang et al., 2007). The ability of INH to inhibit CYP in *M. tuberculosis* may contribute to synergy in the RIF-INH plus SPC combination when the active form of INH is not rapidly eliminated inside *M. tuberculosis* and at the same time, the drugs act on multiple targets.

There are prospects of combining SPC with RIF-INH . SPC, given by intramuscular injection to achieve therapeutic concentrations in serum of about 100 mg/L 1 h after a single 2-g dose, a ≥4-fold increase in its effectiveness within the triple combination would potentially allow for oral formulation. This is critical, especially in treating TB out-patients. In summary, these *in vitro* and *ex vivo* results suggests that the RIF-INH plus triple-

combination, may be an effective therapeutic option for the treatment of both the drug susceptible and resistant *M. tuberculosis* infections. In overall, these investigations suggest that synergy can be exploited to potentially improve treatment.

Chapter 4

Delineating bactericidal versus bacteriostatic agents

4.1. Background

Despite the achievements realized with whole-cell (WCS) assays that have yielded numerous hit compounds against TB, the development and validation of methods for rapidly selecting bactericidal compounds still remains a challenge. Approaches such as Microplate Alamar Blue (MABA) and the Resazurin-based Microplate Assay (REMA) merely provide MIC information and do not predict the cidality of the test compounds. Moreover, the reporter genes such as luciferase (*lux*) or *gfp* require modifications for each strain (Primm & Franzblau, 2007). So far, the conventional gold standard method of delineating bactericidal compounds involves plating of bacilli following drug exposure and enumerating the colony forming units (CFUs) after 3-4 weeks. This is labour intensive, difficult to automate and slow, and so is not easy to adopt for hit prioritization of small molecules emanating from HTS cascade.

The main aim of chapter 4 was to develop simple, rapid and robust assays that would act as preliminary screening tool(s) to enable the initial assessment and determination of bactericidal compounds. Such understanding would aid in the prioritization of hits for the progression into drug discovery programmes. In addition, this chapter explored methodologies that allow for a fast and reliable monitoring of mycobacterial physiological state as well as cell growth, particularly within the context of new TB drug discovery.

A modified "spot-assay" technique, reported by Kaur *et al.* was employed to rapidly delineate bactericidal and bacteriostatic drugs, **Chapter 4 section 4.2.2** (Kaur et al., 2015). The modified spot-assay method relied on establishing a correlation by a visual comparison

of the bacterial outgrowth in the 24-well agar plate containing the test agents (4X, 2X, 1X and ½X MIC) with the wells having the reference bactericidal/static agents. The determination of MIC_{90} formed the starting point for the spot-assay on a 96-well plate, **(Appendix 3)**. The fast-growing surrogate *M. smegmatis* mc^2155::gfp was used to enable rapid assessment of the drugs susceptibility profiles. Plating was subsequently carried out on a 24-well plate upon antibiotic treatment at 4X, 2X, 1X and ½X MICs and compared with that of the reference drugs. The absence or very few colonies at concentrations ≥ 1X MIC implied bactericidal effect of the test agents; also exhibited by the reference drug, DCS. On the other hand, bacteriostatic agents displayed the presence of bacterial colonies at 1X MIC or possibly higher concentrations. This modified approach has the advantage of offering a simple, economical and qualitative HTS with the potential to impact on the TB drug discovery process.

In addition to the spot assay, **section 4.2.3** of this chapter illustrated the work employed through the use of flow cytometry (FCM) and the fluorescent microscopy techniques for rapid assessment of mycobacterial physiological state as well as the growth inhibitory effect of antibiotic drugs against *M. smegmatis*, a fast growing surrogate. This is key, considering the slow growth of *M. tuberculosis*, coupled with the challenges of working with a human pathogen under biological safety level 3 conditions. This has contributed to difficulty of gaining insight into the organism's physiology and metabolism (Warner, 2014). The fluorescent techniques and other optical detector methods are opted for, to provide a rapid and real-time assessment of bacterial viability upon antibiotic treatment.

4.2. Results

4.2.1. Bactericidal/static evaluation of antibiotic drugs using the spot assay technique

The MICs of the selected drugs were determined against *M. smegmatis* and are listed in **Table 4.1**

Table 4-1 MIC_{90} of the selected test drugs against *M. smegmatis*

Compound	**Abbreviation**	**MIC_{90} (µM)**
Capreomycin	CAP	0.8
Ethambutol	EMB	1.0
Bedaquiline	BDQ	0.2
Isoniazid	INH	13.0
Spectinomycin	SPC	50.0
Rifampicin	RIF	10.0
Erythromycin	ERY	8.0
Streptomycin	STR	0.5
Hygromycin	HYG	4.1
Fusidic acid	FSA	80.8
D-cycloserine	DCS	75.0

A time-curve assay was used to determine the bactericidal-static activity of FSA against *M. smegmatis* **(Figure 4.1)**. At MIC_{90} of 80.8 µM, FSA exhibited bacteriostatic activity over the 24 h period. Information on the bactericidal activity of DCS against *M. smegmatis* was obtained from previously reported studies (Feng & Barletta, 2003; Peteroy et al., 2000).

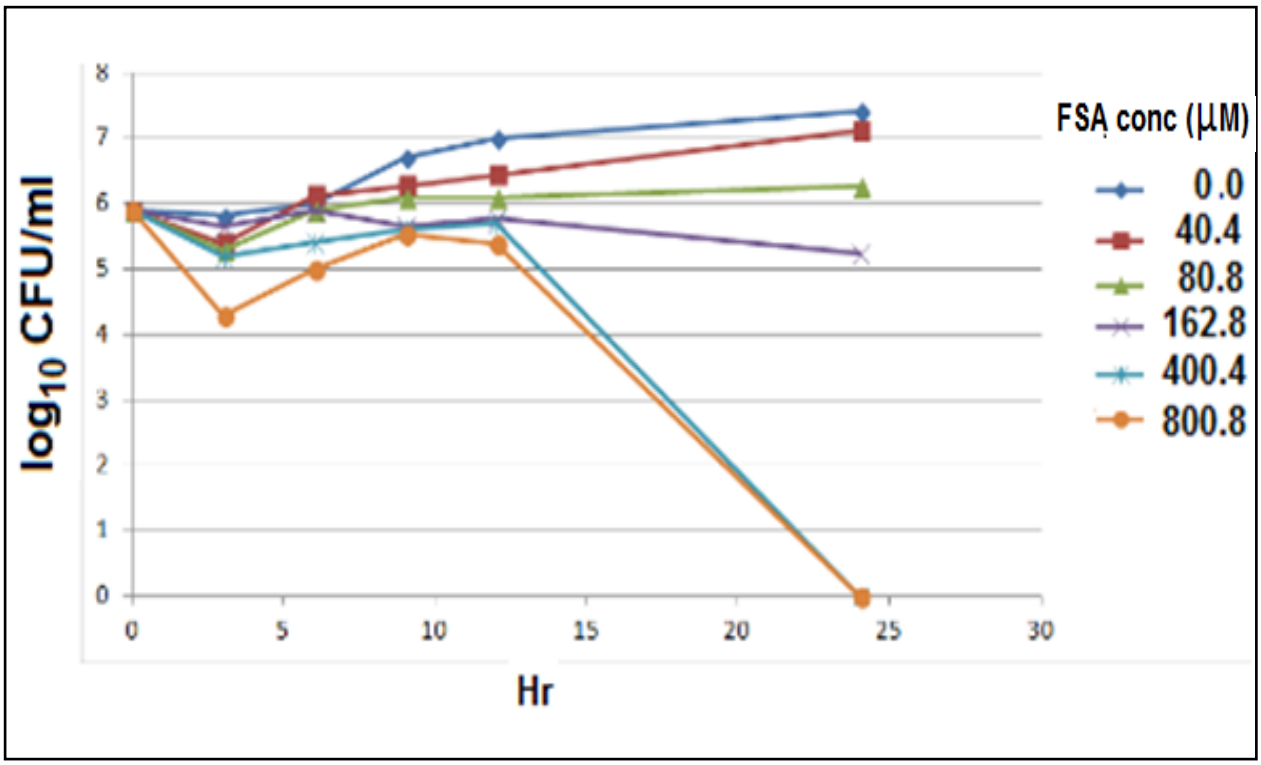

Figure 4-1 Bacteriostatic effect of FSA at MIC_{90} of 80.8 µM. Time-kill experiments for *M. smegmatis* following exposure to FSA concentrations 0, 40.4, 80.8, 162.6, 400.4 and 800.8 µM. Viable cell concentrations were determined by plating on Middlebrook 7H10 agar. Data are from the representative experiment performed in technical duplicate.

FSA and DCS, the two selected drugs, showed distinct patterns in the observed colony forming units **(Figure 4-2)**. Using FSA, a fairly dense population was observed on the culture medium of the 24-well plate that consisted of 1X MIC drug. A similar population density was seen with the 2X MIC population, an indication of the bacteriostatic tendency of the drug. DCS, on the other hand showed remarkably few colonies at 1X MIC and no CFU were observed at 2X MIC presumably because of its bactericidal effect. CAP and ERY exhibited dense mycobacterial populations at the 1X MICs respectively, suggesting bacteriostatic effects. HYG, STR, RIF, EMB and SPC manifested bactericidal activity whereas BDQ yielded an intermediate profile which was difficult to define unequivocally.

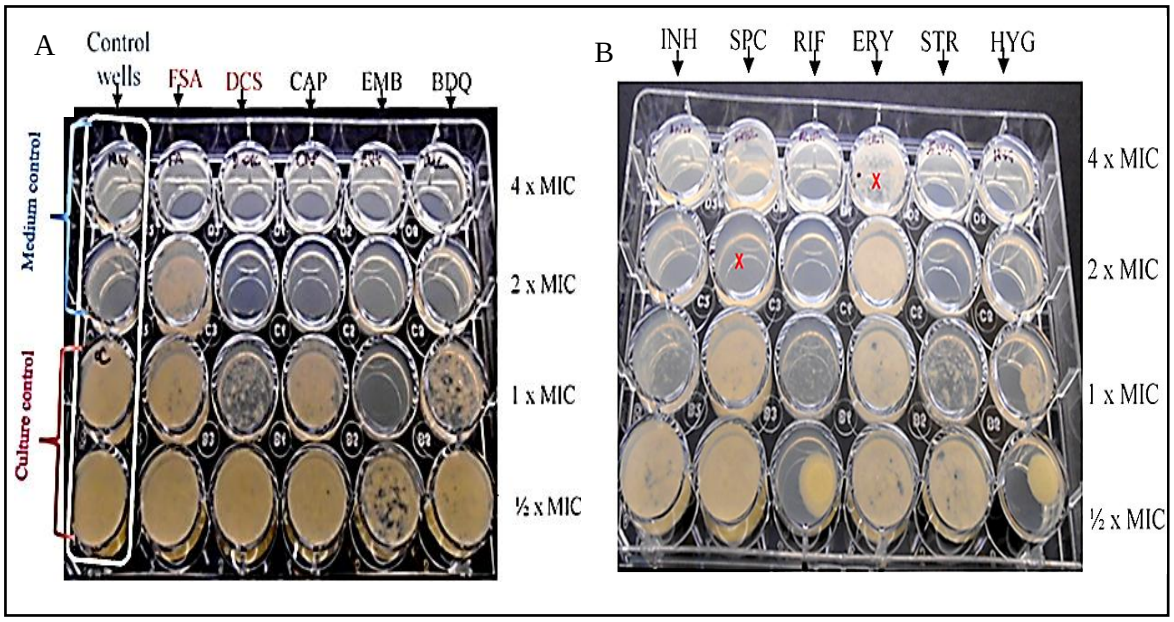

Figure 4-2 Bactericidal versus static effects: 24-well plate spot-assay of selected drugs at 4X, 2X, X and ½X MIC 14 days post incubation. FSA and DCS used as reference for bacteriostatic and bactericidal drugs respectively. CFUs on wells containing the test agents (CAP, EMB, BDQ, INH, SPC, RIF, ERY, STR and HYG) are visually compared with those of reference drugs at their respective concentrations. X- indicates 1 x MIC_{90} wells for SPC and ERY.

These preliminary findings were compared with the reported data from previous studies on *M. smegmatis* **(Table 4.2).**

Table 4-2 Comparison of bacteriostatic/bactericidal activity inferred from the spot assay with the reported data

Compound	**Abbrev.**	**Experimental inference**	**Reported in *M.smegmatis***	**Method used**	**Reference**
Capreomycin	CAP	Static	Cidal	Time-kill	Lin et al., 2014
Ethambutol	EMB	Cidal	Static	Enzyme inhibition	Forbes et al., 2015
Bedaquiline	BDQ	Not clear	Cidal	Oxygen consumption rate	Hards et al., 2015
Isoniazid	INH	Cidal	Cidal	Time-kill	da Silva etal.,, 2009
Spectinomycin	SPC	Cidal	Static	Spot-assay	Kaur et al., 2015
Rifampicin	RIF	Cidal	Cidal	Oxidation and binding	Staudinger et, 2014
Erythromycin	ERY	Static	Static	MBC/MIC assay	Pankey & Sabath, 2004
Streptomycin	STR	Cidal	Cidal	MBC/MIC assay	Heifets & Lindholm-Levy, 1989
Hygromycin	HYG	Cidal	Cidal	Enzyme inhibition	Rosen & Mobashery, 2012

4.2.1 Profiling bacillary populations in log and stationary phases.

FSA and SPC were selected as antibiotic agents owing to their potential for further development as a combination therapy on the basis of the synergy described above **(Chapter 2**). *M. smegmatis* was adopted as proxy for *M. tuberculosis* in developing the assays. Calcein-AM (CA-AM) was used a marker for viable cell; retention of CA-AM by the cells indicate enzyme activity as well as membrane integrity. Propidium iodide (PI) was used a marker for non-viable (membrane-compromised) cells, because it is excluded by intact plasma membranes

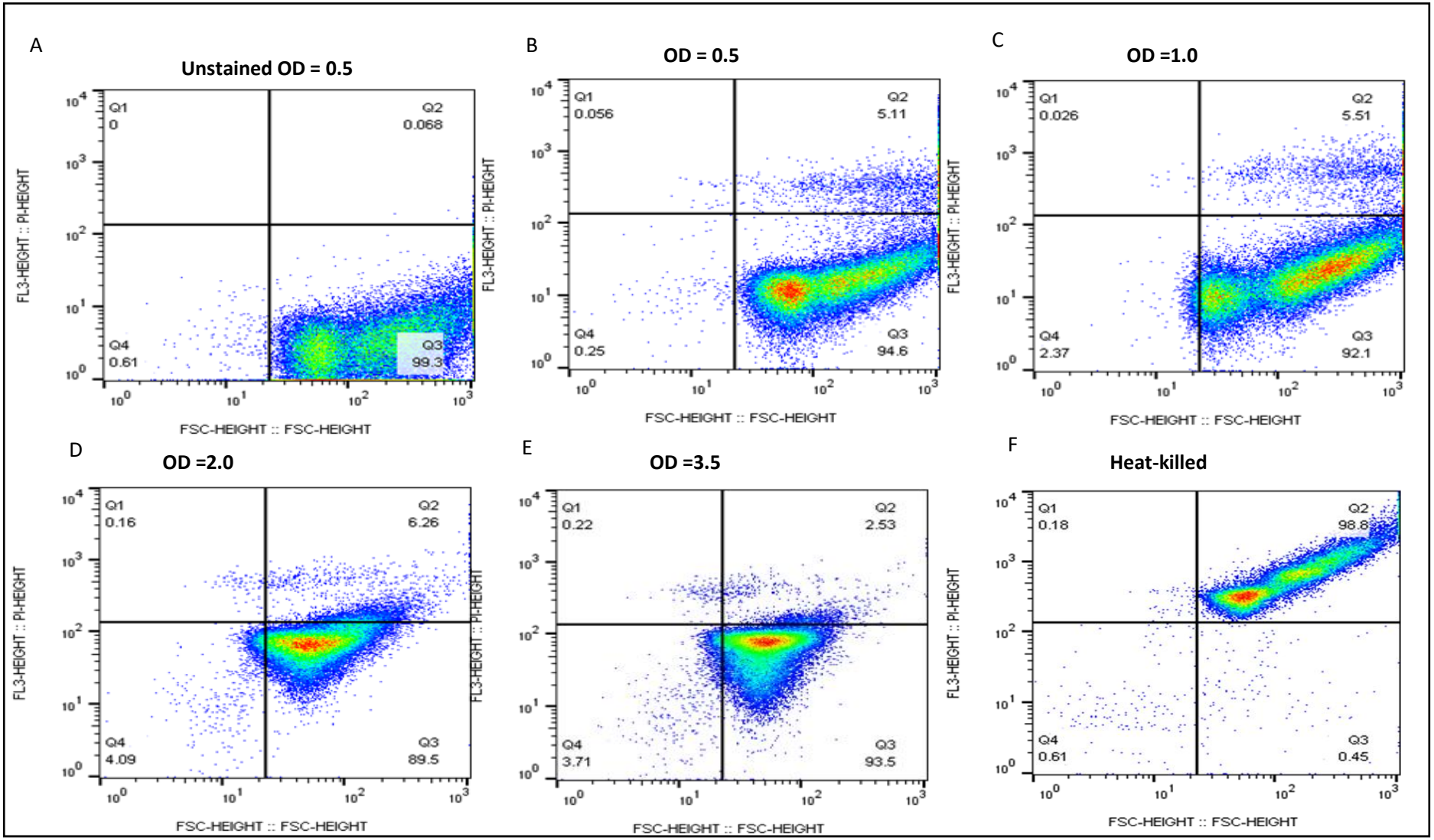
A
Unstained OD = 0.5
Q1
0
Q2
0.068
Q4
0.61
Q3
99.3
B
OD = 0.5
Q1
0.056
Q2
5.11
Q4
0.25
Q3
94.6
C
OD =1.0
Q1
0.026
Q2
5.51
Q4
2.37
Q3
92.1
D
OD =2.0
Q1
0.16
Q2
6.26
Q4
4.09
Q3
89.5
E
OD =3.5
Q1
0.22
Q2
2.53
Q4
3.71
Q3
93.5
F
Heat-killed
Q1
0.18
Q2
98.8
Q4
0.61
Q3
0.45
FL3-HEIGHT :: PI-HEIGHT
FSC-HEIGHT :: FSC-HEIGHT

Figure 4-3 FCM dot plots of *M. smegmatis* (A) unstained at OD_{600} 0.5, and stained with PI at OD_{600} of (B) 0.5 (C) 1.0 (D) 2.0 (E) 3.5 (F) Heat-killed cells. Data are representative from experiments performed in biological duplicate.

In order to assess membrane integrity in both actively replicating and stationary phase bacilli, single-staining by propidium iodide (PI) was utilized. The staining profiles observed during the two phases of growth are shown in **Figure 4-3**. Distinct fluorescence was observed between the stained and unstained cell populations. As the culture progressed from exponential phase to stationary phase, the PI fluorescence intensity measured on the FL3 detector increased, perhaps indicating the presence of more permeabilized cells owing to cell death or injury. At an $OD6_{00}$ of 0.5, indicative of mid-exponential growth phase, less PI fluorescence intensity was observed than at higher OD values - that is, at OD_{600} readings of 1.0, 2.0 and 3.5. In addition, a more compact or homogenous population was evident in the stationary phase culture (OD_{600} of 2.0 and 3.5), which contrasted with the heterogeneity evident in the log phase culture. The inverse profile was observed using the CA-AM stain **(Figure 4-4)**.

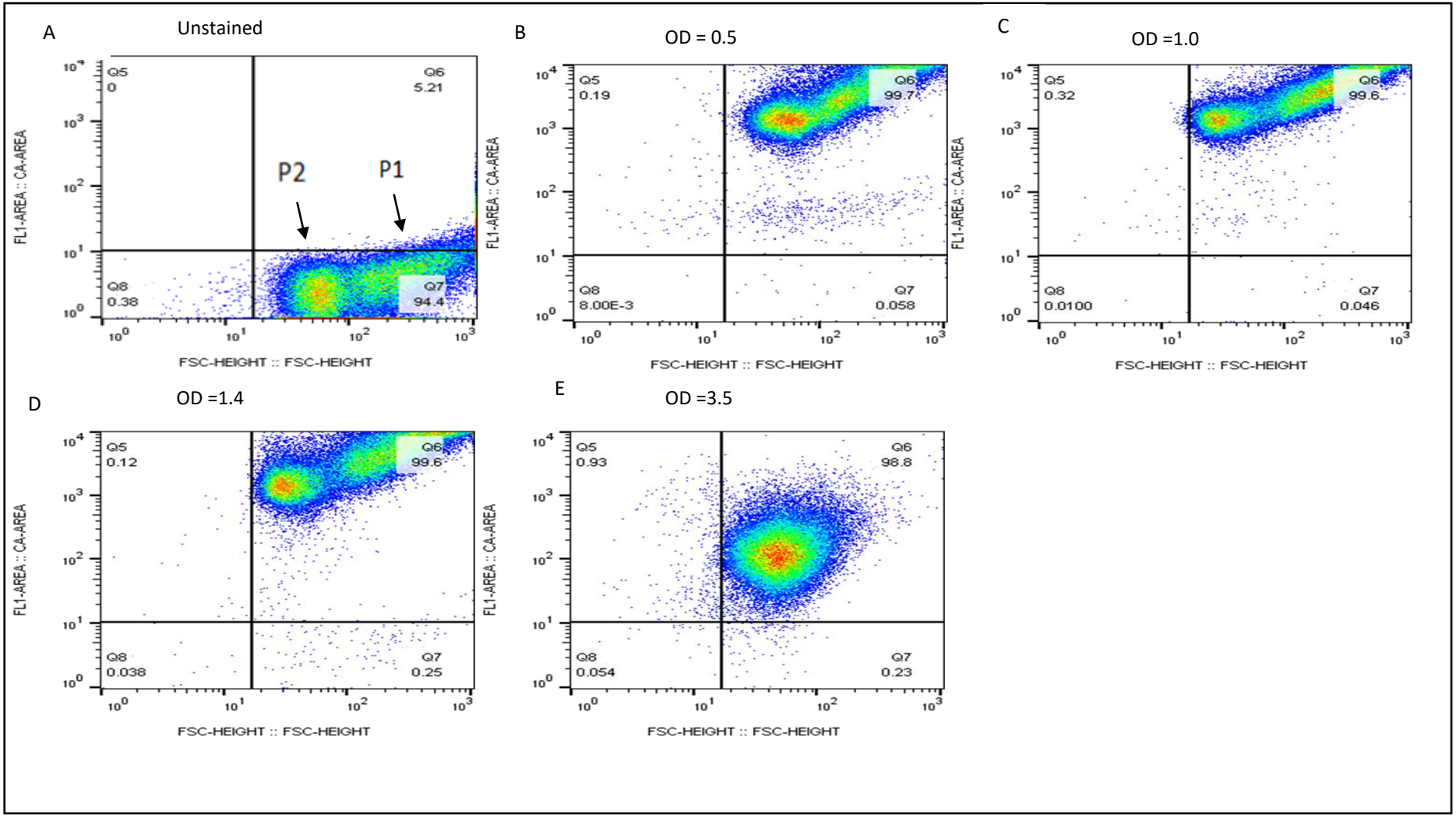

Figure 4-4 **FCM dot plots of *M. smegmatis* (A) unstained at OD_{600} 0.5, and stained with CA-AM at OD_{600} of (B) 0.5 (C) 1.0 (D) 1.4 (E) 3.5.** Data are representative from experiments performed in biological duplicate.

Higher CA-AM fluorescence was observed with log-phase cultures (OD 0.5, 1.0 and 1.4) compared to stationary phase (OD 3.5). That is, the proportion of PI and CA-AM stained populations correlated negatively. For both PI and CA-AM stained cells, the stationary phase population (OD_{600} 2.0 or 3.5) profiled by the forward-scatter height (FSC-H), exhibited a shift towards the left relative to the sub-population of the exponentially growing culture, OD_{600} 0.5, **(Figure 4-5)**.

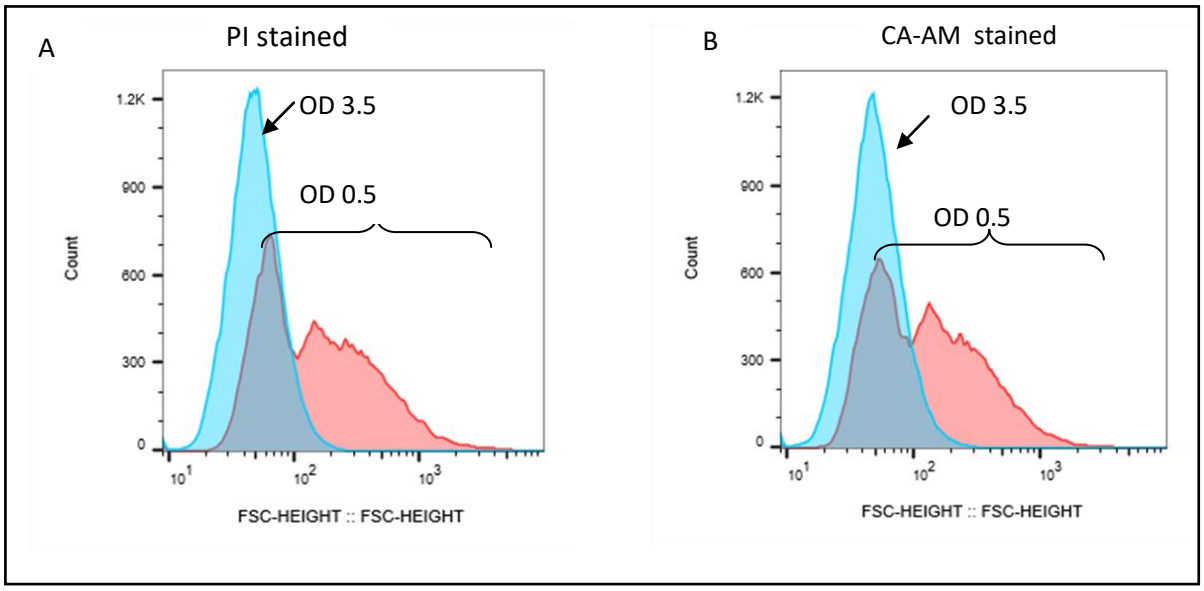

Figure 4-5 FCM histogram overlays of *M. smegmatis* FSC-height (A) PI (B) CA-AM stained at log phase OD_{600} 0.5 and stationary phase OD_{600} 3.5

FSC-H provides a measure of the distribution of cell sizes; therefore, the pattern observed reinforced the interpretation that stationary phase cells are smaller and more homogenous.

To further explore the two sub-populations, P1 and P2, these gated cells were sorted and some sample slides examined under bright-field and fluorescent microscopy for evidence of the differential aggregation. Slides mounted with the P1 sub-population revealed aggregated cells, a triplet and single cells. On the other hand, P2 sub-population displayed mainly doublet and single cells **(Figure 4-6)** which might suggest differential composition in P1 and P2 sub-populations.

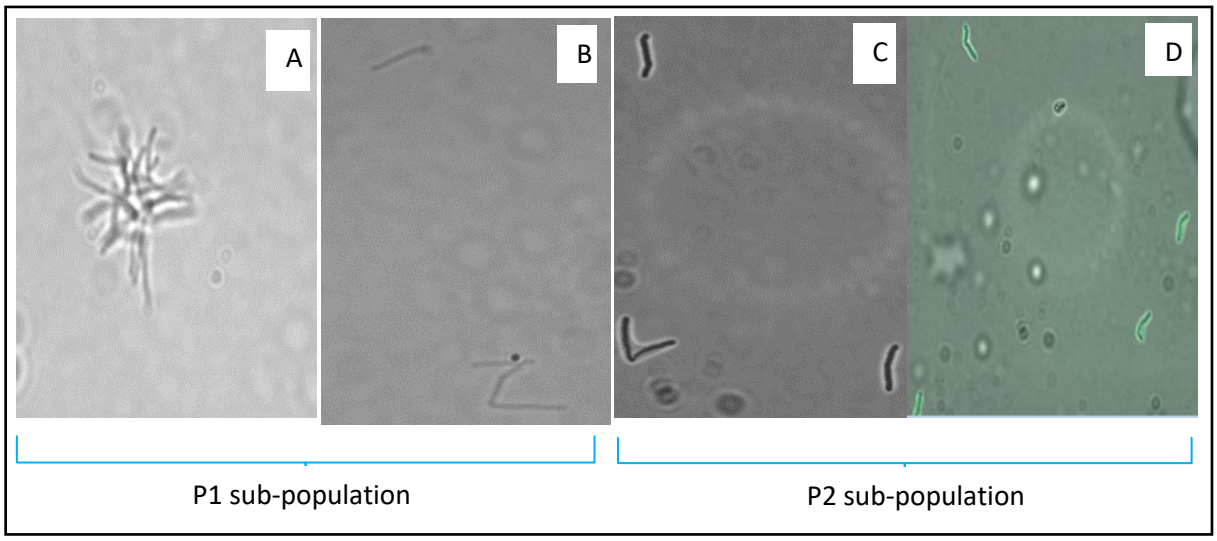

Figure 4-6 Representative microscopic images in bright-field (A-C) and fluorescent microscopy (D) showing *M. smegmatis* after cell-sorting of the two sub-populations; P1 and P2. (A) aggregated cells (B) a singlet and triplet (C) singlets and a doublet (D) singlets bacteria . Selected slides from P1 sub-population manifested aggregated cells, triplets and singlets. On the other hand, viewed slides with P2 sub-population displayed mainly doublets and singlets with notable absence of aggregated cells and triplets. Data are representative of three biological replicate.

4.2.2 Impact of the selected antibiotics on *M. smegmatis* viability and cell damage.

FCM was used to evaluate the viability of *M. smegmatis* after incubation with various concentrations of FSA and SPC. The cells were stained with CA-AM. "Viable cells" were defined as those that were able to reproduce; their reproductive capacity requires both metabolic activity and membrane integrity.(Nebe-von-Caron et al., 2000). The MIC_{90} values of the test drugs were determined using the conventional approach against an *M. smegmatis* gfp mutant.

Exposure to FSA

The respective histograms of the untreated *M. smegmatis* populations; the unstained cells used as a negative control, CA-AM stained at 0 h and CA-AM stained after a 72 h incubation are shown, **(Figure 4-7)**.

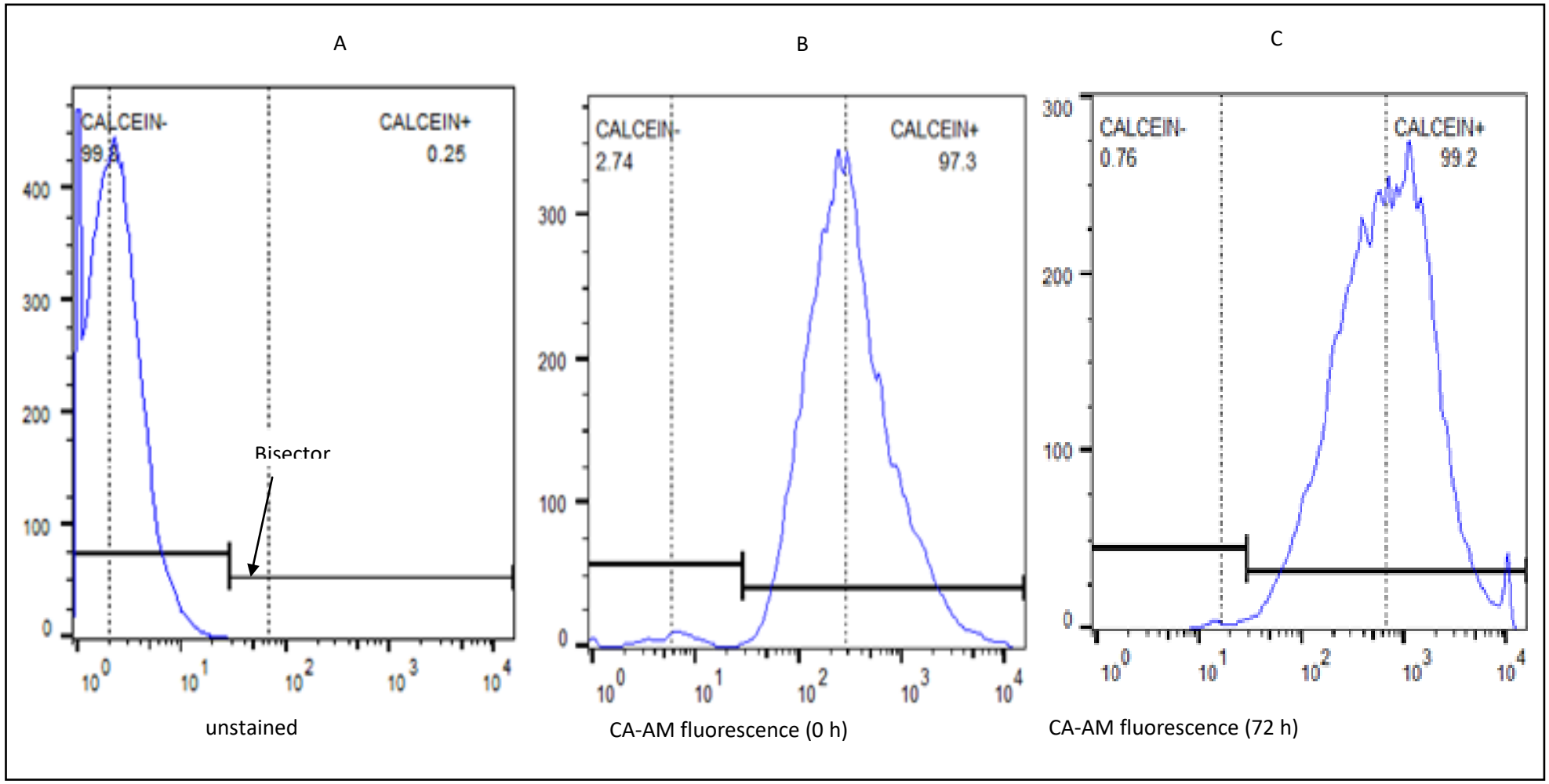

Figure 4-7 Fluorescence histograms of *M. smegmatis* showing untreated culture controls CA-AM (–ve) and CA-AM (+ve) on the left and right hand-side of the bisector line respectively. (A) unstained cells (B) stained with CA-AM 1µM for 60 min at the start of the experiment (0 h) , (C) stained with CA-AM 1µM for 60 min after 72 h of incubation. Data are representative of experiments performed in duplicate.

M. smegmatis cells were treated with FSA at ½X, 1X and 5X MIC and incubated over a 72 h time-course, **Figure 4-8**. The CA-AM stained cells were analysed at various time-points throughout the time-period. At a concentration of ½X MIC of FSA, the population of CA-AM stained positive cells remained above 98% over the 72 h period, similar to the untreated population . In contrast, the number of bacilli which returned a positive CA-AM signal with FSA treatment at 1X MIC was reduced by about 54% in 72 h. At an FSA concentration of 5X MIC, a more significant inhibitory effect was observed; the CA-AM stained population reduced to 0.01% at the 72 h time period. However, earlier time-points - that is, 24 and 48 treatment with 5X MIC - did not reveal any notable difference compared to the effect observed with 1X MIC.

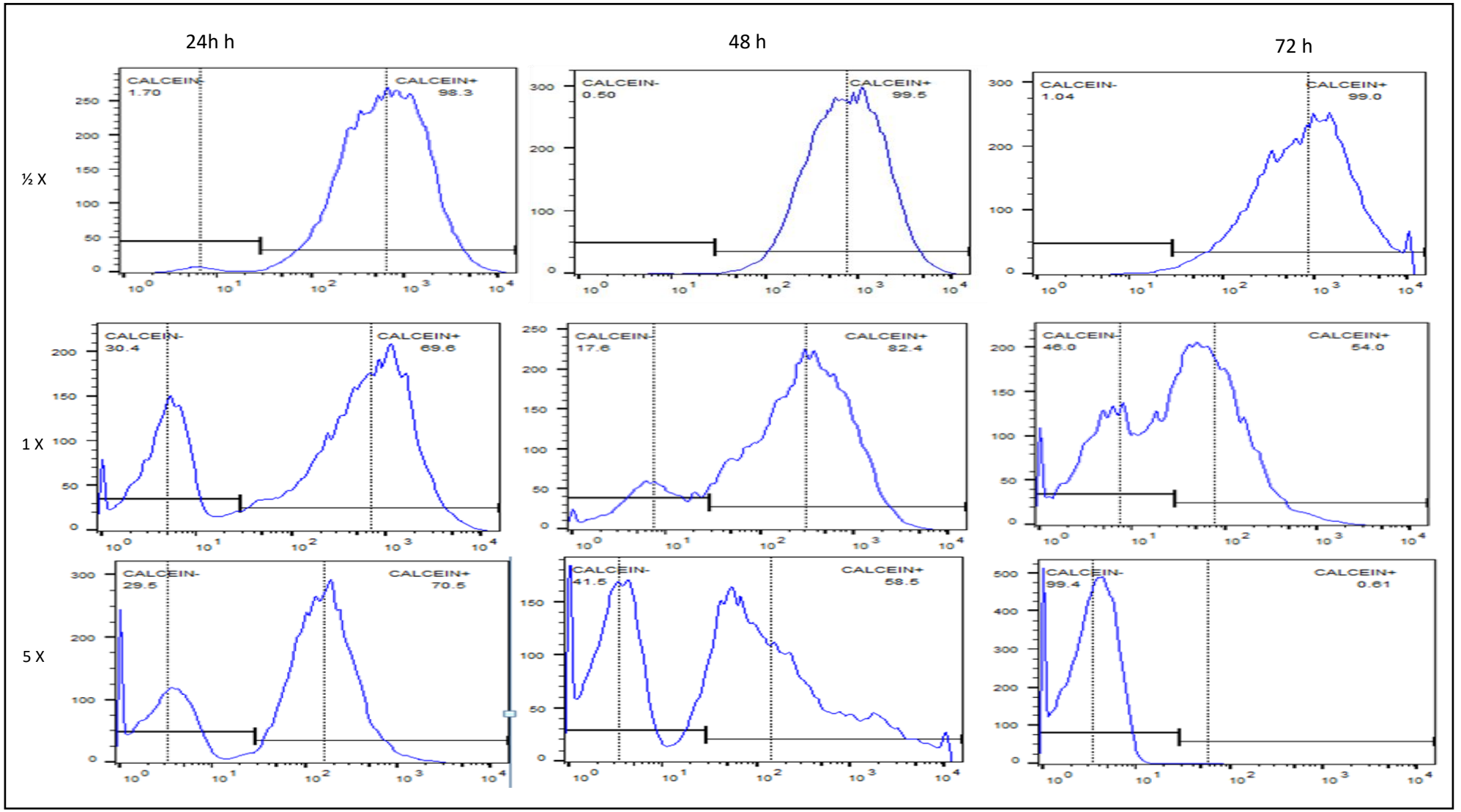
24h h
48 h
72 h
½ X
1 X
5 X
CALCEIN-
1.70
CALCEIN+
98.3
CALCEIN-
0.50
CALCEIN+
99.5
CALCEIN-
1.04
CALCEIN+
99.0
CALCEIN-
30.4
CALCEIN+
69.6
CALCEIN-
17.6
CALCEIN+
82.4
CALCEIN-
46.0
CALCEIN+
54.0
CALCEIN-
29.5
CALCEIN+
70.5
CALCEIN-
41.5
CALCEIN+
58.5
CALCEIN-
99.4
CALCEIN+
0.61

Figure 4-8 Fluorescence histograms of *M. smegmatis* treated with FSA at 24, 48 and 72 h. CA-AM (–ve) and CA-AM (+ve) on the left and right hand-side of the bisector line respectively.

Exposure to SPC

SPC showed the greatest inhibitory effect at ½X MIC during the 24, 48 and 72 h period in contrast to that of ½X MIC FSA **(Figure 4-9)** over the same time period. However, the treatment with 1X MIC SPC showed similar histograms with that of ½X MIC since the CA-AM positive cells were maintained at about 80% in both cases. Furthermore, treatment with 5X MIC SPC manifested in greater than 90% inhibition at the 72 h time-point, evident by a Calcein –ve population of 93.3% **(Figure 4-9,** bottom-right panel**)**. In stark contrast to the FSA activity, the area under curve for the CA-AM negative histogram of 5X MIC SPC was observed to be much smaller at the 72 h time-point. This implied a significant reduction in the overall bacterial population— possibly a result of cell lysis.

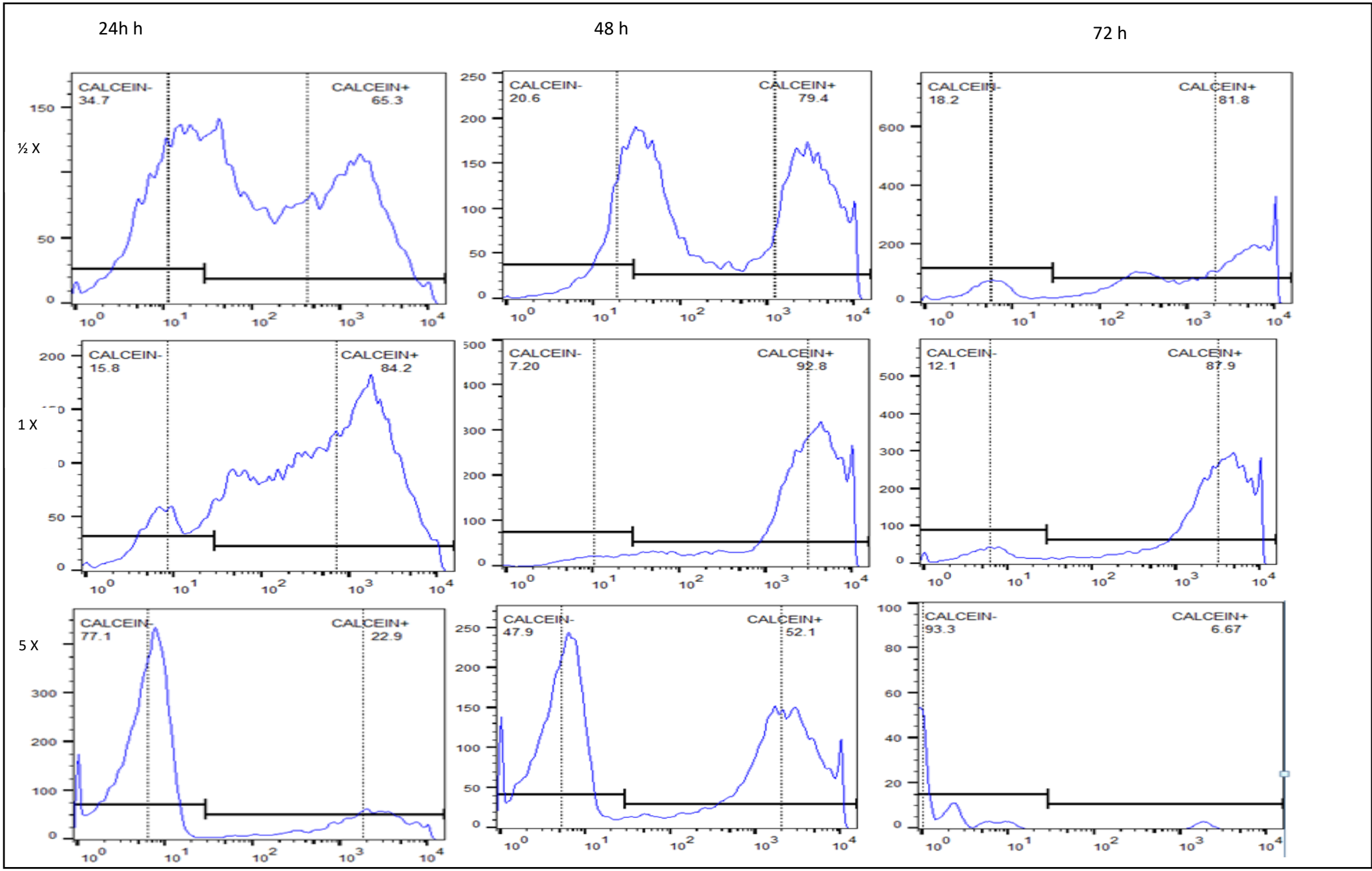
24h h
48 h
72 h
½ X
1 X
5 X
CALCEIN-
34.7
CALCEIN+
65.3
CALCEIN-
20.6
CALCEIN+
79.4
CALCEIN-
18.2
CALCEIN+
81.8
CALCEIN-
15.8
CALCEIN+
84.2
CALCEIN-
7.20
CALCEIN+
92.8
CALCEIN-
12.1
CALCEIN+
87.9
CALCEIN-
77.1
CALCEIN+
22.9
CALCEIN-
47.9
CALCEIN+
52.1
CALCEIN-
93.3
CALCEIN+
6.67

Figure 4-9 Fluorescence histograms of *M. smegmatis* treated with SPC at 24, 48 and 72 h. CA-AM (–ve) and CA-AM (+ve) on the left and right hand-side of the bisector line respectively. >90% inhibition, that is, the bacterial population with Calcein –ve = 93.3% is exhibited at 72 h of 5 X MIC. In addition, the area under the curve in this panel is much smaller compared to the rest of the panels.

4.3. Discussion

The spot assay strategy for selecting bactericidal agents highlighted a preliminary study, based on a comparative visualization of the test agents with the reference drugs. Compounds emanating from a large HTS screening cascade could potentially be delineated into cidal or static compounds. This would then allow hits' prioritization into the drug discovery programmes.

This assay demonstrated a straight-forward technique that can be used to qualitatively display the extent at which a compound manifests cidality. Based on a simple two-step procedure; (i) MIC determination on a 96-well plate and (ii) spot-assay method on a 24-well agar plate, the assay exhibited some consonance between the experimental outcome and the conventional assays for bactericidal determinations. However, this assay did not suggest any reduction of the incubation time. The other down-side was that the assay could not provide unequivocal proof of the cidal activity of the compounds. For example, the activity of BDQ, could not be determined clearly since it was considered to lie within the 'grey' area. Further wash-out experiments may be required at a later stage in the development for the most promising compounds.

Hendon-Dunn *et al* reported the use of FCM to assess the response of *M. tuberculosis* to antibiotics with different modes of action (Hendon-Dunn et al., 2016). By utilizing RIF and INH, the study illustrated a method for rapid analysis of drugs' susceptibility. Besides, it provided information about the drugs' potential mode of action; antibiotics targeting the cell wall gave a distinctive fluorescence profile compared to those inhibiting intracellular processes (Hendon-Dunn et al., 2016). For example, the inhibitory effect on the bacterial population with the cell wall targeting antibiotics, INH and BTZ-043, displayed an early and steep rise in SYTOX-green (SG) staining; a marker which permeates through damaged

bacteria and binds to DNA (Roth et al., 1997). On the other hand, a steady rise in the SG-stained population was observed for rifampicin exposure as well as other intracellular-targeting antibiotics. In order to further assess the robustness and utility of FCM, **sections 4.2.2** and **4.2.3** of this chapter described the results of the FCM and the fluorescent microscopy techniques applied for a quick assessment of mycobacterial physiological state and their susceptibility to antibiotics. Differences in physiological state of *M. tuberculosis* can be critical for its survival. For example, *M. tuberculosis* can persist for many years within the tissues of the host's lung without causing clinical disease (Orme, 1988). Evidence has suggested that cells survive in nutrient-deprived stationary phase. As a follow-up to this, Smeulders *et al.* studied the stationary-phase survival of *M. smegmatis*, as model for mycobacterial persistence (Smeulders et al., 1999). Emanating from their studies, a transition from late log phase into early stationary phase was associated with the cell's ability to sense the depletion of glycerol and initiate a shut down into stationary phase. This involved, uptake of the remaining glycerol from the medium, cells displayed a reductive cell division, resistance to both osmotic and acid stress and pool mRNA stabilized. Studies conducted with gram-negative species such as *Escherichia coli, Vibrio sp.*, and *Salmonella typhimurium* indicated a decrease in cell size, increased stress resistance, increases in RNA stability, and major changes in protein synthesis as some of the morphological and physiological changes that occur.

Here, analysis with the flow cytometer revealed the physiological heterogeneity within the exponential and stationary phase populations. For example, cultures from the exponential phase of *M. smegmatis*; unstained, and CA-AM stained at OD_{600} 0.5, 1.0 and 1.4, displayed two sub populations, P1 and P2, **(Figure 4-4)**. These subpopulations mainly

consisted of viable cells as indicated with high fluorescence upon staining with CA-AM - a marker for cell viability owing to esterase activity (Díaz et al., 2010).

Moreover, low fluorescence was observed with PI staining **(Figure 4-5)**. The transition of *M. smegmatis* cell population from log phase to stationary phase was also accompanied with a cell size reduction. This may possibly be explained by the rearrangement in peptidoglycan in cell wall of the stationary phase bacteria leading to size reduction (Oliver, 2010). The rearrangement in peptidoglycan can be triggered by various factors: Faghri *et al* reported a change from bacilli to coccoid in *Helicobacter pylori* on exposure for three days to sub MIC antibiotics (Faghri et al., 2014). Yet in another study, Besnard et al. reported morphologic changes following nutrient starvation in *Campylobacter jejuni* (Besnard, Federighi & Cappelier, 2000). Recent work by Wui *et al* on *M. smegmatis* revealed the development of small – cell survival morphotype when the bacteria were exposed to mild starvation conditions (Wu, Gengenbacher & Dick, 2016). Using fluorescence microscopic analyses, small resting cell (SMRC) morphotypes progressed through partitioned multi-nucleoided cell intermediates, which divide to generate mono-nucleoided SMRCs (Wu, Gengenbacher & Dick, 2016).

This work also revealed that FCM could be applied to improve the understanding of antibiotic effect on mycobacteria. In this study, FCM assessment highlighted the succession of cell changes that occurred in antibiotic stressed populations of *M. smegmatis*. Both FSA and SPC were less active against *M. smegmatis* at both ½X and 1X MIC. Even at 5X MIC, considerable esterase activity was maintained with both drugs at 24 h and 48 h treatment. However, at 72 h, a sharp reduction of more than 90% of the respective populations showed cells that lack esterase activity due to injury or death. Moreover, the mean fluorescence intensity observed with both ½X and 1X MIC SPC was higher than that displayed with FSA

or control cells. Curiously, this increase in fluorescence intensity corresponded with the increase in cell count. This may suggest a differential response of the bacteria towards these antibiotics that inhibits different stages of the translation process **(Figure 1-7)**. Alternatively, a more permeable cell wall due to the antibiotic treatment may cause leakage of the CA-AM thereby resulting in false positives. The apparently limited inhibition observed with both FSA and SPC at early time points, 24 h or 48 h, may explain their mechanism of action (Almeida Da Silva & Palomino, 2011). Early inhibition, such as 24 h, indicate that the mode of action could involve a lesion of the cell membrane resulting from the direct damage of the cell membrane while a late inhibition would imply a metabolic impairment leading to secondary damage to the cell membrane. A previous study carried out by Moghoofei *et al.* on *Pseudomonas aeruginosa*, reported that these bacilli could be converted to coccoid form under antibiotic stress (Moghoofei et al., 2015). The conversion may lead to resistance to antibiotics due to changes in cell wall cross-link or decreased metabolic activity (Sachidanandham, Yew-Hoong Gin & Laa Poh, 2005; .McDougald et al., 1998). Similar investigations can be undertaken with mycobacteria. The application of both spot assay and FCM techniques represents powerful tools for rapidly selecting potential lead compounds with either bactericidal or bacteriostatic activity; thereby facilitating drug discovery.

Chapter 5

Conclusions and Future Perspectives

5.1. Conclusions

Urgent measures are required to sustain an active TB drug pipeline, particularly at the pre-clinical phase of development. The major goal of this thesis was to develop and apply improved methods for advancing novel drug combinations in TB drug discovery. Thus, an integrated approach was adopted which encompassed the utilization of different strategies, tools and experimental models. These efforts aimed to deliver synergistic drug candidates that would allow for rapid translation into clinical trials within the current anti-TB drug pipeline.

This thesis fits into two broad categories; (i) evaluation of synergistic drug combinations and (ii) rapid investigation of the mode of action of experimental compounds with demonstrated anti-mycobacterial activity. Chapters 2 and 3 focused on developing and exploring synergistic drug interactions with existing anti-TB antibiotics. Furthermore, a drug repurposing strategy was employed. In defining synergy, the effect elicited by a combination of compounds is greater than that observed from the individual compounds. Consequently, this may result in increased therapeutic efficacy, reduced drug concentration required, shorter treatment duration, and potentially reduced side-effects (Williamson, 2001). In order to identify combinations that display synergistic interactions, a number of techniques were developed and optimized with different experimental models. Using *M. smegmatis*, prior to application in *M. tuberculosis*, allowed the manipulation of various preliminary experiments within the BSL2 laboratory. Furthermore, the faster growth rate of *M. smegmatis* in comparison to *M. tuberculosis* made it possible to carry out formative studies in a shorter period of time, thus minimizing the time-consuming aspect of working with *M. tuberculosis*

at the initial stages. In addition, the use of *M. smegmatis* allowed insight into potential synergistic activity of selected drug combinations that were expected to show good concordance; in that, drugs that synergized with FSA using *M. smegmatis* were similarly expected to synergize with FSA against *M. tuberculosis* owing to their genetic relatedness..

The modified checkerboard combination assay was implemented to uncover potential synergies among the interacting agents. In this assay, the efficacies of the single agents and the resulting combinations could be determined in a single 96-well plate. This single-plate 96-well matrix checkerboard assay can be automated to provide a high-through put screening platform that would allow for hundreds of investigational compounds to be combined in hundreds of possible pairings and dose variations.

The standard two-drug combination assays were extended here to include an innovative 3-D approach that enabled the simultaneous use of 3 agents. Using the 3-drug combination set-up, the *in vitro* synergistic effect of RIF-INH plus SPC was demonstrated against *M. tuberculosis* wild-type strain. Moreover, by applying this method, it was shown that SPC restored the susceptibility of the RIF-R *M. tuberculosis rpoB* mutant to the RIF-INH combination regimen. The exact mode of action underlying the synergy evident in this assay remain to be determined; however, this result suggests the possibility of selecting combination agents that will retain activity even against genetically resistant mutants.

The construction of isoboles, i.e. isoeffective curves, applied in the course of this thesis allowed analysis and a clear representation of synergistic interactions in both the 2- and 3-drug combinations. Although these isobolograms largely demonstrated the drugs' synergistic interactions, their applications are not without limitations. For example, the nature and extent of any interaction may be dose-dependent; that is, a combination of two compounds may act synergistically within one dose range while showing antagonism within another. By

incorporating a large number of data points, it is possible to generate representative isobolograms illustrative of the drug combination's effect at a specific level (Martinez-Irujo et al., 1996).

The potency of TB compounds, as determined by MIC and MBC evaluation, is a key consideration in early drug discovery programmes. As pointed out, the second broad aspect of this thesis engaged different strategies for rapid delineation of bactericidal activity. Drug candidates which exhibited strong synergy including FSA and SPC were prioritized for this study, both individually and in selected combinations. In the MIC and MBC evaluation, a modified *in vitro* cell regrowth assay adopted from Zhang *et al.* demonstrated a simple and robust bactericidal activity assay against *M. tuberculosis* (Zhang et al., 2007). Here, the MIC of test compounds was determined within 7 days followed by MBC determination. Previous work by Andreu *et al.* described the determination of all of standard drugs using a Lux reporter strain and report that MICs for all the drugs tested can be determined by day 3 (Andreu et al., 2012). While this may be true for the standard optimized drugs, some experimental compounds are not likely to be optimized for their killing properties and may need longer exposure time. Therefore, day 7 was seen as optimal time for MIC determination. This aberration may be as a result of the physico-chemical properties of different drugs which can influence their ability to access the bacteria over a period of time. As a result, discrimination between bacteriostatic and bactericidal agents may not be easily ascertained over a shorter period of time. In addition to the fact that the regrowth experiment was easy to perform, the time taken for the generation of these results (approximately 14 days) was shorter compared to the conventional method of CFU enumeration.

The FCM approach **(Chapter 4)** was adopted as an efficient alternative due to its ability to monitor viability and growth of mycobacterial cells in response to antibiotic

treatment rapidly and with high sensitivity. As already highlighted, it allows for the detection of viable but non-culturable (VBNC) cells which are not captured by the conventional CFU enumeration (Hendon-Dunn et al., 2016). Herein, FCM assay demonstrated the morphological heterogeneity, based on size/shape, of populations within the exponential growth phase, whereas at a later phase of growth, a more compact homogenous population was observed. The population of stationary phase cells was seen at a lower fluorescence of the FSC-height with FCM analysis, suggesting a reduced cell size compared to the exponential phase population. Bacteriostatic activities of both FSA and SPC against *M. smegmatis* were indicated, however SPC manifested bactericidal tendencies at much higher drug concentrations and after prolonged exposure. As mentioned in **Chapter 4 (section 4.3)**, both FSA and SPC are translational inhibitors, therefore the FCM profiles may be attributed to the delayed response compared to what might be observed with a cell wall inhibitor. Moreover, injured cells, as a result of antibiotic exposure, may not recover and could still retain some enzymatic activity as shown with CA-AM staining. The use of FCM in this thesis for bactericidal analysis may, therefore, be considered as a work in progress at best. While FCM permits the detection of the cells without any requirement that they can grow, our detection of 'viability' was limited to presence of esterase activity determined by CA-AM staining. Furthermore, in antibiotic-stress environments, the metabolic activity may be decreased below the threshold of detection. Besides, prior determination of an optimal dye concentration would be necessary for better resolution. Since CA-AM staining alone may not give a definite indication of the cell's viability, other reporter probes may be useful in the validation for viability analysis.

Besides the application of FCM, a modified qualitative spot assay strategy to elucidate bactericidal and bacteriostatic mycobacteria using *M. smegmatis* displayed a remarkable correlation between the observed experimental activities and those reported using

standard mode of action determinations. The spot assay technique is key, particularly in preliminary medium-throughput assays for the potential discrimination of bactericidal agents coming out of hits in drug discovery. Moreover, it is a useful tool when working with fastidious organisms (Wayne, 2007). However, unlike FCM, the spot assay may not be utilized to identify the bacteria that are in a state of very low metabolic activity and do not divide, but are alive and can become culturable on resuscitation (Shleeva et al., 2004).

5.2. Future Perspectives.

The results obtained from this work underscore the potential to explore compound synergies in TB drug discovery by use of the matrix checkerboard assay. However, further modifications of checkerboard assay may be adopted. As noted by Hsieh *et al*., a major problem inherent in this is the use of two-fold dilutions for the antibiotic concentrations (Hsieh et al., 1993). This exponential increase in dilutions potentially makes this method inherently unsuitable for evaluating synergy, thus, requiring newer methods or modifications. An approach that utilizes multiple plate set-up at different starting concentrations of the test drugs presents a viable alternative.

In this work, higher potency with very low drug concentrations was demonstrated when FSA interacted synergistically with ERY. This is a key consideration for the efficient and rapid elimination of a pathogen. In addition, the ability of more potent drug interactions to circumvent pre-existing resistance even to the extent of restoring drug susceptibility was demonstrated. The delineation of cidal or static antimicrobial agents has been shown to be play a significant role in hit prioritisation. This is mainly reinforced by the fact that the successful use of static drugs to treat infections requires an intact host immune system.

Accordingly, the primary perspective to extend this work will be the *in vivo* evaluation of synergism between FSA with the anti-tubercular drugs and/or other antibiotics

such as ERY and SPC, which have displayed synergy *in vitro*. Secondly, it has been shown that potent combinations have the ability to restore drug susceptibility. This is achieved where there is intrinsic genetic resistance to one of the combination drugs. Therefore, it will be important to prioritize highly potent synergistic combinations for the in vivo drug susceptibility testing against a *M. tuberculosis* H37Rv strain that is resistant to either of the drugs within the combination.

Thirdly, the predictive model adopted in Chapter 2 indicated the potential of FSA and synergizing drugs to penetrate necrotic tuberculosis lesions based on the differential partitioning values, clog P. It might be worth investigating the potential of these drugs to complement other combination partners in their ability to penetrate caseous granulomas.

Finally, the overall and greater vision of this work is to contribute to the enormous task of eradicating TB through new drug development and the application of innovative combination regimens that are rationally designed in the preclinical stages. The general course of this thesis is summarized in **Figure 5-1.**

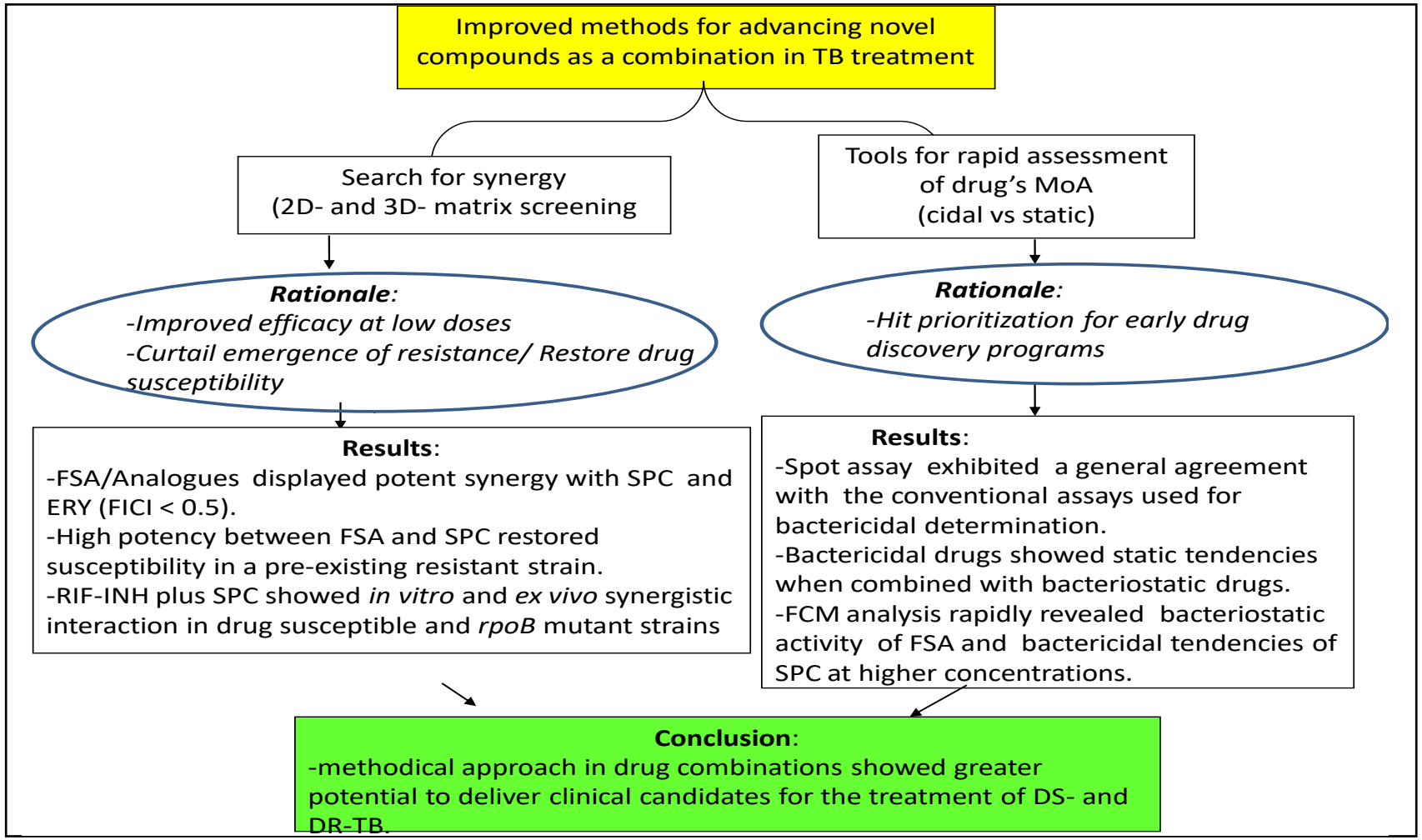

Figure 5-1 Schematic representation highlighting key aspects in the thesis

Chapter 6

Experimental

6.1. Chemicals and reagents

Chemicals and solvents were mainly purchased from Sigma-Aldrich. FSA analogues were synthesized in Kelly Chibale's lab., chemistry department at the University of Cape Town. Bedaquiline (BDQ) was purchased from Asclepia MedChem Solutions (Belgium). A spectinamide, 1599, was donated by Dr. Richard E. Lee, St. Jude Children's Research Hospital & University of Tennessee. 5mM stock concentrations of the drugs were prepared in DMSO at -20°C. Working solutions of the antimicrobial agents were prepared in distilled water.

Table 6-1 Strains and plasmids used in this study

Strain	Description	Reference or source
M. smegmatis		
mc^2155	Wild-type	Laboratory collection
M. tuberculosis		
H37RvMA	Wild-type	(Ioerger *et al*., 2010)
Macrophages		
THP-1	Undifferentiated monocytes	Laboratory collection
Plasmids		
pMSP12::gfp	Rv2390c	(Tan *et al*., 2013)

6.2. Bacterial strains and growth conditions.

The bacterial strains and plasmids used in this study are detailed in Table 6.1. *M. smegmatis* mc^2155 experiments were performed in Middlebrook (MB) 7H9 medium enriched with 10% Glucose salt (v/v), 0.2% Glycerol and 0.05% (v/v) tween-80 for 3 days at 37 °C. Freezer

stocks of *M. tuberculosis* H37Rv (Ma) and H37Rv.pMSP12::*gfp* mutant were grown in Middlebrook (MB) 7H9 supplemented with 10% oleic acid-albumin-dextrose-catalase (OADC) (Difco) at 37 °C for approximately 3 days sub-cultured and grown further to attain an OD_{600} 0.5. The cell suspension was then adjusted to give a final concentration of 10^5 cells/ml at the time of inoculation. 25 µg of kanamycin per ml was added into the *gfp* mutant each time a culture was started.

6.3. Drug susceptibility testing.

The MICs for the selected drugs were determined by the broth microdilution assays according to the clinical and laboratory standards institute (CLSI) guidelines (Wayne, 2007). Briefly, broth microdilution assays were performed in round-bottom 96-well microplates in which drugs were diluted in 7H9 medium using two fold serial dilutions. *M. tuberculosis* strains were grown to OD_{600} ~ 0.2 in 7H9 medium and used as a starting inoculum following five hundred-fold dilution in 7H9 medium. An equal volume of the diluted inoculum strain was added to each well of the plate (final volume of 100 µl per well). To minimize evaporation of the growth medium during the assay, 200 µL of sterile water was added to each outer well of each plate. The plates were incubated for 3 and 8 days for *M. smegmatis* and *M. tuberculosis* respectively. After the addition of resazurin, the plates were further incubated for 1 day in the case of *M. smegmatis* and 2 to 3 additional days for *M. tuberculosis* (Ramon-Garcia et al., 2011). A change from blue to pink indicated growth of bacteria, and the MIC_{90} was defined as the lowest concentration of drug that prevented this color change. For *gfp*-based-measurement, MIC determinations were performed in black, clear-bottom, 96-well microplates and fluorescence measured with a Fluostar Optima microplate reader (BMG Labtech) using excitation and emission wavelengths of 485 and 508 nm.

6.4. Drug interactions (synergy, no interaction, antagonism).

6.4.1. Checkerboard assay

2D Checkerboard

Two-dimensional drug interactions were determined by checkerboard titration in a 96-well plate **(Figure 6-1)**. The two-drug microdilution was carried out with slight modification as described by Chen *et al* (Chen et al., 2006). Briefly, the first serially diluted drug was dispensed (2 µl) along the x-axis (columns 3 to 11) at a concentration 100 times higher than the final concentration in the well and the second serially diluted (2 µl)) drug in the y-axis (row B to H) at a concentration 50 times higher than the final concentration in the 96-well microtitre plate. The first column (column 1) and last column (column 12) contained drug-free control and a control drug concentration giving maximum inhibition respectively. The second column from B2-H2, and first row from A3-A11 contained individual drugs. Synergy was described by the fractional inhibitory concentration (FIC) index expressed as FICI = $FIC_A + FIC_B = C_A^{comb}/MIC_A^{alone} + C_B^{comb}/MIC_B^{alone}$ where MIC_A^{alone} and MIC_B^{alone} are MICs of drugs A and B when acting alone and C_A^{comb} and C_B^{comb} are the concentrations of drugs A and B at the iso-effective combinations respectively. FICI $\leq$ 0.5 represented synergy; FICI > 4 antagonism and in between represents no interaction (Odds, 2003).

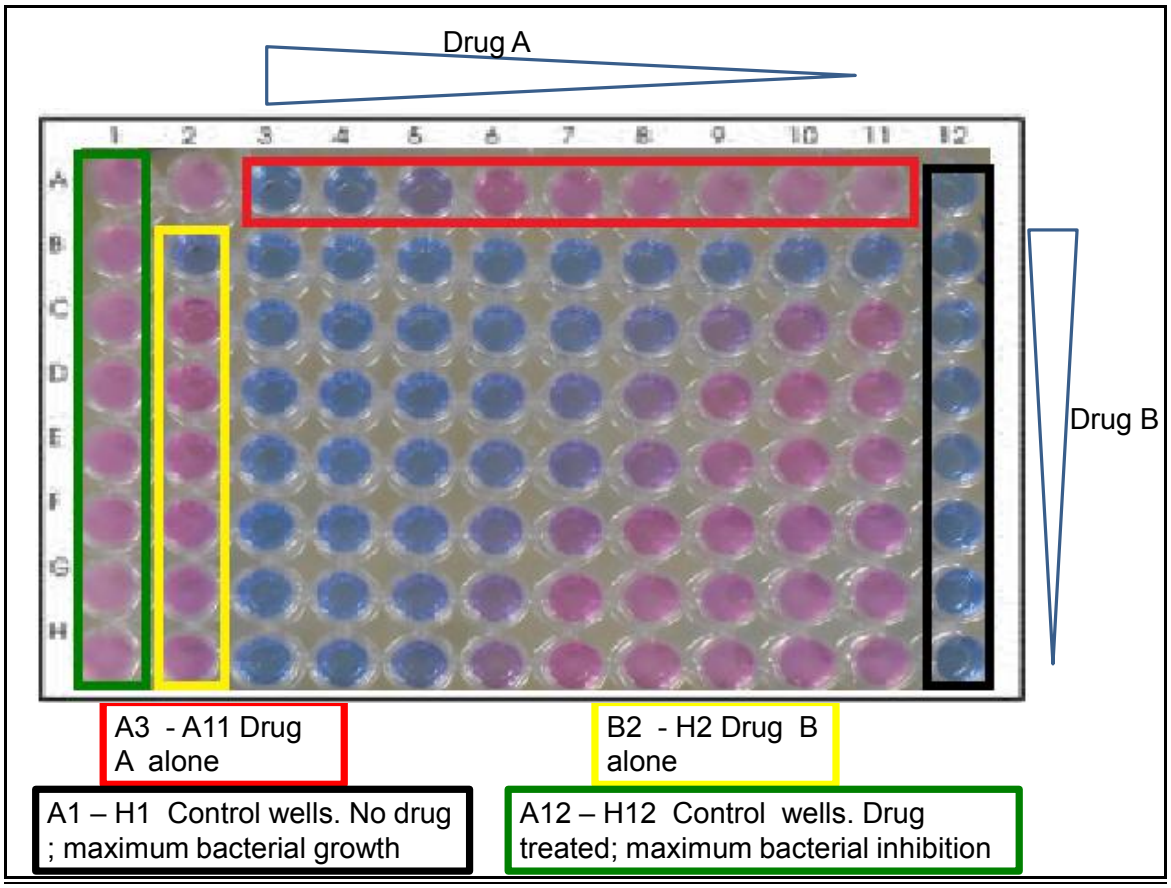

Figure 6-1 Schematic representation of a 2D plate layout

3D Checkerboard

In the three-drug combinations **(Figure 6-2)**, microdilutions were principally based on the standard two-dimensional checkerboard assay. The third drug (2 µl) were then added at a concentration 50 times higher than the final concentration in the well as an overlay at sub-inhibitory concentrations ranging from 1/32 to ½ of the MIC. Well A2 on all plates contained the third drug only. After inoculation with a log-phase culture of *M tuberculosis* (50µl) to each well, the plates were placed in zip-lock bags and incubated for about 2 weeks at 37°C before the results were read in the BD plate reader (excitation at 485nm and emission at 520nm). The mean for the maximum inhibition wells (column 12) was used as a background substraction for all other wells. Percent inhibition was defined as 1-(test well fluorescence units/mean fluorescence units of max. inhibition wells) x 100 on day 14 of incubation. The

lowest drug concentration effecting inhibition of 90% was considered the MIC. Resazurin dye was used to visualize the 96-well microtitre plates inoculated with H37Rv (Ma).

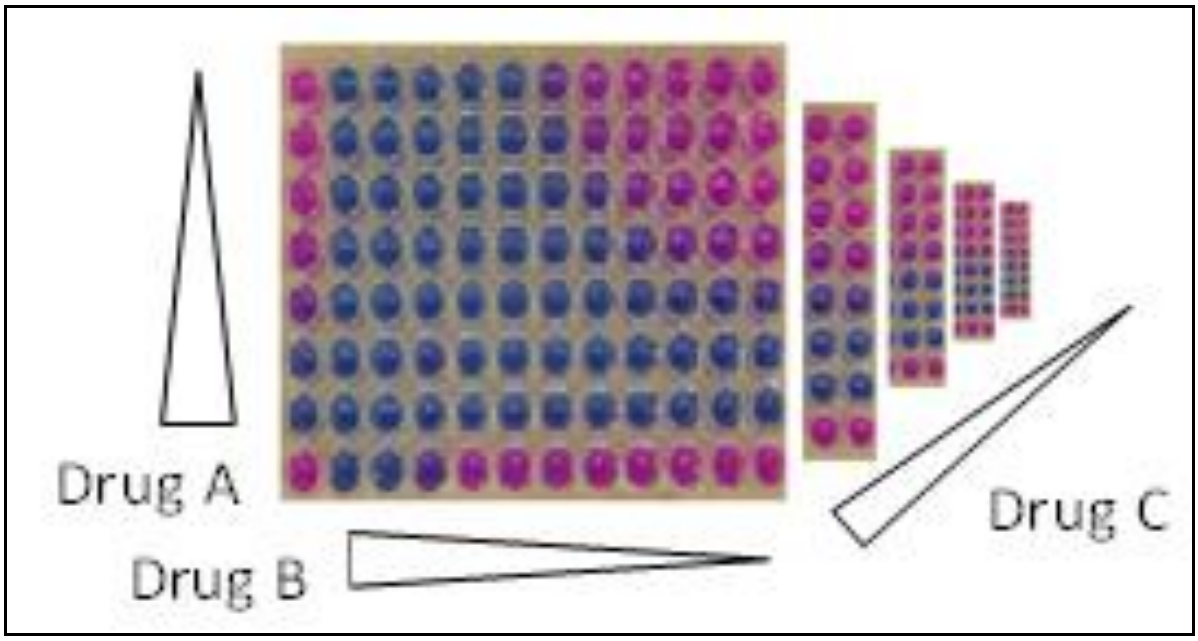

Figure 6-2 Representation of a 3-drug (3D) combination layout in a 96-well plate

6.4.2. Time-kinetics assay

To validate the synergy detected by CB, time-kill analysis was performed. Drug combinations and the respective individual drugs were used at their optimal synergistic concentration. Briefly, *M. tuberculosis* strain was grown in 7H9 broth containing 0.05% tween-80 with an inoculum of approximately 5 X 10^6 CFU/ml. Tissue flasks were prepared containing each antibiotic alone and their combinations including a control tube without antibiotics. Each tissue flask (final volume 10 ml) was inoculated with 100 µl of a 3-day old broth culture to give an initial inoculum of approximately 5 x 10^5 CFU/ml. The flasks were incubated at 37 °C. 100 µl aliquots withdrawn at different time points over a period of 14 days. Ten-fold dilutions of the aliquots were be prepared on 7H9/OADC media and 100 µl

each dilution plated onto 7H10 agar plates containing 10% OADC supplement. Colony forming units were then determined after a further 21 days of incubation.

6.5. Ex-vivo interaction study

6.5.1. Macrophage Growth and Infection

A 1 ml freezer stock of THP-1 macrophages were thawed by rubbing between gloved hands as quickly as possible. To wash out excess DMSO and serum from the cells, the thawed freezer stock was added into 9 ml RPMI-1640 of pre-warmed media, supplemented with 10% foetal bovine serum (FBS). This was followed by gentle centrifugation, 100 x g for 5 minutes. The old media was discarded and the pellet resuspended in 10 ml of fresh media. Cells were then grown in a 37°C CO_2 incubator to a density of between 8 x10^5/ml and 1.0 x 10^6/ml (achieved within 3-4 days) on 50 ml tissue flasks. Afterwards, the cells were washed by centrifuging at x 1400g and resuspending in fresh media. An automated cell counter was used test the macrophage viability. The media was changed every 3 days. THP-1 cells were passaged only 5 times. No antibiotic was used during the macrophage growth.

THP-1 cells were then differentiated with 100 nM phorbol 12-myristate 13-acetate (PMA) for 24 h. Thereafter, ~5x10^5 THP-1 macrophages were infected at a multiplicity of infection of 1: 10 bacteria for 3 h at 37°C. Cells were then washed with the media. To release the bacteria, macrophages were lysed once with 1x PBS and then with diH_2O, with the latter being removed immediately. Then, 100 µl of diH_20 was added and the cells were incubated at 24°C for 15 minutes. Finally, 100 µl volume containing lysed cells were pipetted into 900 µl of 7H9 medium with 0.05% Tween-80 and serially diluted. The serial dilutions were inoculated into the 7H10 agar plates, incubated for 14-21 weeks for CFU enumeration.

6.5.2. Synergistic drug interactions against M. tuberculosis-macrophage culture

Infected macrophage lysates were treated with the selected anti-TB drugs and/or translational inhibitors as single agents or in combination. As a control, free drug macrophages were included. The MICs for the selected drugs were determined by the broth microdilution assays according to the clinical and laboratory standards institute (CLSI) guidelines **(section 6.3)**. THP-1 cells in the presence of drugs were incubated at 37°C for the required duration of the experiment. Afterwards, 20 µl of 0.01% resazurin was added per well and the plate incubated for another 24 h. Fluorescence was measured at the excitation and emission wavelengths of 544 nm and 590 nm respectively for viability determination.

6.6. Bactericidal versus bacteriostatic analysis

6.6.1. MBC: MIC Ratio

In this assay, an established technique was used to differentiate the bacteriostatic or bactericidal effect of a single drug or drug combination **(Figure 6-3)**. Briefly, the MIC_{90} of the drugs against *M. tuberculosis* H37Rv::gfp or wild-type strain were first determined in 7H9 broth using the standard microdilution method on a 96-well plate. Briefly, 2-µl of the test drugs were added to the 7H9 medium to make a total of 100µl. This was followed by 2-fold dilutions on a 96-well plate. 50-µl of mid-log phase culture (OD_{600} 0.6) adjusted to approximately 10^5 CFU/ml were added to the wells. The plates are then packed in zip-lock bags and incubated at 37°C for 7 days.

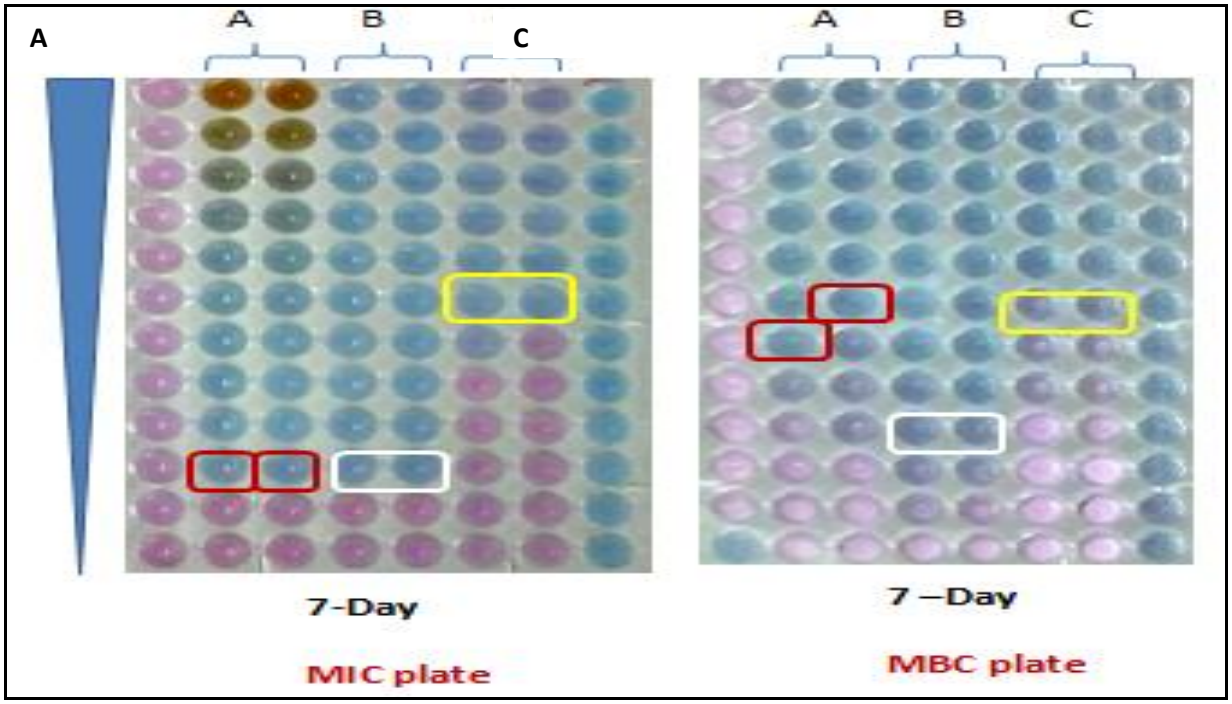

Figure 6-3 Bactericidal vs bacteriostatic: Representation of (A) MIC (B) MBC plates with resazurin dye. The standard MIC plate was set-up and incubated for 7 days. Before resazurin was added, 5 µl from every well was transferred to 200 µl of a drug-free medium, MBC plate and processed in the same way as the MICplate. Resazurin was added to the MBC plate, incubated for a further 24 – 48 h and the lowest concentrations of the drugs that resisted colour change from blue to pink in both plates compare. The respective concentrations were used to analyze the MBC/MIC ratios. MBC/MIC ≤ 2 was considered bactericidal

Thereafter, the MIC_{90} was established by measuring fluorescence using the BD microplate reader with excitation and emission wavelengths of 485nm and 520nm, respectively. 5- µl from every well was later transferred to 100- µl of a drug-free medium in another 96-well plate, MBC plate, and incubated at 37°C for a further 7 days. Fluorescence was measured on day 7. The concentration at which there was 90% or greater inhibition of RFU compared to those of untreated cells was defined as the bactericidal concentration. A compound or drug combination was considered bactericidal if the ratio between the minimal bactericidal concentration MBC_{99} and the MIC_{90} was equal to or smaller than 2, that is MBC/MIC ≤ 2. Alternatively, when the wild-type strain was utilized, the transfer of 5- µl was effected before

adding 10- µl per well of resazurin blue, this was then incubated for 24 h. A change from blue to pink indicated growth of bacteria, and the MIC was defined as the lowest concentration of drug that prevented this colour change. INH, a bactericidal drug was used as a positive control.

6.6.2. "Spot-assay" experiment

A modified assay by Kaur *et al*. was adopted for this study (Kaur et al., 2015). The spot-assay began with a 96-well culture plate, MIC/assay plate, **(Figure 6-4)**. In brief, 50µl of 7H9/OADC media was first dispensed across all the wells. Rows 1 and 12 were used as media and culture controls respectively. Rows B to G contained the compounds under investigation and reference drug controls, FSA and DCS serially diluted from column 1 to 12. *M. smegmatis* pMSP12 gfp strain cells were added to each well of the 96-well plate at approximately 7 x 10^4 CFU/ml. Incubation was performed at 37°C for 3-4 days. After the incubation the MIC_{90} data were recorded using a BD plate reader and the fluorescence intensity measured in the bottom-reading mode with excitation at 485nm and emission at 520nm.

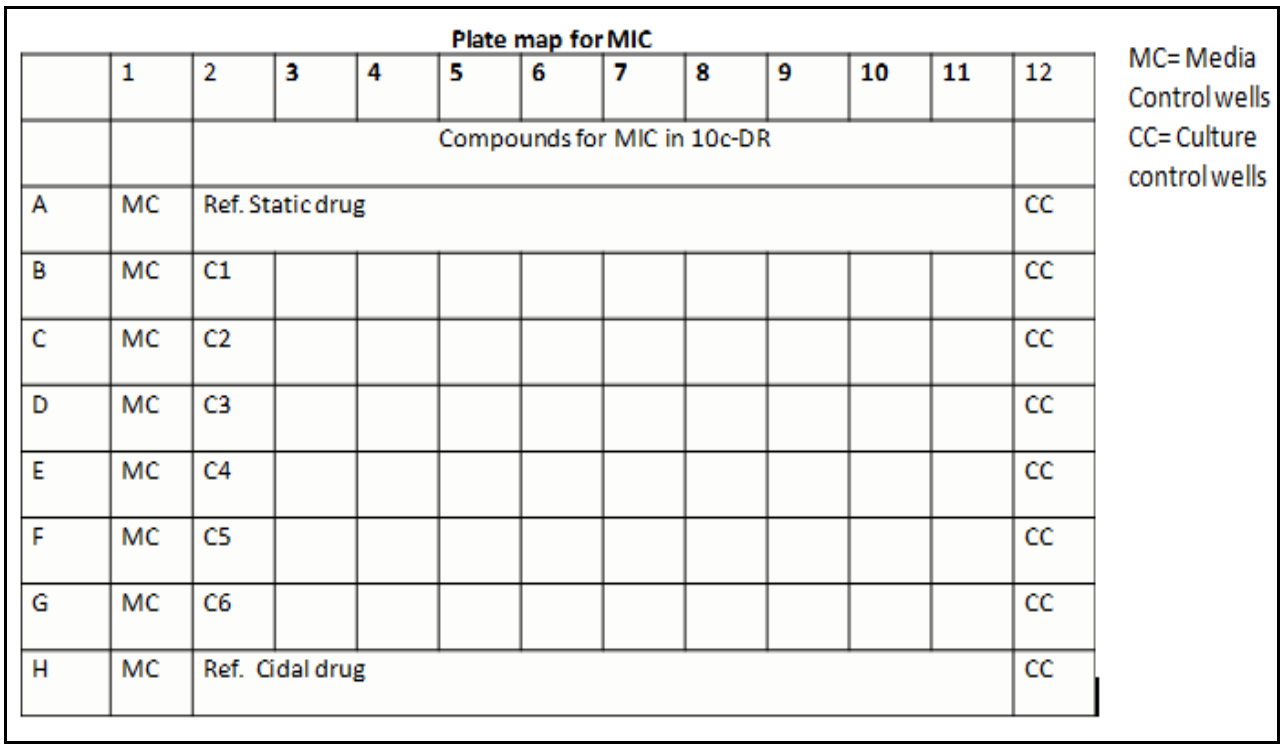

Figure 6-4 A plate map for the MIC in a 96-well plate. Six test drugs (C1-C6) are subjected to MIC test as a 10-concentration dose response. The 1st and 8th rows = reference drug controls (static and cidal drug). *M. smegmatis* culture addition was performed with the multi-channel pipette and incubation undertaken at 37°C for 3-4 days. Post – incubation, the MIC data were recorded on BD plate reader.

The spot-assay was performed by accurately dispensing 10-µl culture volumes from the 96-well plate onto 24-well agar plates at 4X, 2X, X and 0.5X MICs **(Figure 6-5)** , swirled using glass beads and incubated at 37°C for 3 days. Visualization assessment was performed once growth/colonies appeared on the culture control wells. We hypothesized that under colony visualization on the 24-well solid plates, wells consisting of cidal drugs at 1X MIC and above would exhibit clean solid plates or far less colonies as compared to those wells containing bacteriostatic drugs which do not kill the bacteria but merely stops their replication at the MIC drug concentration.

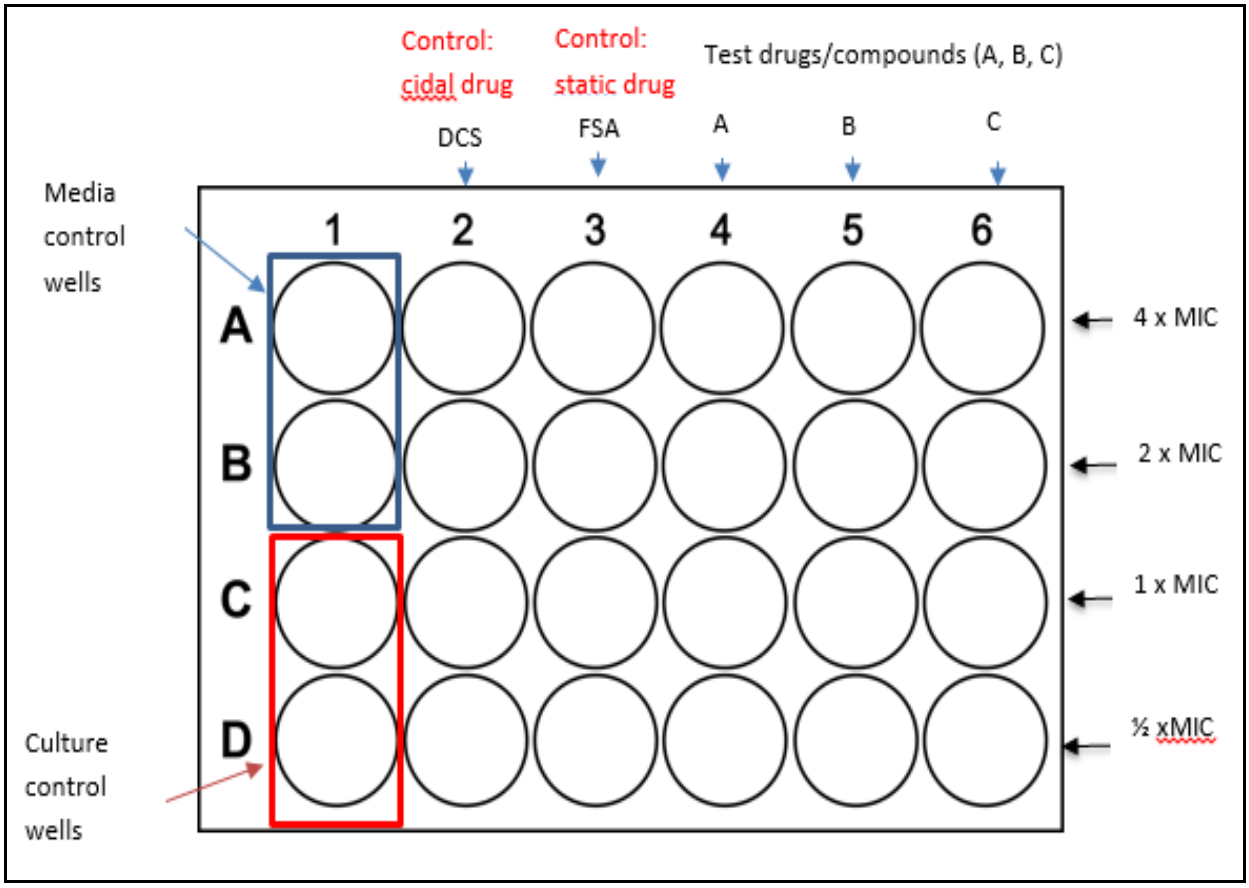

Figure 6-5 Twenty-four well, 7H10 agar plate. 10µl of culture dispensed in each well containing 4X, 2X, 1X and ½ x MIC of test drugs (A, B, C). FSA and DCS used as reference static and cidal drugs respectively.

6.7. Isolation of mutants of *M. tuberculosis*

To isolate spontaneous mutants, cultures of wild-type *M. tuberculosis* were grown at 37°C to OD600 = 0.6, pelleted by centrifugation, and resuspended in Middlebrook 7H9 broth supplemented with glycerol, OADC, and 0.05% Tween 80. Aliquots containing 10^7, 10^8 and 10^9 cells were then plated on Middlebrook 7H10 agar media supplemented with glycerol and OADC in the presence of drug at 5 x and 10 x the MIC_{90} value determined in liquid culture. Colonies arising after 1 weeks' incubation were then picked and sub cultured in Middlebrook 7H9 containing drug at 1 x MIC_{90}. The bacterial strain was then retested for susceptibility with the respective drugs.

6.8. Assessment of mycobacterial physiological state and antibiotic treatment

6.8.1. Membrane integrity and cell viability assay

The determination of mycobacterial's physiological states in exponential and stationary phases was perfomed with *M. smegmatis* mc^2155 using PI and CA-AM.

PI staining: A method by Gonzalez et al., was used with modifications (Gonzalez-y-Merchand, Jorge A 2012). Bacterial suspensions at different phases, OD_{600} = 0.5, 2.0 and 3.5 were adjusted to~10^6 bacteria per ml and mixed with 1 µM of 1 mg/ml PI fluorescent stain (Sigma, USA). Bacterial cells containing PI stain were incubated for 30 min at 24°C. Analysis was performed with a fluorescence-activated cell sorting (FACS) Scan Calibur flow 140 cytometer (BD, Becton Dickinson, USA). PI stain is a fluorescent dye that penetrates through the compromised membrane of dead or injured cells. Forward and side scatter parameters (both in a logarithmic settings) were measured. Fluorescence of 20000 events were analysed with FL3-FSC dot plots.

CA-AM staining: M. smegmatis staining was performed according to Kramer *et al*., (Kramer, Wiechert & Kohlheyer, 2016). A 1 mM solution was prepared by dissolving 50µg sample in 50 µl DMSO. Approximately 10^6 cells were stained with 1 µM CA-AM, incubated for 30 min at 37°C before FCM analysis. Fluorescence of 20000 events were analysed with FL1-FSC dot plots.

6.8.2. Cell sorting

M. smegmatis sub-populations analysed by FCM had their sort gates defined on an FL1 vs FSC dot plot of CA-AM stained cells. The sorter was set on purity mode, and sorted cells collected in two 5-ml tubes. Sorting was stopped after the acquisition of between 100,000 – 200, 000 cells in each tube. Filter-sterilized PBS was used as the sheath fluid. The sorted cells

were centrifuged at 4000 x g for 5 min, the supernatant removed. The remaining volume with sorted cells used for microscopy evaluation.

6.8.3. Fluorescence microscopy

Bacterial cell suspensions in 1 x PBS, after cell-sorting were spread on glass slides and cover slips mounted. The slides were placed on a 42°C heating block for 3 min to allow the adhesion of *M. smegmatis* onto the slides before examination under a fluorescence microscope (Zeiss AX10 microscope, Carl Zeiss MicroImaging GmbH, Jena, Germany). A fluorescence immersion oil was used for the observation at high objective (x100).

6.8.4. Sample preparation and FCM data acquisistion

Antimycobacterial agents were prepared with 7H9 broth in 12-ml falcon tubes.Eachdilution was then inoculated with ~10^6 cells. Untreated bacterial suspensions were also included as controls. The tubes were incubated at 37°C for 72 h and data acquisition on FCM performed at 0, 24, 48 and 72 h time points. For FCM analysis, 1µl of 1 mM CA-AM solution was added to the suspensions to yield a final concentration of 1 µM. The samples were incubated at 37°C for 30min before being analysed with a 488nm argon laser (FACScanflow cytometer; Becton Dickinson Immunocytometry Systems) using FACProSort software.

6.8.5. Flow cytometric statistical analysis.

Samples were analyzed by examining histogram profiles of CA-AM fluorescence with Flowjo v.10 software. The percentage of CA-AM -ve and +ve cells upon antibiotic treatment was evaluated.

APPENDICES

Appendix 1: Culture media

All media were made to a final volume of 1L with distilled water. Media were sterilized by autoclaving at 121°C for 15 min.

7H10/OADC Agar

19 g Middlebrook 7H10 agar powder (DifcoTM, USA), 5 ml glycerol (Merck, Germany)

100 ml Middlebrook OADC Enrichment (BD Microbiology Systems, USA) added after autoclaving.

7H9/OADC Liquid

4.7 g Middlebrook 7H9 broth powder (DifcoTM, USA), 2 ml glycerol (Merck, Germany) 100 ml OADC Middlebrook OADC Enrichment (BD Microbiology Systems, USA) added after autoclaving.

Appendix 2: *In vitro* MIC_{90} of FSA and its selected derivatives against *M. tuberculosis* H37Rv (wild-type) strain and FSA-R mutant

Compound	**14 day 7H9/OADC MIC_{90} (µM) with H37Rv**	**14 day 7H9/OADC MIC_{90} (µM) with FSA-R**
FSA	2.4	20
GKFA17	33	80
GKFA37	0.5	80
GKFA51	5.2	160
GKFA 61	14	>160

Appendix 3: Spot Assay: MIC_{90} 96-well microtitre plate experiment for the MIC_{90} analysis against *M. smegmatis*::gfp

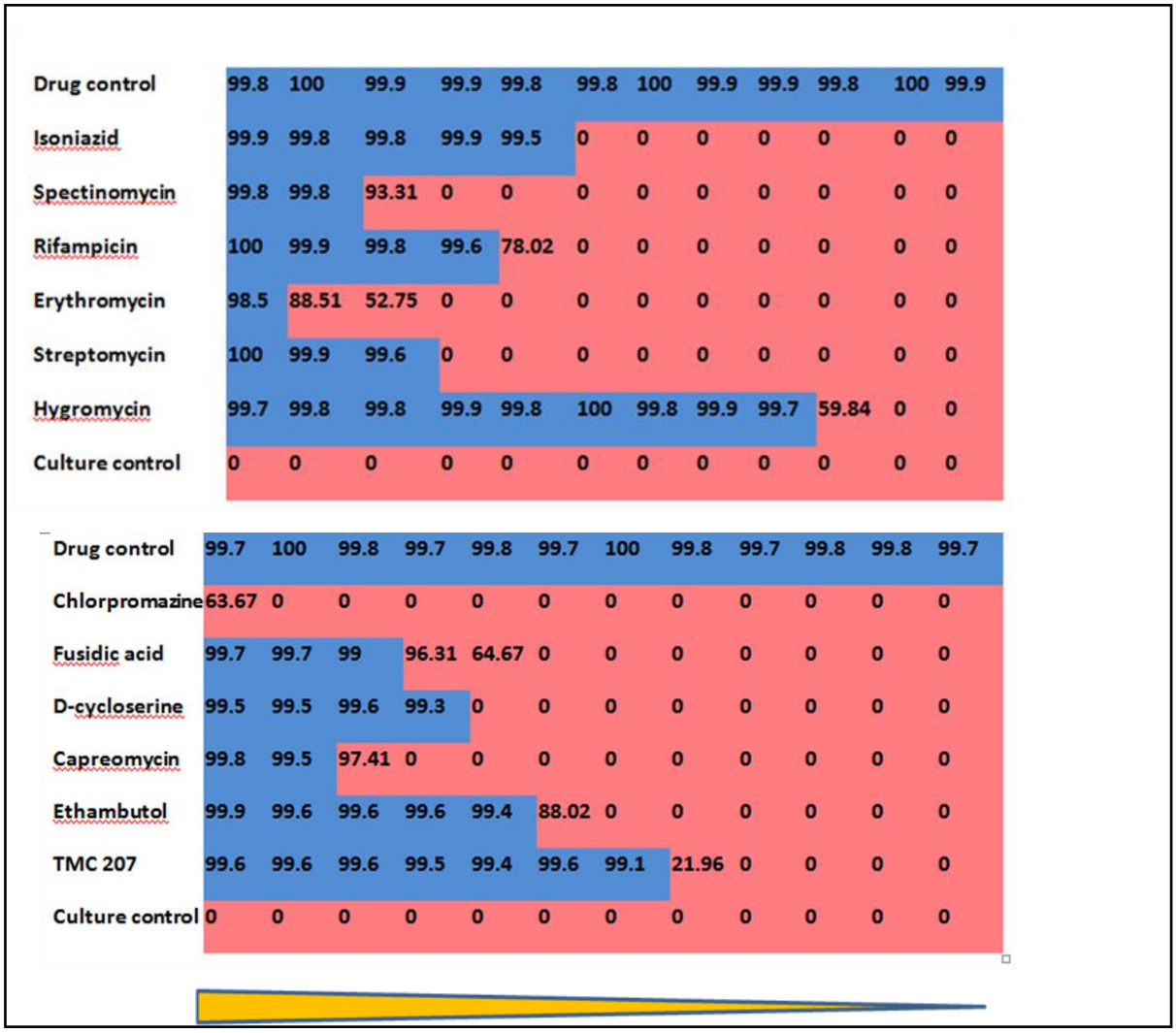

Drug control	99.8	100	99.9	99.9	99.8	99.8	100	99.9	99.9	99.8	100	99.9
Isoniazid	99.9	99.8	99.8	99.9	99.5	0	0	0	0	0	0	0
Spectinomycin	99.8	99.8	93.31	0	0	0	0	0	0	0	0	0
Rifampicin	100	99.9	99.8	99.6	78.02	0	0	0	0	0	0	0
Erythromycin	98.5	88.51	52.75	0	0	0	0	0	0	0	0	0
Streptomycin	100	99.9	99.6	0	0	0	0	0	0	0	0	0
Hygromycin	99.7	99.8	99.8	99.9	99.8	100	99.8	99.9	99.7	59.84	0	0
Culture control	0	0	0	0	0	0	0	0	0	0	0	0

Drug control	99.7	100	99.8	99.7	99.8	99.7	100	99.8	99.7	99.8	99.8	99.7
Chlorpromazine	63.67	0	0	0	0	0	0	0	0	0	0	0
Fusidic acid	99.7	99.7	99	96.31	64.67	0	0	0	0	0	0	0
D-cycloserine	99.5	99.5	99.6	99.3	0	0	0	0	0	0	0	0
Capreomycin	99.8	99.5	97.41	0	0	0	0	0	0	0	0	0
Ethambutol	99.9	99.6	99.6	99.6	99.4	88.02	0	0	0	0	0	0
TMC 207	99.6	99.6	99.6	99.5	99.4	99.6	99.1	21.96	0	0	0	0
Culture control	0	0	0	0	0	0	0	0	0	0	0	0

REFERENCES

Ali, J.A., Jackson, A.P., Howells, A.J. & Maxwell, A. 1993. The 43-kilodalton N-terminal fragment of the DNA gyrase B protein hydrolyzes ATP and binds coumarin drugs. *Biochemistry.* 32(10):2717-2724.

Almeida Da Silva, P.E. & Palomino, J.C. 2011. Molecular basis and mechanisms of drug resistance in *Mycobacterium tuberculosis*: classical and new drugs. *The Journal of Antimicrobial Chemotherapy.* 66(7):1417-1430. DOI:10.1093/jac/dkr173 [doi].

Almeida, d.S.P., Ainsa, J., Palomino, J., Leão, S. & Ritacco, V. 2007. Drugs and drug interactions. *Tuberculosis.*

Andreu, N., Fletcher, T., Krishnan, N., Wiles, S. & Robertson, B.D. 2012. Rapid measurement of antituberculosis drug activity in vitro and in macrophages using bioluminescence. *The Journal of Antimicrobial Chemotherapy.* 67(2):404-414. DOI:10.1093/jac/dkr472 [doi].

Andries, K., Verhasselt, P., Guillemont, J., Gohlmann, H.W., Neefs, J.M., Winkler, H., Van Gestel, J., Timmerman, P. et al. 2005. A diarylquinoline drug active on the ATP synthase of *Mycobacterium tuberculosis*. *Science (New York, N.Y.).* 307(5707):223-227. DOI:1106753 [pii].

Ankomah, P., Johnson, P.J. & Levin, B.R. 2013. The pharmaco–, population and evolutionary dynamics of multi-drug therapy: Experiments with S. aureus and E. coli and computer simulations. *PLoS Pathog.* 9(4):e1003300.

Ashtekar, D.R., Costa-Periera, R., Shrinivasan, T., Iyyer, R., Vishvanathan, N. & Rittel, W. 1991. Oxazolidinones, a new class of synthetic antituberculosis agent. In vitro and in vivo activities of DuP-721 against *Mycobacterium tuberculosis*. *Diagnostic Microbiology and Infectious Disease.* 14(6):465-471.

Atkins, B. & Gottlieb, T. 1999. Fusidic acid in bone and joint infections. *International Journal of Antimicrobial Agents.* 12:S79-S93.

Baggot, J.D. 1998. Antimicrobial selection, administration and dosage: continuing education. *Journal of the South African Veterinary Association.* 69(4):174-185.

Barco, P., Cardoso, R.F., Hirata, R.D., Leite, C.Q., Pandolfi, J.R., Sato, D.N., Shikama, M.L., de Melo, F.F. et al. 2006. pncA mutations in pyrazinamide-resistant *Mycobacterium tuberculosis* clinical isolates from the southeast region of Brazil. *The Journal of Antimicrobial Chemotherapy.* 58(5):930-935. DOI:dkl363 [pii].

Barry, C.E.,3rd, Lee, R.E., Mdluli, K., Sampson, A.E., Schroeder, B.G., Slayden, R.A. & Yuan, Y. 1998. Mycolic acids: structure, biosynthesis and physiological functions. *Progress in Lipid Research.* 37(2-3):143-179. DOI:S0163-7827(98)00008-3 [pii].

Barry, V.C., BELTON, J.G., CONALTY, M.L., DENNENY, J.M., EDWARD, D.W., O'SULLIVAN, J.F., TWOMEY, D. & WINDER, F. 1957. A new series of phenazines (rimino-compounds) with high antituberculosis activity. *Nature.* 179(4568):1013-1015.

Basu, S. & Galvani, A. 2008. The transmission and control of XDR TB in South Africa: an operations research and mathematical modelling approach. *Epidemiology and Infection.* 136(12):1585-1598.

Berenbaum, M.C. 1978. A method for testing for synergy with any number of agents. *The Journal of Infectious Diseases.* 137(2):122-130.

Besnard, V., Federighi, M. & Cappelier, J. 2000. Development of a direct viable count procedure for the investigation of VBNC state in *Listeria monocytogenes*. *Letters in Applied Microbiology.* 31(1):77-81.

Bhusal, Y., Shiohira, C.M. & Yamane, N. 2005. Determination of in vitro synergy when three antimicrobial agents are combined against *Mycobacterium tuberculosis*. *International Journal of Antimicrobial Agents.* 26(4):292-297. DOI:S0924-8579(05)00208-6 [pii].

Biava, M., Porretta, G., Poce, G., Supino, S. & Sleiter, G. 2007. New pyrroles with potential antimycobacterial, antifungal and selective COX-2 inhibiting activities. Synthetic methodologies. *Current Organic Chemistry.* 11(12):1092-1112.

Bilgin, N., Claesens, F., Pahverk, H. & Ehrenberg, M. 1992. Kinetic properties of *Escherichia coli* ribosomes with altered forms of S12. *Journal of Molecular Biology.* 224(4):1011-1027.

Black, W.A. & McNellis, D.A. 1970. Susceptibility of Nocardia species to modern antimicrobial agents. *Antimicrobial Agents and Chemotherapy.* 10:346-349.

Bohman, K., Ruusala, T., Jelenc, P. & Kurland, C. 1984. Kinetic impairment of restrictive streptomycin-resistant ribosomes. *Molecular and General Genetics MGG.* 198(1):90-99.

Bollenbach, T. 2015. Antimicrobial interactions: mechanisms and implications for drug discovery and resistance evolution. *Current Opinion in Microbiology*. 27:1-9.

Brauner, A., Fridman, O., Gefen, O. & Balaban, N.Q. 2016. Distinguishing between resistance, tolerance and persistence to antibiotic treatment. *Nature Reviews Microbiology*. 14(5):320-330.

Bruhn, D.F., Scherman, M.S., Liu, J., Scherbakov, D., Meibohm, B., Bottger, E.C., Lenaerts, A.J. & Lee, R.E. 2015. In vitro and in vivo Evaluation of Synergism between Anti-Tubercular Spectinamides and Non-Classical Tuberculosis Antibiotics. *Scientific Reports*. 5:13985. DOI:10.1038/srep13985 [doi].

Caminero, J. 2010. Multidrug-resistant tuberculosis: epidemiology, risk factors and case finding [State of the art series. Drug-resistant tuberculosis. Edited by CY. Chiang. Number 4 in the series]. *The International Journal of Tuberculosis and Lung Disease*. 14(4):382-390.

Carvalho-Netto, E., Markham, C., Blanchard, D., Nunes-de-Souza, R. & Blanchard, R. 2006. Physical environment modulates the behavioral responses induced by chemical stimulation of dorsal periaqueductal gray in mice. *Pharmacology Biochemistry and Behavior*. 85(1):140-147.

Chain, E., Florey, H., Jennings, M. & Williams, T. 1943. Helvolic acid, an antibiotic produced by *Aspergillus fumigatus*, mut. helvola Yuill. *British Journal of Experimental Pathology*. 24(3):108.

Chait, R., Craney, A. & Kishony, R. 2007. Antibiotic interactions that select against resistance. *Nature*. 446(7136):668-671.

Chen, P., Gearhart, J., Protopopova, M., Einck, L. & Nacy, C.A. 2006. Synergistic interactions of SQ109, a new ethylene diamine, with front-line antitubercular drugs in vitro. *The Journal of Antimicrobial Chemotherapy.* 58(2):332-337. DOI:dkl227 [pii].

Cholo, M.C., Steel, H.C., Fourie, P.B., Germishuizen, W.A. & Anderson, R. 2012. Clofazimine: current status and future prospects. *The Journal of Antimicrobial Chemotherapy.* 67(2):290-298. DOI:10.1093/jac/dkr444 [doi].

Chopra, I. 1976. Mechanisms of resistance to fusidic acid in *Staphylococcus aureus*. *Microbiology.* 96(2):229-238.

Chou, T.C. 2006. Theoretical basis, experimental design, and computerized simulation of synergism and antagonism in drug combination studies. *Pharmacological Reviews.* 58(3):621-681. DOI:58/3/621 [pii].

Christiansen, K. 1999. Fusidic acid adverse drug reactions. *International Journal of Antimicrobial Agents.* 12:S3-S9.

Cicek-Saydam, C., Cavusoglu, C., Burhanoglu, D., Hilmioglu, S., Ozkalay, N. & Bilgic, A. 2001. In vitro susceptibility of *Mycobacterium tuberculosis* to fusidic acid. *Clinical Microbiology and Infection.* 7(12):700-702.

Cocito, C., Di Giambattista, M., Nyssen, E. & Vannuffel, P. 1997. Inhibition of protein synthesis by streptogramins and related antibiotics. *The Journal of Antimicrobial Chemotherapy.* 39 Suppl A:7-13.

Cohen, J. 2013. Infectious disease. Approval of novel TB drug celebrated--with restraint. *Science (New York, N.Y.).* 339(6116):130. DOI:10.1126/science.339.6116.130 [doi].

Cole, S.T. & Riccardi, G. 2011. New tuberculosis drugs on the horizon. *Current Opinion in Microbiology.* 14(5):570-576. DOI:10.1016/j.mib.2011.07.022 [doi].

Collignon, P. & Turnidge, J. 1999. Fusidic acid in vitro activity. *International Journal of Antimicrobial Agents.* 12 Suppl 2:S45-58.

Cordone, A., Audrain, B., Calabrese, I., Euphrasie, D. & Reyrat, J. 2011. Characterization of a *Mycobacterium smegmatis* uvrA mutant impaired in dormancy induced by hypoxia and low carbon concentration. *BMC Microbiology.* 11(1):231.

Cuenca-Estrella, M. 2004. Combinations of antifungal agents in therapy--what value are they? *The Journal of Antimicrobial Chemotherapy.* 54(5):854-869. DOI:10.1093/jac/dkh434 [doi].

Cynamon, M.H., Klemens, S.P., Sharpe, C.A. & Chase, S. 1999. Activities of several novel oxazolidinones against *Mycobacterium tuberculosis* in a murine model. *Antimicrobial Agents and Chemotherapy.* 43(5):1189-1191.

da Silva, J.L., Mesquita, A.R. & Ximenes, E.A. 2009. In vitro synergic effect of ²-lapachone and isoniazid on the growth of *Mycobacterium fortuitum* and *Mycobacterium smegmatis*. *Memórias do Instituto Oswaldo Cruz.* 104(4):580-582.

Daffe, M. & Draper, P. 1998. The envelope layers of mycobacteria with reference to their pathogenicity. *Advances in Microbial Physiology.* 39:131-203.

Dahlfors, A.A.R. & Kurland, C.G. 1990. Novel mutants of elongation factor G. *Journal of Molecular Biology.* 215(4):549-557.

Darley, E.S. & MacGowan, A.P. 2004. Antibiotic treatment of gram-positive bone and joint infections. *The Journal of Antimicrobial Chemotherapy.* 53(6):928-935. DOI:10.1093/jac/dkh191 [doi].

Dartois, V. 2014. The path of anti-tuberculosis drugs: from blood to lesions to mycobacterial cells. *Nature Reviews.Microbiology.* 12(3):159-167. DOI:10.1038/nrmicro3200 [doi].

Davis, J.M. & Ramakrishnan, L. 2009. The role of the granuloma in expansion and dissemination of early tuberculous infection. *Cell.* 136(1):37-49.

Dey, T., Brigden, G., Cox, H., Shubber, Z., Cooke, G. & Ford, N. 2013. Outcomes of clofazimine for the treatment of drug-resistant tuberculosis: a systematic review and meta-analysis. *The Journal of Antimicrobial Chemotherapy.* 68(2):284-293. DOI:10.1093/jac/dks389 [doi].

Dheda, K., Barry 3rd, C. & Maartens, G. 2015. Tuberculosis. Lancet 2015; published online Sept 13. http://dx. doi. org/10.1016/S0140-6736 (15) 00151-

Díaz, M., Herrero, M., García, L.A. & Quirós, C. 2010. Application of flow cytometry to industrial microbial bioprocesses. *Biochemical Engineering Journal.* 48(3):385-407.

Díaz, J.C.R., Ruiz, M., Lopez, M. & Royo, G. 2003. Synergic activity of fluoroquinolones and linezolid against *Mycobacterium tuberculosis*. *International Journal of Antimicrobial Agents.* 21(4):354-356.

DiMasi, J.A., Feldman, L., Seckler, A. & Wilson, A. 2010. Trends in risks associated with new drug development: success rates for investigational drugs. *Clinical Pharmacology and Therapeutics.* 87(3):272.

Dooley, S. & Simone, M. 1994. The extent and management of drug-resistant tuberculosis: the American experience. In *Clinical tuberculosis.* Chapman & Hall Medical Londres. 171-189.

Drlica, K. & Zhao, X. 1997. DNA gyrase, topoisomerase IV, and the 4-quinolones. *Microbiology and Molecular Biology Reviews : MMBR.* 61(3):377-392.

Drusano, G.L., Sgambati, N., Eichas, A., Brown, D.L., Kulawy, R. & Louie, A. 2010. The combination of rifampin plus moxifloxacin is synergistic for suppression of resistance but antagonistic for cell kill of *Mycobacterium tuberculosis* as determined in a hollow-fiber infection model. *MBio.* 1(3):10.1128/mBio.00139-10. DOI:10.1128/mBio.00139-10 [doi].

Dubee, V., Triboulet, S., Mainardi, J.L., Etheve-Quelquejeu, M., Gutmann, L., Marie, A., Dubost, L., Hugonnet, J.E. et al. 2012. Inactivation of *Mycobacterium tuberculosis* l,d-transpeptidase LdtMt(1) by carbapenems and cephalosporins. *Antimicrobial Agents and Chemotherapy.* 56(8):4189-4195. DOI:10.1128/AAC.00665-12 [doi].

Ducati, R.G., Ruffino-Netto, A., Basso, L.A. & Santos, D.S. 2006. The resumption of consumption -- a review on tuberculosis. *Memorias do Instituto Oswaldo Cruz.* 101(7):697-714. DOI:S0074-02762006000700001 [pii].

Duvold, T., Sørensen, M.D., Björkling, F., Henriksen, A.S. & Rastrup-Andersen, N. 2001. Synthesis and conformational analysis of fusidic acid side chain derivatives in relation to antibacterial activity. *Journal of Medicinal Chemistry.* 44(19):3125-3131.

England, K., Boshoff, H.I., Arora, K., Weiner, D., Dayao, E., Schimel, D., Via, L.E. & Barry, C.E.,3rd 2012. Meropenem-clavulanic acid shows activity against *Mycobacterium*

tuberculosis in vivo. *Antimicrobial Agents and Chemotherapy*. 56(6):3384-3387. DOI:10.1128/AAC.05690-11 [doi].

Entenza, J. & Moreillon, P. 2009. Tigecycline in combination with other antimicrobials: a review of in vitro, animal and case report studies. *International Journal of Antimicrobial Agents.* 34(1):8. e1-8. e9.

Faghri, J., Poursina, F., Moghim, S., Esfahani, H.Z., Esfahani, B.N., Fazeli, H., Mirzaei, N., Jamshidian, A. et al. 2014. Morphological and bactericidal effects of different antibiotics on *Helicobacter pylori*. *Jundishapur Journal of Microbiology.* 7(1).

Feng, Z. & Barletta, R.G. 2003. Roles of *Mycobacterium smegmatis* D-alanine:D-alanine ligase and D-alanine racemase in the mechanisms of action of and resistance to the peptidoglycan inhibitor D-cycloserine. *Antimicrobial Agents and Chemotherapy.* 47(1):283-291.

Forbes, L., Ebsworth-Mojica, K., DiDone, L., Li, S., Freundlich, J.S., Connell, N., Dunman, P.M. & Krysan, D.J. 2015. A High Throughput Screening Assay for Anti-Mycobacterial small molecules based on adenylate kinase release as a reporter of cell lysis. *PloS One.* 10(6):e0129234.

Fortun, J., Martin-Davila, P., Navas, E., Perez-Elias, M.J., Cobo, J., Tato, M., De la Pedrosa, E.G., Gomez-Mampaso, E. et al. 2005. Linezolid for the treatment of multidrug-resistant tuberculosis. *The Journal of Antimicrobial Chemotherapy.* 56(1):180-185. DOI:dki148 [pii].

Franzblau, S.G., DeGroote, M.A., Cho, S.H., Andries, K., Nuermberger, E., Orme, I.M., Mdluli, K., Angulo-Barturen, I. et al. 2012. Comprehensive analysis of methods used

for the evaluation of compounds against *Mycobacterium tuberculosis*. *Tuberculosis.* 92(6):453-488.

Gao, Y.G., Selmer, M., Dunham, C.M., Weixlbaumer, A., Kelley, A.C. & Ramakrishnan, V. 2009. The structure of the ribosome with elongation factor G trapped in the posttranslocational state. *Science (New York, N.Y.).* 326(5953):694-699. DOI:10.1126/science.1179709 [doi].

GARROD, L.P. & WATERWORTH, P.M. 1962. Methods of testing combined antibiotic bactericidal action and the significance of the results. *Journal of Clinical Pathology.* 15:328-338.

Gengiah, T.N., Gray, A.L., Naidoo, K. & Karim, Q.A. 2011. Initiating antiretrovirals during tuberculosis treatment: a drug safety review. *Expert Opinion on Drug Safety.* 10(4):559-574. DOI:10.1517/14740338.2011.546783 [doi].

Giffin, R. & Robinson, S. 2009. *Addressing the Threat of Drug-Resistant Tuberculosis:: A Realistic Assessment of the Challenge: Workshop Summary*. National Academies Press.

Gilchrist, J.E., Campbell, J.E., Donnelly, C.B., Peeler, J.T. & Delaney, J.M. 1973. Spiral plate method for bacterial determination. *Applied Microbiology.* 25(2):244-252.

Gillespie, S.H. & Billington, O. 1999. Activity of moxifloxacin against mycobacteria. *The Journal of Antimicrobial Chemotherapy.* 44(3):393-395.

Gler, M.T., Skripconoka, V., Sanchez-Garavito, E., Xiao, H., Cabrera-Rivero, J.L., Vargas-Vasquez, D.E., Gao, M., Awad, M. et al. 2012. Delamanid for multidrug-resistant

pulmonary tuberculosis. *The New England Journal of Medicine.* 366(23):2151-2160. DOI:10.1056/NEJMoa1112433 [doi].

Global Alliance for TB Drug Development 2001. Tuberculosis. Scientific blueprint for tuberculosis drug development. *Tuberculosis (Edinburgh, Scotland).* 81 Suppl 1:1-52. DOI:S1472979201902884 [pii].

Godtfredsen, W. & Vangedal, S. 1962. The structure of fusidic acid. *Tetrahedron.* 18(9):1029-1048.

Godtfredsen, W., Von Daehne, W., Tybring, L. & Vangedal, S. 1966. Fusidic acid derivatives. I. Relationship between structure and antibacterial activity. *Journal of Medicinal Chemistry.* 9(1):15-22.

Gonzalez-y-Merchand, J.A., Zaragoza-Contreras, R., Guadarrama-Medina, R., Helguera-Repetto, A.C., Rivera-Gutierrez, S., Cerna-Cortes, J.F., Santos-Argumedo, L. & Cox, R.A. 2012. Evaluation of the cell growth of mycobacteria using *Mycobacterium smegmatis* mc2 155 as a representative species. *Journal of Microbiology.* 50(3):419-425.

Gopal, P., Yee, M., Sarathy, J., Low, J.L., Sarathy, J.P., Kaya, F., Dartois, V., Gengenbacher, M. et al. 2016. Pyrazinamide resistance is caused by two distinct mechanisms: prevention of Coenzyme A depletion and loss of virulence factor synthesis. *ACS Infectious Diseases.* 2(9):616-626.

Greco, W.R., Bravo, G. & Parsons, J.C. 1995. The search for synergy: a critical review from a response surface perspective. *Pharmacological Reviews.* 47(2):331-385.

Green, L.J., Marder, P., Mann, L.L., Chio, L.C. & Current, W.L. 1999. LY303366 exhibits rapid and potent fungicidal activity in flow cytometric assays of yeast viability. *Antimicrobial Agents and Chemotherapy.* 43(4):830-835.

Gupta, S., Agarwal, R. & Srivastava, S. 2014. *Textbook on Clinical Ocular Pharmacology & Therapeutics.* JP Medical Ltd.

Hards, K., Robson, J.R., Berney, M., Shaw, L., Bald, D., Koul, A., Andries, K. & Cook, G.M. 2015. Bactericidal mode of action of bedaquiline. *The Journal of Antimicrobial Chemotherapy.* 70(7):2028-2037. DOI:10.1093/jac/dkv054 [doi].

Hartkoorn, R.C., Uplekar, S. & Cole, S.T. 2014. Cross-resistance between clofazimine and bedaquiline through upregulation of MmpL5 in *Mycobacterium tuberculosis. Antimicrobial Agents and Chemotherapy.* 58(5):2979-2981. DOI:10.1128/AAC.00037-14 [doi].

Harvey, R. 1978. Interaction of two inhibitors which act on different enzymes of a metabolic pathway. *Journal of Theoretical Biology.* 74(3):411-437.

Heifets, L. & Lindholm-Levy, P. 1989. Comparison of bactericidal activities of streptomycin, amikacin, kanamycin, and capreomycin against *Mycobacterium avium* and *M. tuberculosis*. *Antimicrobial Agents and Chemotherapy.* 33(8):1298-1301.

Hendon-Dunn, C.L., Doris, K.S., Thomas, S.R., Allnutt, J.C., Marriott, A.A., Hatch, K.A., Watson, R.J., Bottley, G. et al. 2016. A flow cytometry method for rapidly assessing *M. tuberculosis* responses to antibiotics with different modes of action. *Antimicrobial Agents and Chemotherapy.* DOI:AAC.02712-15 [pii].

Hirashima, A. & Kaji, A. 1973. Role of elongation factor G and a protein factor on the release of ribosomes from messenger ribonucleic acid. *The Journal of Biological Chemistry.* 248(21):7580-7587.

Hoagland, D., Zhao, Y. & E Lee, R. 2016. Advances in Drug Discovery and Development for Pediatric Tuberculosis. *Mini Reviews in Medicinal Chemistry.* 16(6):481-497.

Hoeksema, H. & Knight, J.C. 1975. The production of dihydrospectinomycin by *Syreptomyces spect abilis*. *The Journal of Antibiotics.* 28(3):240-241.

Hoffner, S., Olsson-Liljequist, B., Rydgård, K., Svenson, S. & Källenius, G. 1990. Susceptibility of mycobacteria to fusidic acid. *European Journal of Clinical Microbiology and Infectious Diseases.* 9(4):294-297.

Hoffner, S.E., Cristea, M., Klintz, L., Petrini, B. & Kallenius, G. 1996. RNA amplification for direct detection of *Mycobacterium tuberculosis* in respiratory samples. *Scandinavian Journal of Infectious Diseases.* 28(1):59-61.

Horita, Y., Maeda, S., Kazumi, Y. & Doi, N. 2014. In vitro susceptibility of *Mycobacterium tuberculosis* isolates to an oral carbapenem alone or in combination with beta-lactamase inhibitors. *Antimicrobial Agents and Chemotherapy*. 58(11):7010-7014. DOI:10.1128/AAC.03539-14 [doi].

Hsieh, M.H., Chen, M.Y., Victor, L.Y. & Chow, J.W. 1993. Synergy assessed by checkerboard a critical analysis. *Diagnostic Microbiology and Infectious Disease.* 16(4):343-349.

Hugonnet, J.E. & Blanchard, J.S. 2007. Irreversible inhibition of the *Mycobacterium tuberculosis* beta-lactamase by clavulanate. *Biochemistry.* 46(43):11998-12004. DOI:10.1021/bi701506h [doi].

Jewetz E., Gunnison, J.B., Bruff, J.B. & Coleman, V.R. 1952. Studies on antibiotic synergism and antagonism. Synergism among seven antibiotics against various bacteria in vitro. *Journal of Bacteriology.* 64(1):29-39.

Jia, J., Zhu, F., Ma, X., Cao, Z.W., Li, Y.X. & Chen, Y.Z. 2009. Mechanisms of drug combinations: interaction and network perspectives. *Nature Reviews Drug Discovery.* 8(2):111-128.

Johanson, U. & Hughes, D. 1994. Fusidic acid-resistant mutants define three regions in elongation factor G of *Salmonella typhimurium*. *Gene.* 143(1):55-59.

Johnson, R., Streicher, E.M., Louw, G.E., Warren, R.M., Van Helden, P.D. & Victor, T. 2007. Drug resistance in M. tuberculosis. *Understanding the Mechanisms of Drug Resistance in Enhancing Rapid Molecular Detection of Drug Resistance in Mycobacterium Tuberculosis.* 7.

Johnson, M.D., MacDougall, C., Ostrosky-Zeichner, L., Perfect, J.R. & Rex, J.H. 2004. Combination antifungal therapy. *Antimicrobial Agents and Chemotherapy.* 48(3):693-715.

Kaneko, T., Cooper, C. & Mdluli, K. 2011. Challenges and opportunities in developing novel drugs for TB. *Future Medicinal Chemistry.* 3(11):1373-1400.

Kang, D.D., Lin, Y., Moreno, J., Randall, T.D. & Khader, S.A. 2011. Profiling early lung immune responses in the mouse model of tuberculosis. *PloS One.* 6(1):e16161.

Karimi, R., Pavlov, M.Y., Buckingham, R.H. & Ehrenberg, M. 1999. Novel roles for classical factors at the interface between translation termination and initiation. *Molecular Cell.* 3(5):601-609.

Kaufmann, S.H. & Schaible, U.E. 2005. 100th anniversary of Robert Koch's Nobel Prize for the discovery of the tubercle bacillus. *Trends in Microbiology.* 13(10):469-475. DOI:S0966-842X(05)00202-7 [pii].

Kaur, P., Ghosh, A., Krishnamurthy, R.V., Bhattacharjee, D.G., Achar, V., Datta, S., Narayanan, S., Anbarasu, A. et al. 2015. A high-throughput cidality screen for *Mycobacterium tuberculosis*. *PloS One.* 10(2):e0117577.

Keith, C.T., Borisy, A.A. and Stockwell, B.R., 2005. Multicomponent therapeutics for net worked systems. *Nature reviews Drug discovery*, *4*(1), pp.71-78.

Kigondu, E.V.M. 2015. *Repurposing Chlorpromazine and its Metabolites for Antituberculosis Drug Discovery.*

Kim, H.S. & Fay, J.C. 2007. Genetic variation in the cysteine biosynthesis pathway causes sensitivity to pharmacological compounds. *Proceedings of the National Academy of Sciences of the United States of America.* 104(49):19387-19391. DOI:0708194104 [pii].

Kitano, H. 2007. A robustness-based approach to systems-oriented drug design. *Nature Reviews Drug Discovery.* 5(3):202-210.

Kloss, P., Xiong, L., Shinabarger, D.L. & Mankin, A.S. 1999. Resistance mutations in 23 S rRNA identify the site of action of the protein synthesis inhibitor linezolid in the ribosomal peptidyl transferase center. *Journal of Molecular Biology.* 294(1):93-101. DOI:10.1006/jmbi.1999.3247 [doi].

Kohanski, M.A., Dwyer, D.J., Hayete, B., Lawrence, C.A. & Collins, J.J. 2007. A common mechanism of cellular death induced by bactericidal antibiotics. *Cell.* 130(5):797-810.

Koripella, R.K., Chen, Y., Peisker, K., Koh, C.S., Selmer, M. & Sanyal, S. 2012. Mechanism of elongation factor-G-mediated fusidic acid resistance and fitness compensation in *Staphylococcus aureus*. *The Journal of Biological Chemistry.* 287(36):30257-30267. DOI:10.1074/jbc.M112.378521 [doi].

Koul, A., Arnoult, E., Lounis, N., Guillemont, J. & Andries, K. 2011. The challenge of new drug discovery for tuberculosis. *Nature.* 469(7331):483-490. DOI:10.1038/nature09657 [doi].

Kramer, C.E., Wiechert, W. & Kohlheyer, D. 2016. Time-resolved, single-cell analysis of induced and programmed cell death via non-invasive propidium iodide and counterstain perfusion. *Scientific Reports.* 6:32104. DOI:10.1038/srep32104 [doi].

Kumar, A., Farhana, A., Guidry, L., Saini, V., Hondalus, M. & Steyn, A.J. 2011. Redox homeostasis in mycobacteria: the key to tuberculosis control? *Expert Reviews in Molecular Medicine.* 13:e39. DOI:10.1017/S1462399411002079 [doi].

Kurien, S. & Lorian, V. 1980. Discrepancies between results obtained by agar and broth techniques in testing of drug combinations. *Journal of Clinical Microbiology.* 11(5):527-529.

Leach, K.L., Brickner, S.J., Noe, M.C. & Miller, P.F. 2011. Linezolid, the first oxazolidinone antibacterial agent. *Annals of the New York Academy of Sciences.* 1222:49-54. DOI:10.1111/j.1749-6632.2011.05962.x [doi].

Lee, C.S., Gambertoglio, J.G., Brater, D.C. & Benet, L.Z. 1977. Kinetics of oral ethambutol in the normal subject. *Clinical Pharmacology and Therapeutics.* 22(5 Pt 1):615-621.

Lee, R.E., Hurdle, J.G., Liu, J., Bruhn, D.F., Matt, T., Scherman, M.S., Vaddady, P.K., Zheng, Z. et al. 2014. Spectinamides: a new class of semisynthetic antituberculosis agents that overcome native drug efflux. *Nature Medicine.* 20(2):152-158. DOI:10.1038/nm.3458 [doi].

Lehár, J., Krueger, A.S., Avery, W., Heilbut, A.M., Johansen, L.M., Price, E.R., Rickles, R.J., Short Iii, G.F. et al. 2009. Synergistic drug combinations tend to improve therapeutically relevant selectivity. *Nature Biotechnology.* 27(7):659-666.

Levy, S.B. & Marshall, B. 2004. Antibacterial resistance worldwide: causes, challenges and responses. *Nature Medicine.* 10:S122-S129.

Li, W., Sanchez-Hidalgo, A., Jones, V., de Moura, Vinicius Calado Nogueira, North, E.J. & Jackson, M. 2017. Synergistic interactions of MmpL3 inhibitors with antitubercular compounds in vitro. *Antimicrobial Agents and Chemotherapy.* :AAC. 02399-16.

Lin, Y., Li, Y., Zhu, N., Han, Y., Jiang, W., Wang, Y., Si, S. & Jiang, J. 2014. The antituberculosis antibiotic capreomycin inhibits protein synthesis by disrupting interaction between ribosomal proteins L12 and L10. *Antimicrobial Agents and Chemotherapy.* 58(4):2038-2044. DOI:10.1128/AAC.02394-13 [doi].

LOEWE, S. 1953. The problem of synergism and antagonism of combined drugs. *Arzneimittel-Forschung.* 3(6):285-290.

Lomovskaya, O., Lee, A., Hoshino, K., Ishida, H., Mistry, A., Warren, M.S., Boyer, E., Chamberland, S. et al. 1999. Use of a genetic approach to evaluate the consequences of inhibition of efflux pumps in Pseudomonas aeruginosa. *Antimicrobial Agents and Chemotherapy.* 43(6):1340-1346.

Lorian, V. 2005. *Antibiotics in laboratory medicine.* Lippincott Williams & Wilkins.

Lyutzkanova, D., Distler, J. & Altenbuchner, J. 1997. A spectinomyciin resistance determinant from the spectinomycin producerStreptomyces flavopersicus. *Microbiology.* 143(7):2135-2143.

Macvanin, M. & Hughes, D. 2005. Hyper-susceptibility of a fusidic acid-resistant mutant of Salmonella to different classes of antibiotics. *FEMS Microbiology Letters.* 247(2):215-220. DOI:S0378-1097(05)00289-2 [pii].

Macvanin, M., Johanson, U., Ehrenberg, M. & Hughes, D. 2000. Fusidic acid-resistant EF-G perturbs the accumulation of ppGpp. *Molecular Microbiology.* 37(1):98-107. DOI:mmi1967 [pii].

Makarov, V., Manina, G., Mikusova, K., Mollmann, U., Ryabova, O., Saint-Joanis, B., Dhar, N., Pasca, M.R. et al. 2009. Benzothiazinones kill *Mycobacterium tuberculosis* by blocking arabinan synthesis. *Science (New York, N.Y.).* 324(5928):801-804. DOI:10.1126/science.1171583 [doi].

Marcoli, R., Iida, S. & Bickle, T.A. 1980. The DNA sequence of an IS1-flanked transposon coding for resistance to chloramphenicol and fusidic acid. *FEBS Letters*. 110(1):11-14.

Markham, P.N. 1999. Inhibition of the emergence of ciprofloxacin resistance in Streptococcus pneumoniae by the multidrug efflux inhibitor reserpine. *Antimicrobial Agents and Chemotherapy*. 43(4):988-989.

Markham, P.N. & Neyfakh, A.A. 1996. Inhibition of the multidrug transporter NorA prevents emergence of norfloxacin resistance in *Staphylococcus aureus*. *Antimicrobial Agents and Chemotherapy*. 40(11):2673-2674.

Martemyanov, K.A., Liljas, A., Yarunin, A.S. & Gudkov, A.T. 2001. Mutations in the G-domain of elongation factor G from Thermus thermophilus affect both its interaction with GTP and fusidic acid. *The Journal of Biological Chemistry*. 276(31):28774-28778. DOI:10.1074/jbc.M102023200 [doi].

Martinez-Irujo, J.J., Villahermosa, M.L., Alberdi, E. & Santiago, E. 1996. A checkerboard method to evaluate interactions between drugs. *Biochemical Pharmacology*. 51(5):635-644.

McDougald, D., Rice, S.A., Weichart, D. & Kjelleberg, S. 1998. Nonculturability: adaptation or debilitation? *FEMS Microbiology Ecology*. 25(1):1-9.

Mensa, B., Kim, Y.H., Choi, S., Scott, R., Caputo, G.A. & DeGrado, W.F. 2011. Antibacterial mechanism of action of arylamide foldamers. *Antimicrobial Agents and Chemotherapy*. 55(11):5043-5053. DOI:10.1128/AAC.05009-11 [doi].

Merle, C.S., Fielding, K., Sow, O.B., Gninafon, M., Lo, M.B., Mthiyane, T., Odhiambo, J., Amukoye, E. et al. 2014. A four-month gatifloxacin-containing regimen for treating tuberculosis. *The New England Journal of Medicine.* 371(17):1588-1598. DOI:10.1056/NEJMoa1315817 [doi].

Miesel, L., Weisbrod, T.R., Marcinkeviciene, J.A., Bittman, R. & Jacobs, W.R.,Jr 1998. NADH dehydrogenase defects confer isoniazid resistance and conditional lethality in *Mycobacterium smegmatis*. *Journal of Bacteriology.* 180(9):2459-2467.

Milazzo, I., Blandino, G., Caccamo, F., Musumeci, R., Nicoletti, G. & Speciale, A. 2003. Faropenem, a new oral penem: antibacterial activity against selected anaerobic and fastidious periodontal isolates. *The Journal of Antimicrobial Chemotherapy.* 51(3):721-725.

Miyazaki, E., Miyazaki, M., Chen, J.M., Chaisson, R.E. & Bishai, W.R. 1999. Moxifloxacin (BAY12-8039), a new 8-methoxyquinolone, is active in a mouse model of tuberculosis. *Antimicrobial Agents and Chemotherapy.* 43(1):85-89.

Moadebi, S., Harder, C.K., Fitzgerald, M.J., Elwood, K.R. & Marra, F. 2007. Fluoroquinolones for the treatment of pulmonary tuberculosis. *Drugs.* 67(14):2077-2099. DOI:67147 [pii].

Moghoofei, M., Fazeli, H., Poursina, F., Esfahani, B.N., Moghim, S., Vaez, H., Hadifar, S. & Safaei, H.G. 2015. Morphological and Bactericidal Effects of Amikacin, Meropenem and Imipenem on Pseudomonas aeruginosa. *Jundishapur Journal of Microbiology.* 8(11).

Mueller, M., de la Pena, A. & Derendorf, H. 2004. Issues in pharmacokinetics and pharmacodynamics of anti-infective agents: kill curves versus MIC. *Antimicrobial Agents and Chemotherapy*. 48(2):369-377.

Munsiff, S.S., Kambili, C. & Ahuja, S.D. 2006. Rifapentine for the treatment of pulmonary tuberculosis. *Clinical Infectious Diseases : An Official Publication of the Infectious Diseases Society of America.* 43(11):1468-1475. DOI:CID39133 [pii].

Murray, R.A., Siddiqui, M.R., Mendillo, M., Krahenbuhl, J. & Kaplan, G. 2007. Mycobacterium leprae inhibits dendritic cell activation and maturation. *Journal of Immunology (Baltimore, Md.: 1950).* 178(1):338-344. DOI:178/1/338 [pii].

Myint, K.B., Sing, L.C. & Wei, Z. 2013. Tannic Acid as Phytochemical Potentiator for Antibiotic Resistance Adaptation. *APCBEE Procedia.* 7:175-181.

Nagaev, I., Björkman, J., Andersson, D.I. & Hughes, D. 2001. Biological cost and compensatory evolution in fusidic acid-resistant *Staphylococcus aureus*. *Molecular Microbiology*. 40(2):433-439.

Naylor, D.M. 2015. Therapeutic Drug Repurposing, Repositioning and Rescue. *Drug Discovery*. :57.

Nebe-von-Caron, G., Stephens, P., Hewitt, C., Powell, J. & Badley, R. 2000. Analysis of bacterial function by multi-colour fluorescence flow cytometry and single cell sorting. *Journal of Microbiological Methods.* 42(1):97-114.

Nguta, J.M., Appiah-Opong, R., Nyarko, A.K., Yeboah-Manu, D. & Addo, P.G. 2015. Current perspectives in drug discovery against tuberculosis from natural products. *International Journal of Mycobacteriology.* 4(3):165-183.

Nichols, R.J., Sen, S., Choo, Y.J., Beltrao, P., Zietek, M., Chaba, R., Lee, S., Kazmierczak, K.M. et al. 2011. Phenotypic landscape of a bacterial cell. *Cell.* 144(1):143-156.

Ntziora, F. & Falagas, M.E. 2007. Linezolid for the treatment of patients with [corrected] mycobacterial infections [corrected] a systematic review. *The International Journal of Tuberculosis and Lung Disease : The Official Journal of the International Union Against Tuberculosis and Lung Disease.* 11(6):606-611.

Nygaard, H.B., van Dyck, C.H. & Strittmatter, S.M. 2014. Fyn kinase inhibition as a novel therapy for Alzheimer's disease. *Alzheimer's Research & Therapy.* 6(1):1.

Nzila, A., Ma, Z. & Chibale, K. 2011. Drug repositioning in the treatment of malaria and TB. *Future Medicinal Chemistry.* 3(11):1413-1426.

Ocampo, P.S., Lazar, V., Papp, B., Arnoldini, M., Abel zur Wiesch, P., Busa-Fekete, R., Fekete, G., Pal, C. et al. 2014. Antagonism between bacteriostatic and bactericidal antibiotics is prevalent. *Antimicrobial Agents and Chemotherapy.* 58(8):4573-4582. DOI:10.1128/AAC.02463-14 [doi].

Odds, F.C. 2003. Synergy, antagonism, and what the chequerboard puts between them. *The Journal of Antimicrobial Chemotherapy.* 52(1):1. DOI:10.1093/jac/dkg301 [doi].

O'Donnell, M., Padayatchi, N. & Metcalfe, J. 2016. Elucidating the role of clofazimine for the treatment of tuberculosis. *The International Journal of Tuberculosis and Lung Disease.* 20(12):S52-S57.

Okuda, S., Iwasaki, S., Tsuda, K., Sano, Y., Hata, T., Udagawa, S., Nakayama, Y. & Yamaguchi, H. 1964. The structure of helvolic acid. *Chemical and Pharmaceutical Bulletin.* 12(1):121-124.

Okura, A., KINOSHITA, T. & TANAKA, N. 1971. Formation of fusidic acid-G factor-GDP-ribosome complex and the relationship to the inhibition of GTP hydrolysis. *The Journal of Antibiotics.* 24(10):655-661.

Oliver, J.D. 2010. Recent findings on the viable but nonculturable state in pathogenic bacteria. *FEMS Microbiology Reviews.* 34(4):415-425. DOI:10.1111/j.1574-6976.2009.00200.x [doi].

Orme, I.M. 1988. Characteristics and specificity of acquired immunologic memory to *Mycobacterium tuberculosis* infection. *Journal of Immunology (Baltimore, Md.: 1950).* 140(10):3589-3593.

Owens, C.P., Chim, N., Graves, A.B., Harmston, C.A., Iniguez, A., Contreras, H., Liptak, M.D. & Goulding, C.W. 2013. The *Mycobacterium tuberculosis* secreted protein Rv0203 transfers heme to membrane proteins MmpL3 and MmpL11. *The Journal of Biological Chemistry.* 288(30):21714-21728. DOI:10.1074/jbc.M113.453076 [doi].

Pankey, G.A. & Sabath, L.D. 2004. Clinical relevance of bacteriostatic versus bactericidal mechanisms of action in the treatment of Gram-positive bacterial infections. *Clinical*

Infectious Diseases : An Official Publication of the Infectious Diseases Society of America. 38(6):864-870. DOI:10.1086/381972 [doi].

Paparella, A., Taccogna, L., Aguzzi, I., Chaves-López, C., Serio, A., Marsilio, F. & Suzzi, G. 2008. Flow cytometric assessment of the antimicrobial activity of essential oils against Listeria monocytogenes. *Food Control.* 19(12):1174-1182.

Payen, M., De Wit, S., Martin, C., Sergysels, R., Muylle, I., Van Laethem, Y. & Clumeck, N. 2012. Clinical use of the meropenem-clavulanate combination for extensively drug-resistant tuberculosis [Case study]. *The International Journal of Tuberculosis and Lung Disease.* 16(4):558-560.

Peteroy, M., Severin, A., Zhao, F., Rosner, D., Lopatin, U., Scherman, H., Belanger, A., Harvey, B. et al. 2000. Characterization of a *Mycobacterium smegmatis* mutant that is simultaneously resistant to D-cycloserine and vancomycin. *Antimicrobial Agents and Chemotherapy*. 44(6):1701-1704.

Peterson, L.R. & Shanholtzer, C.J. 1992. Tests for bactericidal effects of antimicrobial agents: technical performance and clinical relevance. *Clinical Microbiology Reviews.* 5(4):420-432.

Pethe, K., Bifani, P., Jang, J., Kang, S., Park, S., Ahn, S., Jiricek, J., Jung, J. et al. 2013. Discovery of Q203, a potent clinical candidate for the treatment of tuberculosis. *Nature Medicine.* 19(9):1157-1160. DOI:10.1038/nm.3262 [doi].

Phee, L.M., Betts, J.W., Bharathan, B. & Wareham, D.W. 2015. Colistin and Fusidic Acid, a Novel Potent Synergistic Combination for Treatment of Multidrug-Resistant

Acinetobacter baumannii Infections. *Antimicrobial Agents and Chemotherapy.* 59(8):4544-4550. DOI:10.1128/AAC.00753-15 [doi].

Plotz, P.H. & Davis, B.D. 1962. Synergism between streptomycin and penicillin: a proposed mechanism. *Science (New York, N.Y.).* 135(3508):1067-1068.

Podolsky, S.H. & Greene, J.A. 2011. Combination drugs—hype, harm, and hope. *New England Journal of Medicine.* 365(6):488-491.

Porse, B.T. & Garrett, R.A. 1999. Sites of interaction of streptogramin A and B antibiotics in the peptidyl transferase loop of 23 S rRNA and the synergism of their inhibitory mechanisms. *Journal of Molecular Biology.* 286(2):375-387.

Prideaux, B., Via, L.E., Zimmerman, M.D., Eum, S., Sarathy, J., O'Brien, P., Chen, C., Kaya, F. et al. 2015. The association between sterilizing activity and drug distribution into tuberculosis lesions. *Nature Medicine.* 21(10):1223-1227. DOI:10.1038/nm.3937 [doi].

Primm, T.P. & Franzblau, S.G. 2007. Recent advances in methodologies for the discovery of antimycobacterial drugs. *Current Bioactive Compounds.* 3(3):201-208.

Ramani, R. & Chaturvedi, V. 2000. Flow cytometry antifungal susceptibility testing of pathogenic yeasts other than Candida albicans and comparison with the NCCLS broth microdilution test. *Antimicrobial Agents and Chemotherapy.* 44(10):2752-2758.

Ramaswamy, S. & Musser, J.M. 1998. Molecular genetic basis of antimicrobial agent resistance in*Mycobacterium tuberculosis*: 1998 update. *Tubercle and Lung Disease.* 79(1):3-29.

Ramon-Garcia, S., Mick, V., Dainese, E., Martin, C., Thompson, C.J., De Rossi, E., Manganelli, R. & Ainsa, J.A. 2012. Functional and genetic characterization of the tap efflux pump in Mycobacterium bovis BCG. *Antimicrobial Agents and Chemotherapy.* 56(4):2074-2083. DOI:10.1128/AAC.05946-11 [doi].

Ramon-Garcia, S., Ng, C., Anderson, H., Chao, J.D., Zheng, X., Pfeifer, T., Av-Gay, Y., Roberge, M. et al. 2011. Synergistic drug combinations for tuberculosis therapy identified by a novel high-throughput screen. *Antimicrobial Agents and Chemotherapy.* 55(8):3861-3869. DOI:10.1128/AAC.00474-11 [doi].

Reddy, V.M., Einck, L., Andries, K. & Nacy, C.A. 2010. In vitro interactions between new antitubercular drug candidates SQ109 and TMC207. *Antimicrobial Agents and Chemotherapy.* 54(7):2840-2846. DOI:10.1128/AAC.01601-09 [doi].

Reeves, D.S. 1987. The pharmacokinetics of fusidic acid. *The Journal of Antimicrobial Chemotherapy.* 20(4):467-476.

Ribeiro, A.L., Degiacomi, G., Ewann, F., Buroni, S., Incandela, M.L., Chiarelli, L.R., Mori, G., Kim, J. et al. 2011. Analogous mechanisms of resistance to benzothiazinones and dinitrobenzamides in *Mycobacterium smegmatis*. *PloS One.* 6(11):e26675. DOI:10.1371/journal.pone.0026675 [doi].

Rivers, E.C. & Mancera, R.L. 2008. New anti-tuberculosis drugs in clinical trials with novel mechanisms of action. *Drug Discovery Today.* 13(23-24):1090-1098. DOI:10.1016/j.drudis.2008.09.004 [doi].

Rolinson, G.N. 1998. Forty years of beta-lactam research. *The Journal of Antimicrobial Chemotherapy.* 41(6):589-603.

Rosen, B.P. & Mobashery, S. 2012. *Resolving the antibiotic paradox: progress in understanding drug resistance and development of new antibiotics.* Springer Science & Business Media.

Roth, B.L., Poot, M., Yue, S.T. & Millard, P.J. 1997. Bacterial viability and antibiotic susceptibility testing with SYTOX green nucleic acid stain. *Applied and Environmental Microbiology.* 63(6):2421-2431.

Russell, D.G. 2001. *Mycobacterium tuberculosis*: here today, and here tomorrow. *Nature Reviews Molecular Cell Biology.* 2(8):569-586.

Sachidanandham, R., Yew-Hoong Gin, K. & Laa Poh, C. 2005. Monitoring of active but non-culturable bacterial cells by flow cytometry. *Biotechnology and Bioengineering.* 89(1):24-31.

Sanders, D.A., Staines, A.G., McMahon, S.A., McNeil, M.R., Whitfield, C. & Naismith, J.H. 2001. UDP-galactopyranose mutase has a novel structure and mechanism. *Nature Structural Biology.* 8(10):858-863. DOI:10.1038/nsb1001-858 [doi].

Sandgren, A., Strong, M., Muthukrishnan, P., Weiner, B.K., Church, G.M. & Murray, M.B. 2009. Tuberculosis drug resistance mutation database. *PLoS Med.* 6(2):e1000002.

Sarathy, J.P., Zuccotto, F., Hsinpin, H., Sandberg, L., Via, L.E., Marriner, G.A., Masquelin, T., Wyatt, P. et al. 2016. Prediction of drug penetration in tuberculosis lesions. *ACS Infectious Diseases.* 2(8):552-563.

Savelsbergh, A., Rodnina, M.V. & Wintermeyer, W. 2009. Distinct functions of elongation factor G in ribosome recycling and translocation. *RNA (New York, N.Y.).* 15(5):772-780. DOI:10.1261/rna.1592509 [doi].

Scannell, J.W., Blanckley, A., Boldon, H. & Warrington, B. 2012. Diagnosing the decline in pharmaceutical R&D efficiency. *Nature Reviews Drug Discovery.* 11(3):191-200.

Schurek, K.N., Wiebe, R., Karlowsky, J.A., Rubinstein, E., Hoban, D.J. & Zhanel, G.G. 2007. Faropenem: review of a new oral penem. *Expert Review of Anti-Infective Therapy.* 5(2):185-198.

Scorpio, A. & Zhang, Y. 1996. Mutations in pncA, a gene encoding pyrazinamidase/nicotinamidase, cause resistance to the antituberculous drug pyrazinamide in tubercle bacillus. *Nature Medicine.* 2(6):662-667.

Shi, W., Zhang, X., Jiang, X., Yuan, H., Lee, J.S., Barry, C.E.,3rd, Wang, H., Zhang, W. et al. 2011. Pyrazinamide inhibits trans-translation in *Mycobacterium tuberculosis*. *Science (New York, N.Y.).* 333(6049):1630-1632. DOI:10.1126/science.1208813 [doi].

Shleeva, M., Mukamolova, G.V., Young, M., Williams, H.D. & Kaprelyants, A.S. 2004. Formation of 'non-culturable'cells of *Mycobacterium smegmatis* in stationary phase in response to growth under suboptimal conditions and their Rpf-mediated resuscitation. *Microbiology.* 150(6):1687-1697.

Singh, R., Manjunatha, U., Boshoff, H.I., Ha, Y.H., Niyomrattanakit, P., Ledwidge, R., Dowd, C.S., Lee, I.Y. et al. 2008. PA-824 kills nonreplicating *Mycobacterium*

tuberculosis by intracellular NO release. *Science (New York, N.Y.).* 322(5906):1392-1395. DOI:10.1126/science.1164571 [doi].

Smalley, K.S., Haass, N.K., Brafford, P.A., Lioni, M., Flaherty, K.T. & Herlyn, M. 2006. Multiple signaling pathways must be targeted to overcome drug resistance in cell lines derived from melanoma metastases. *Molecular Cancer Therapeutics.* 5(5):1136-1144. DOI:5/5/1136 [pii].

Small, B.G., McColl, B.W., Allmendinger, R., Pahle, J., López-Castejón, G., Rothwell, N.J., Knowles, J., Mendes, P., Brough, D. and Kell, D.B., 2011. Efficient discovery of anti-inflammatory small-molecule combinations using evolutionary computing. *Nature chemical biology*, *7*(12), pp.902-908.

Smeulders, M.J., Keer, J., Speight, R.A. & Williams, H.D. 1999. Adaptation of *Mycobacterium smegmatis* to stationary phase. *Journal of Bacteriology.* 181(1):270-283.

Spitzer, M., Griffiths, E., Blakely, K.M., Wildenhain, J., Ejim, L., Rossi, L., De Pascale, G., Curak, J., Brown, E., Tyers, M. and Wright, G.D., 2011. Cross-species discovery of syncretic drug combinations that potentiate the antifungal fluconazole. *Molecular Systems Biology*, *7*(1), p.499

Staudinger, T., Redl, B. & Glasgow, B.J. 2014. Antibacterial activity of rifamycins for M. smegmatis with comparison of oxidation and binding to tear lipocalin. *Biochimica Et Biophysica Acta (BBA)-Proteins and Proteomics.* 1844(4):750-758.

Stefanovic-Racic, M., Yang, X., Turner, M.S., Mantell, B.S., Stolz, D.B., Sumpter, T.L., Sipula, I.J., Dedousis, N. et al. 2012. Dendritic cells promote macrophage infiltration and comprise a substantial proportion of obesity-associated increases in CD11c+ cells in adipose tissue and liver. *Diabetes.* 61(9):2330-2339. DOI:10.2337/db11-1523 [doi].

Strittmatter, S.M. 2014. Overcoming drug development bottlenecks with repurposing: old drugs learn new tricks. *Nature Medicine.* 20(6):590-591.

Sühnel, J. 1990. Evaluation of synergism or antagonism for the combined action of antiviral agents. *Antiviral Research.* 13(1):23-39.

Tabernero, J., Rojo, F., Calvo, E., Burris, H., Judson, I., Hazell, K., Martinelli, E., Ramon y Cajal, S. et al. 2008. Dose- and schedule-dependent inhibition of the mammalian target of rapamycin pathway with everolimus: a phase I tumor pharmacodynamic study in patients with advanced solid tumors. *Journal of Clinical Oncology : Official Journal of the American Society of Clinical Oncology.* 26(10):1603-1610. DOI:10.1200/JCO.2007.14.5482 [doi].

Taburet, A.M., Guibert, J., Kitzis, M.D., Sorensen, H., Acar, J.F. & Singlas, E. 1990. Pharmacokinetics of sodium fusidate after single and repeated infusions and oral administration of a new formulation. *The Journal of Antimicrobial Chemotherapy.* 25 Suppl B:23-31.

Tahlan, K., Wilson, R., Kastrinsky, D.B., Arora, K., Nair, V., Fischer, E., Barnes, S.W., Walker, J.R. et al. 2012. SQ109 targets MmpL3, a membrane transporter of trehalose monomycolate involved in mycolic acid donation to the cell wall core of *Mycobacterium tuberculosis*. *Antimicrobial Agents and Chemotherapy.* 56(4):1797-1809. DOI:10.1128/AAC.05708-11 [doi].

Takayama, K. & Kilburn, J.O. 1989. Inhibition of synthesis of arabinogalactan by ethambutol in *Mycobacterium smegmatis*. *Antimicrobial Agents and Chemotherapy.* 33(9):1493-1499.

Tekin, E., Beppler, C., White, C., Mao, Z., Savage, V.M. & Yeh, P.J. 2016. Enhanced identification of synergistic and antagonistic emergent interactions among three or more drugs. *Journal of the Royal Society Interface.* 13(119):20160332.

Torella, J.P., Chait, R. & Kishony, R. 2010. Optimal drug synergy in antimicrobial treatments. *PLoS Comput Biol.* 6(6):e1000796.

Trefzer, C., Rengifo-Gonzalez, M., Hinner, M.J., Schneider, P., Makarov, V., Cole, S.T. & Johnsson, K. 2010. Benzothiazinones: prodrugs that covalently modify the decaprenylphosphoryl-β-D-ribose 2′-epimerase DprE1 of *Mycobacterium tuberculosis*. *Journal of the American Chemical Society.* 132(39):13663-13665.

Tuomanen, E., Durack, D.T. & Tomasz, A. 1986. Antibiotic tolerance among clinical isolates of bacteria. *Antimicrobial Agents and Chemotherapy.* 30(4):521-527.

Turnidge, J. & Collignon, P. 1999. Resistance to fusidic acid. *International Journal of Antimicrobial Agents.* 12:S35-S44.

Vanderhaeghe, H., Van Dijck, P. & De Somer, P. 1965. Identity of ramycin with fusidic acid. *Nature.* 205(4972):710-711.

Vannuffel, P. & Cocito, C. 1996. Mechanism of action of streptogramins and macrolides. *Drugs.* 51(1):20-30.

Verbist, L. 1990. The antimicrobial activity of fusidic acid. *The Journal of Antimicrobial Chemotherapy.* 25 Suppl B:1-5.

Von Daehne, W., Godtfredsen, W. & Rasmussen, P. 1979. Structure-activity relationships in fusidic acid-type antibiotics. *Advances in Applied Microbiology.* 25:95-146.

WALLGREN, A. 1948. B.C.G. vaccination; is it of any value in control of tuberculosis? *British Medical Journal.* 1(4562):1126-1129.

Warner, D.F. 2014. *Mycobacterium tuberculosis* metabolism. *Cold Spring Harbor Perspectives in Medicine.* 5(4):10.1101/cshperspect.a021121. DOI:10.1101/cshperspect.a021121 [doi].

Wayne, P. 2007. Clinical and laboratory standards institute. *Performance Standards for Antimicrobial Susceptibility Testing.* 17.

Weinstein, E.A., Yano, T., Li, L.S., Avarbock, D., Avarbock, A., Helm, D., McColm, A.A., Duncan, K. et al. 2005. Inhibitors of type II NADH:menaquinone oxidoreductase represent a class of antitubercular drugs. *Proceedings of the National Academy of Sciences of the United States of America.* 102(12):4548-4553. DOI:0500469102 [pii].

WHO, T. Global tubeculosis report 2016.

WHO, W. 2012. Global tuberculosis report 2012. *World Health Organization, Geneva Http://apps.Who.int/iris/bitstream/10665/91355/1/9789241564656_eng.Pdf.*

Williamson, E.M. 2001. Synergy and other interactions in phytomedicines. *Phytomedicine.* 8(5):401-409.

Willie, G.R., Richman, N., Godtfredsen, W. & Bodley, J.W. 1975a. Translocation. XV. Characteristics of and structural requirements for the interaction of 24, 25-dihydrofusidic acid with ribosome. elongation factor G complexes. *Biochemistry.* 14(8):1713-1718.

Willie, G.R., Richman, N., Godtfredsen, W. & Bodley, J.W. 1975b. Translocation. XV. Characteristics of and structural requirements for the interaction of 24, 25-dihydrofusidic acid with ribosome. elongation factor G complexes. *Biochemistry.* 14(8):1713-1718.

Wilson, D.N. 2009. The A–Z of bacterial translation inhibitors. *Critical Reviews in Biochemistry and Molecular Biology.* 44(6):393-433.

Winder, F. & Collins, P. 1970. Inhibition by isoniazid of synthesis of mycolic acids in *Mycobacterium tuberculosis*. *Microbiology.* 63(1):41-48.

Winglee, K., Lun, S., Pieroni, M., Kozikowski, A. & Bishai, W. 2015. Mutation of Rv2887, a marR-like gene, confers Mycobacterium tuberculosis resistance to an imidazopyridine-based agent. *Antimicrobial Agents and Chemotherapy.* 59(11):6873-6881. DOI:10.1128/AAC.01341-15 [doi].

World Health Organization 2014. Companion handbook to the WHO guidelines for the programmatic management of drug-resistant tuberculosis.

World Health Organization 2015. Global tuberculosis report 2015.

Wright, G.D. 2016. Antibiotic Adjuvants: Rescuing Antibiotics from Resistance. *Trends in Microbiology.*

Wu, M., Gengenbacher, M. & Dick, T. 2016. Mild nutrient starvation triggers the development of a small-cell survival morphotype in mycobacteria. *Frontiers in Microbiology.* 7.

Yang, H., Chen, G., Hu, L., Liu, Y., Cheng, J., Ye, Y. & Li, J. 2016. Enhanced efficacy of imipenem-colistin combination therapy against multiple-drug-resistant Enterobacter cloacae: in vitro activity and a Galleria mellonella model. *Journal of Microbiology, Immunology and Infection.*

Yang, C., Lei, H., Wang, D., Meng, X., He, J., Tong, A., Zhu, L., Jiang, Y. et al. 2012. In vitro activity of linezolid against clinical isolates of *Mycobacterium tuberculosis*, including multidrug-resistant and extensively drug-resistant strains from Beijing, China. *Japanese Journal of Infectious Diseases.* 65(3):240-242.

Yang, C., Shen, X., Peng, Y., Lan, R., Zhao, Y., Long, B., Luo, T., Sun, G. et al. 2015. Transmission of *Mycobacterium tuberculosis* in China: a population-based molecular epidemiologic study. *Clinical Infectious Diseases : An Official Publication of the Infectious Diseases Society of America.* 61(2):219-227. DOI:10.1093/cid/civ255 [doi].

Yano, T., Kassovska-Bratinova, S., Teh, J.S., Winkler, J., Sullivan, K., Isaacs, A., Schechter, N.M. & Rubin, H. 2011. Reduction of clofazimine by mycobacterial type 2 NADH:quinone oxidoreductase: a pathway for the generation of bactericidal levels of reactive oxygen species. *The Journal of Biological Chemistry.* 286(12):10276-10287. DOI:10.1074/jbc.M110.200501 [doi].

Yeh, P., Tschumi, A.I. & Kishony, R. 2006. Functional classification of drugs by properties of their pairwise interactions. *Nature Genetics.* 38(4):489-494. DOI:ng1755 [pii].

Yonath, A. 2005. Antibiotics targeting ribosomes: resistance, selectivity, synergism, and cellular regulation. *Annu.Rev.Biochem.* 74:649-679.

Zhang, L., Yan, K., Zhang, Y., Huang, R., Bian, J., Zheng, C., Sun, H., Chen, Z. et al. 2007. High-throughput synergy screening identifies microbial metabolites as combination agents for the treatment of fungal infections. *Proceedings of the National Academy of Sciences of the United States of America.* 104(11):4606-4611. DOI:0609370104 [pii].

Zhang, Y., Wade, M.M., Scorpio, A., Zhang, H. & Sun, Z. 2003. Mode of action of pyrazinamide: disruption of *Mycobacterium tuberculosis* membrane transport and energetics by pyrazinoic acid. *The Journal of Antimicrobial Chemotherapy.* 52(5):790-795. DOI:10.1093/jac/dkg446 [doi].

Zignol, M., Hosseini, M.S., Wright, A., Weezenbeek, C.L., Nunn, P., Watt, C.J., Williams, B.G. & Dye, C. 2006. Global incidence of multidrug-resistant tuberculosis. *The Journal of Infectious Diseases.* 194(4):479-485. DOI:JID36035 [pii].

Zimmermann, G.R., Lehar, J. & Keith, C.T. 2007. Multi-target therapeutics: when the whole is greater than the sum of the parts. *Drug Discovery Today.* 12(1):34-42.

Zumla, A., George, A., Sharma, V., Herbert, R.H.N., of Ilton, B.M., Oxley, A. & Oliver, M. 2015. The WHO 2014 global tuberculosis report—further to go. *The Lancet Global Health.* 3(1):e10-e12.

Zumla, A., Nahid, P. & Cole, S.T. 2013. Advances in the development of new tuberculosis drugs and treatment regimens. *Nature Reviews Drug Discovery.* 12(5):388-404.

Zumla, A.I., Gillespie, S.H., Hoelscher, M., Philips, P.P., Cole, S.T., Abubakar, I., McHugh, T.D., Schito, M. et al. 2014. New antituberculosis drugs, regimens, and adjunct therapies: needs, advances, and future prospects. *The Lancet.Infectious Diseases.* 14(4):327-340. DOI:10.1016/S1473-3099(13)70328-1 [doi].

Zurenko, G.E., Yagi, B.H., Schaadt, R.D., Allison, J.W., Kilburn, J.O., Glickman, S.E., Hutchinson, D.K., Barbachyn, M.R. et al. 1996. In vitro activities of U-100592 and U-100766, novel oxazolidinone antibacterial agents. *Antimicrobial Agents and Chemotherapy*. 40(4):839-845.